UNIVERSITY OF CALIFORNIA,
IRVINE

Volatile Organic Compounds in OCWD Water Samples and Volatile Organic Biomarkers in Exhaled Breath and Plasma of Overweight and Type 2 Diabetes Subjects

Dissertation

submitted in partial satisfaction of the requirements for the degree of

DOCTOR OF PHILOSOPHY

in Chemistry

by

Yu-Hsin Hung

Dissertation Committee:
Professor Donald R. Blake, Chair
Professor Barbara J. Finlayson-Pitts
Professor Sergey A. Nizkorodov

2014

ProQuest LLC.
789 East Eisenhower Parkway
P.O. Box 1346
Ann Arbor, MI 48106 - 1346

DEDICATION

To my parents, my brother, and my aunt.

To all the good friends in my life.

To my teachers, mentors, the Rowland-Blake group, the Galassetti group, UCI Institute for Clinical Translational Science (ICTS) staff members, UCI Chemistry Department staff members.

TABLE OF CONTENTS

LIST OF FIGURES

LIST OF TABLES

LIST OF EQUATIONS

ACKNOWLEDGEMENTS

I would like to thank my advisor and mentor, Professor Donald R. Blake for his support, positive encouragement, scientific thinking and inspiration over the years. None of this would happen without him.

I also appreciate all the help from my dear workers in the Rowland-Blake Group. I would like to thank Simone Meinardi for providing all kinds of help and his knowledge of the instrument and experiments. I would like to Gloria Liu Weitz and Brent Love for always being heartwarming, patient and supportive. I also want to give thanks to Barbara Chisholm, Hyun-Ji (Julie) Lee, Barbara Barletta, Isobel Simpson, Matthew Gartner, Josette Marrero, and Gregory Hartt for their advice and assistance. I also want to thank all the group members for making the group such a good one.

I want to give my thanks to Professor Pietro R. Galassetti and Dr. Stacy R. Oliver for their experiment coordination, support, inspiration and advice. My thank also goes to the UCI ICTS staff members.

I would also like to thank Professor William J. Cooper for providing the help and being enthusiastic. I thank Ken Ishida for his knowledge and support.

I would like to thank my committee members, Professor Barbara J. Finlayson-Pitts and Professor Sergey A. Nizkorodov for their time and helpful advice.

Finally, I would like to give thank to my parents and family for being supportive all the time and trying to do whatever they can do for me.

CURRICULUM VITAE

Yu-Hsin Hung

University of California, Irvine, CA
Ph. D. in Chemistry (2014)

University of California, Irvine, CA
Teaching Assistant, Chemistry Department (2010-2011)

National Taiwan Normal University, Taipei, Taiwan
M.S. in Chemistry (2008)

National Taiwan Normal University, Taipei, Taiwan
Teaching Assistant, Chemistry Department (2007-2008)

National Taiwan Normal University, Taipei, Taiwan
B.S. in Chemistry (2006)

Publications

Hsueh-Ju Liu, Yu-Hsin Hung, Chang-Chuan Chou and Chan-Cheng Su. "Proton-controllable Fluorescent Switch Based on Interconversion of Polynuclear and Dinuclear Copper(II) Complexes." Chemical Communication, 5 (2007) 495-497

Yu-Hsin Hung, Stacy R. Oliver, Hyun Ji Lee, Brian D. Tran, Pietro R. Galassetti, Donald R. Blake. "Breath/Plasma Gas Ratio as a Biomarker of Altered Metabolism in Obesity and Type 2 Diabetes." Diabetes. 61 (2012) A711

ABSTRACT OF THE DISSERTATION

Volatile Organic Compounds in OCWD Water Samples and Volatile Organic Biomarkers in Exhaled Breath and Plasma Of Overweight and Type 2 Diabetes Subjects

By

Yu-Hsin Hung

Doctor of Philosophy in Chemistry

University of California, Irvine, 2014

Professor Donald R. Blake, Chair

The objective of water sample study is to determine and monitor change of volatile organic compounds in water samples during two steps in the water treatment process at the OCWD, reverse osmosis and ultraviolet(UV)-H_2O_2 based UV advanced oxidation processes. In order to optimize water reclamation for mitigation of ever-increasing water demand, the production and elimination of pollutants (both known and unidentified) during the water treatment process need to be thoroughly investigated. Volatile organic compounds were collected by purging water samples with ultra high purity helium and collection in 1.9 L stainless canisters. Degassed samples were analyzed with multiple column/detector combinations simultaneously to detect known and unidentified compounds. Chloromethane and four trihalomethanes (Br, Cl) were found, but well below the legal or suggested levels. Increase of methyl

nitrate and *i*-propyl nitrate after the UV-H_2O_2 based UV advanced oxidation process were observed as well. Estimation of methyl nitrate and *i*-propyl nitrate annual production based on current results demonstrates no significant air quality effect.

The objective of breath and plasma studies among overweight and type 2 diabetes mellitus (T2DM) groups is to determine possible biomarkers for screening of pre-diabetes and diabetes. Financial cost, possible complications of diabetes, and the finger pricking blood sugar monitoring routine are overwhelming for diabetic patients. Biomarkers for pre-diabetes and diabetes may facilitate diabetes screening and/or inspire non-invasive blood sugar monitoring techniques. Exhaled breath, ambient room air, and plasma degas samples were analyzed with multi column/detector combinations. Plasma and/or delta breath isoprene, acetone, and methanol are substantially higher in males than females for overweight and T2DM groups. A larger group covering various age ranges can help further determine the distribution of these three and maybe determine other gases among groups (healthy, overweight, and T2DM) that can serve as diabetes screening biomarkers.

Chapter 1: Introduction

1.1. Volatile Organic Compounds in the Atmosphere

The atmosphere is mostly composed of nitrogen, oxygen, argon, carbon dioxide and noble gases. Volatile organic compounds (VOCs) compose less than 0.0001% of the atmosphere. Even though VOCs in the atmosphere are at low concentrations, their variety and reactivity make them important. Volatile organic compounds in the atmosphere have anthropogenic and biogenic sources. For example, forests are an important biogenic source of isoprene, α-pinene, β-pinene, methanol, aldehydes, and ketones (Graedel et al., 1993). Photolysis reactions in seawater are important sources of alkyl nitrates (Atlas, 1993; Moore & Blough, 2002). Biomass burning is also a substantial source for atmospheric VOCs, including methane and non methane hydrocarbons (NMHCs) such as alkanes, alkenes, aromatics, halocarbons, alkyl nitrates (Blake, Smith, Chen, Whipple, & Rowland, 1994; Lacaux et al., 1995; Simpson et al., 2002; Ward et al., 1992). Human activities such as petroleum refinement, vehicle exhaust, solvent usage, and agriculture emit a variety of hydrocarbons and halocarbons (Derwent, Hester, & Harrison, 1995; Piccot, Watson, & Jones, 1992).

The photochemical reactivity and the resulting products make atmospheric VOCs important in local and regional atmospheric chemistry. Major atmospheric VOCs include hydrocarbons, halocarbons, oxygenates, and organosulfur compounds. Oxidation by hydroxyl radicals is the most important reaction for hydrocarbons.

Equation 1.1 $$RH + \cdot OH \rightarrow R\cdot + H_2O$$

Upon oxidation, VOCs can react with nitrogen oxide in sunlight producing tropospheric ozone and oxygenates (Finlayson-Pitts & Pitts Jr, 2000; Haagen-Smit, Bradley, & Fox, 1953).

Equation 1.2 $$R\cdot + O_2 \rightarrow \cdot RO_2$$

Equation 1.3 $$\cdot RO_2 + NO \rightarrow \cdot RO + NO_2$$

Equation 1.4 $$NO_2 \xrightarrow{h\nu\ (\lambda < 420)} NO + O(^3P)$$

Equation 1.5 $$O(^3P) + O_2 \rightarrow O_3$$

Equation 1.6 $$O_3 \xrightarrow{h\nu\ (\lambda = 310nm)} O(^1D) + O_2$$

Equation 1.7 $$O(^1D) + H_2O \rightarrow 2OH$$

As a result of different reactivities in the atmosphere, each compound has a unique lifetime. Air masses carrying VOCs usually have a similar ratio between compounds as that of their source when first released. However, more reactive species diminish faster than those less reactive. Therefore, by comparing the ratio between different components, one can estimate the age of the sampled air mass or determine possible origins of it.

Volatile organic compounds in the environment can affect human health via several different paths, such as drinking water, aspiration, and skin contact (Sato & Nakajima, 1987). The study of VOCs emitted during human metabolic processes can provide useful information. Volatile organic compounds can also be studied in different media, such as in aqueous solutions, bio fluids, atmospheric samples and human breath.

Volatile organic compounds can travel between an aqueous solution and the atmosphere; and between bio fluids and human breath. Thus, it is important to learn how the VOC profiles correlate with each other from these different fluid/air scenarios.

1.2. Breath VOCs

It is well known that VOCs are exchanged in alveolar cells. Therefore, human breath contains VOCs that reveal an individual's metabolic condition. In ancient Greece, it was noted that diabetic patients had a sweet smell in their breath (Phillips, 1992). Also, a fish smell in breath, resulting from an increase of nitrogenous compounds, was found in patients with renal or liver diseases (Wills & Savory, 1981). By 1971, Pauling and co-workers were able to quantify around 250 substances from exhaled breath (1971). In 1988, O'Neill and colleagues observed 19 VOCs in exhaled breath including alkanes, alkenes, oxygenates, were thought to be the a breath fingerprint of lung cancer (1988). Later, Phillips et al. found a set of nine breath markers composed of C_4-C_{14} hydrocarbons, which distinguished lung cancer patients from non-lung cancer subjects with higher than 60% precision (2003; 1999). Phillips et al. also found that a group of methylated hydrocarbons, which were proposed as peroxidation products of polyunsaturated fatty acids, distinguished female breast cancer patients from non-breast cancer patients (precision > 73%) (2006; 2003). Studies of breath VOCs and their relation to diseases and/or physical conditions demonstrate that the utility of human breath for diagnostic or screening purposes is feasible. In fact, the U.S. Food and Drug Administration (FDA) has

approved about 40 breath devices for the detection of diseases or conditions, such as asthma, Helicobacter pylori, and breath ethanol (Paschke, Mashir, & Dweik, 2010).

Table 1.1: Some of FDA approved breath devices. Adapted from F1000 Medicine Reports 2010, 2:56 (Paschke et al., 2010).

Disease/Condition	**Molecule Detected**
Asthma, airway inflammation	NO
Helicobacter pylori	$^{13}CO_2/^{12}CO_2$
Lactose malabsorption	H_2
Grade 3 heart transplant rejection	(C_4-C_{20}) alkanes, monomethylalkanes
Ventilation	CO_2
Breath ethanol	Ethanol

1.3. Blood VOCs

Screening techniques for diseases and for the onset of diseases are with ever-increasing importance since people have learned that prevention is more cost effective. Changes of metabolic products and/or by-products due to altered metabolic processes are expected. Therefore, measurements of these changes have a high potential to provide biomarkers for the design of screening, diagnostic, and monitoring methodologies. Studying the signals (host response, metabolic products, and by-products) given off at different stages of the process of disease development is crucial. which are proposed to be caused by diseases and medical treatments, for Alzheimer's disease (Han, M. Holtzman, W. McKeel, Kelley, & Morris, 2002), type 2 diabetes (C. Wang et al., 2005; Yuan, Kong, Guan, Yang, & Xu, 2007), and lung cancer (Filipiak et al., 2010). Blood is a good candidate to observe metabolites. Blood carries nutrients such as amino acids and glucose to cells throughout the body, and also transports metabolic products and/or waste from cells. Therefore, blood gases are a likely source of valuable information for normal and altered metabolic processes.

1.4. Obesity and Type 2 Diabetes Mellitus (T2DM)

According to the 2011 National Diabetes Fact Sheet, 25.6 % of adults over the age of 20 in the U.S.A have diabetes (Centers for Disease Control and Prevention. National diabetes fact sheet: national estimates and general information on diabetes and prediabetes in the United States, 2011). In a healthy human body, the pancreas secretes insulin when there is an increase of blood glucose. Then, insulin signals muscles to uptake glucose for storage for future energy production. Type 1 diabetic mellitus is usually diagnosed at young ages, because patients are born with defected insulin production ability, whereas T2DM is high blood glucose resulting from the poor response of cells to endogenous insulin. There is also gestational diabetes mellitus (GDM), which occurs during pregnancy. Statistics show that some GDM patients become healthy after delivery, but are at a higher risk to develop T2DM within 1-2 decades (Bellamy, Casas, Hingorani, & Williams, 2009; Halbritter et al., 2012). Diabetic patients also have an increased risk of complications, such as heart disease, kidney disease, and vision damage. Obesity is found to cause or to worsen diseases such as heart disease, hypertension, and T2DM (Kopelman, 2000). Obesity alters the metabolic status in the human body and triggers the onset of T2DM by making liver and muscles less responsive to blood insulin. For example, after a healthy human eats, their blood glucose increase and this causes their pancreas to secrete insulin. The endogenous insulin stops the liver from secreting glucose and signals the muscle to uptake glucose from the blood stream. Obesity subject have an increased amount of fat cells, which interact with the liver and the muscle resulting in their poor response efficiency to insulin. The development of less responsive liver and muscles of obese people leads to blood sugar remaining at dangerously high

levels. Therefore, at the onset of hyperglycemia (high blood glucose), the pancreas compensates by releasing more insulin and the blood glucose is able to go down to a normal range. As months and years pass, the amount of insulin that the body needs to bring down glucose level rises. The pancreas is gradually damaged during the process, and is gradually incapable of producing the amount of insulin needed to lower blood glucose. Subjects become hyperglycemic and are diagnosed with T2DM.

Many T2DM patients are overweight. Studies also show that there is a positive correlation of body mass index (BMI) and relative risk of developing T2DM (Willett, Dietz, & Colditz, 1999). As a result, a study of the differences and similarities between overweight and T2DM patients is warranted. Type 2 diabetic mellitus is considered a progressive disease. The metabolic changes that occur during leading to T2DM can help us better understand the disease. Observations of the disease development may also provide strategies for drug design and prevention of overweight subjects from developing T2DM.

In 2009, Kim and colleagues studied the urine of mice that were on high-fat diets and those on normal diets via ^{1}H-nuclear magnetic resonance (NMR) spectrometry. They found a group of compounds relating to glucose breakdown (pyruvate and lactate) and energy production by fat (such as acetone) that were markedly higher in mice with high-fat diets than in mice that had normal diets (2009). In 2011, Spagou et al. compared the metabolic profiles of the plasma of mice that were either on high-fat diets for 12 month or low-fat diets for 15 month (2011). The conclusion of the study was that rats on high-fat diets had an increased amount of metabolic products from ketosis, which is a process of fat breakdown for energy production, similar to that observed in obese human populations (Spagou et al., 2011). While both reports had similar conclusions, Spagou et al. reminded readers that there exist some subtle differences for mice even in the same group (2011). Mice on the same high fat diet had different body weights at the end of the study (Spagou et al., 2011). When interpreting results, Spagou et al. indicated that one must consider individual differences even among the same group of subjects (2011).

Though breath VOCs have been useful for the detection of some disease, its application in studying T2DM is still not clear. In 2010, Greiter et al. used proton transfer reaction-mass spectrometry (PTR-MS) to compare breath profiles of T2DM and healthy subjects. By using acetone, butanol, dimethyl sulfide, isoprene, and five unknown compounds (mass = 49, 126, 135, 140, 157), they distinguished T2DM subjects from healthy subjects with high accuracy (90% sensitivity, 92% specificity) (Greiter et al., 2010). However, the authors also mentioned that further investigation to validate the results is needed (Greiter et al., 2010). In 2012, Halbritter et al. studied exhaled VOCs of 52 pregnant women and found that the concentration changes of acetone and some thiols

in breath samples trace the change of subjects' blood glucose level (Halbritter et al., 2012). They also observed less dimethyl sulfides and methanol for GDM subjects compared to the rest of the study group (Halbritter et al., 2012).

Volatile organic compounds were also predictors of blood metabolite levels, such as glucose and triglycerides. Novak et al. studied breath VOCs of 18 T1DM volunteers and found that methyl nitrate correlated well with blood glucose for 16 out of 18 patients (Novak et al., 2007). Galassetti et al. investigated multi-variants prediction for blood glucose from a combination of the following gases from exhaled breath: ethanol, acetone, methyl nitrate, *o*-xylene, *m/p*-xylene, and ethylbenzene (Galassetti et al., 2005; Lee et al., 2009). The demonstrated prediction showed a high correlation (average correlation coefficient > 0.70) with measured blood glucose among all the subjects studied (Galassetti et al., 2005; Lee et al., 2009). Minh and colleagues also showed an excellent prediction of blood triglycerides and free fatty acids (FFA) using groups of selected exhaled gases (Minh et al., 2012).

1.5. Water Treatment VOCs

One of the main goals of water treatment is to produce water that does not harm public health. Ideal water treatment processes are meant to eliminate possible pathogens in a healthy and in a cost effective way. Since the early 1900s, chlorine has been used for water treatment in the United States because of its excellent disinfection efficiency. However, it was found that halogenated disinfection by-products, which have potential threat to human health, are generated in chlorine disinfection processes (Bellar, Lichtenberg, & Kroner, 1974). Some techniques, such as reverse osmosis (RO) and

ultraviolet advanced oxidation process (UVAOP) have been used in the water treatment process to help remove pathogens, trace contaminants and disinfection by-products (DBPs). To ensure public heath, the regulated allowance of total trihalomethanes (THMs), a major group of DBPs in drinking water, has been set at 80 ppb in the US (Bond, Huang, Templeton, & Graham, 2011). Besides halohydrocarbons, generation of nitrogenous hydrocarbons were also discovered in water disinfection processes (Krasner et al., 2006). A challenging task for water treatment facilities is to identify unknown DBPs at relatively low concentrations.

1.6. Purge and Trap

Techniques such as purge and trap (P&T), headspace analysis, solvent extraction and solid phase extraction are commonly used for the study of VOCs in fluids. Water and biological fluid samples in our study were purged with purified ultra high purity helium, in order to achieve clean VOCs extraction.

Comparing various methods, P&T has (i) better sensitivity, (ii) no memory effect, (iii) suitable for large and small sample volumes (Golfinopoulos, Lekkas, & Nikolaou, 2001; Matz, Kibelka, Dahl, & Lennemann, 1999). Because of the advantages, P&T has been applied to the study of VOCs contained in solutions for decades. The use of gas streams, such as helium, to extract gas contents of solutions was first reported in 1962 by Swinnerton, Linnenbom and Cheek (1962). Swinnerton et al. purged water samples with a helium stream and instantly directed the helium stream to a gas chromatograph (GC) for

separation and analysis. Swinnerton et al. also believed this technique could be used for a wide range of samples (Swinnerton et al., 1962).

Later on, important alternations were made to achieve better sensitivity and separation. Preconcentration traps are used to remove the purging gas to concentrate collected gases prior to separation and detection, thus, higher detector response is achieved. Therefore, preconcentration traps are common when P&T is used for solution VOC analysis (Dunemann & Hajimiragha, 1993; Leonard, Liu, Brewer, & Sacks, 1998; Matz et al., 1999; J.-L. Wang & Chen, 2001). The two most common preconcentration methods utilized are adsorbent material and cryogenic trapping. When adsorbent materials are used, the resulting gas stream will pass through one or more designed absorbent materials, in which compounds of interest are trapped. Volatile organic compounds are released upon heating. Memory effect occurs when trapped compounds are not 100% volatilized and the residue can contaminate following analyses. Efficient refresh steps are necessary after each injection. For example, in between each sampling time the adsorbent material is kept at high temperature to prevent possible contaminations. Also, sufficiently high temperatures are needed for the release of VOCs from adsorbent material, which can cause potential thermal decomposition for some unstable compounds. Cryogen cooling traps, such as liquid nitrogen or liquid carbon dioxide, are used to condense VOCs in a loop. The clean and efficient release of VOCs can be achieved by immersing the concentration loop into a hot water bath.

For this thesis, studies were designed to investigate VOC profiles in a variety of samples, including (i) water samples at different stages of water treatment in Orange

County Water District (OCWD); and (ii) plasma and breath of overweight (OW) and type 2 diabetes mellitus subjects (T2DM). Purge was used for the preparation of fluid degas samples. A multi-column and multi-detector GC system was used for separation and detection (Colman et al., 2001). The purpose of part of this study was to analyze blood and breath profiles for the same group and evaluate the similarity and differences between the OW and T2DM groups. The water treatment work could lead to improvements for the water treatment stages and demonstrates possible impact that VOCs in treated water may have on their mixing ratios in the atmosphere.

1.6.1. Previous Biofluid Studies Using P&T For VOCs

As P&T was developed in 1970s, it has been used to study VOCs profiles for various types of samples, including foods (Heikes, Jensen, & Fleming-Jones, 1995), aqueous solutions (Golfinopoulos et al., 2001; Kuo, Chian, DeWalle, & Kim, 1977; Leonard et al., 1998; Swinnerton et al., 1962; Warner & Beasley, 1984), and body fluids (Anderson, Thomson, & Harland, 1979; Ashley et al., 1992; Dunemann & Hajimiragha, 1993; Peoples, Pfaffenberger, Shafik, & Enos, 1979). Volatile organic compounds in body fluids as products and/or byproducts of metabolic processes can indicate how the body reacts to disease, environments (Dunemann & Hajimiragha, 1993), and even toxins (Anderson et al., 1979; Houeto, Borron, Marlière, Baud, & Levillain, 2001). So the study of VOCs in blood and other body fluids is of high importance. Two common strategies for the analysis of VOCs in blood include: (i) using deuterated analogues of analytes of interest as internal standards (Ashley et al., 1992), and (ii) making use of the identification power of mass spectrometry (MS) to study profiles of VOCs in bio fluids

comprehensively (Peoples et al., 1979). In 1979, blood cyanide concentrations and the thermal degradation products of nitrogen containing polymers, were investigated for their relation to deaths of fire casualties by Anderson (1979). The blood of controls, fire casualties, and firemen were studied by nitrogen P&T and analyzed by GC-MS and gas-liquid chromatography (Anderson et al., 1979). Also, due to the interest of understanding how VOCs in the environment relate to those in the human body, Dunemann et al. did a comprehensive study with a variety of samples including human milk, whole blood, urine, well water and waste water (1993). Dunemann et al. focused on 48 VOCs, which are known to pose health risks. Purge and trap coupled with GC was used to demonstrate concentration levels of VOCs in the environment and also in various human body fluids (1993). Another noted function of blood is the transportation and exchange of metabolic products from the lungs, kidneys and skin while sweeping the metabolic products from the blood stream. This suggests that breath and other bio fluids may also be potential candidates to look for biomarkers.

To better evaluate various VOCs, global profiling is likely helpful in relative studies. When it comes to studying the global profiling of VOCs, MS with superb identification power and good sensitivity is often used. Fiehn (2008) and Pasikanti et al. (2008) pointed out that GC-MS is very powerful in terms of separation, identification of unknowns, reproducibility, and sensitivity.

1.6.2. Previous Water Treatment Studies Using P&T For VOCs

In 1974, Bellar and coworkers utilized P&T techniques to examine the VOCs from drinking water. Results from their report pointed out the existence of halocarbons, such

as trichloromethane ($CHCl_3$), in the drinking water (Bellar et al., 1974). More relative studies were undertaken after Bellar et al. published their results (Leonard et al., 1998; Lepine & Archambault, 1992; Niri, Bragg, & Pawliszyn, 2008). Besides the halogenated byproducts generated during chlorine disinfection process, anthropogenic VOCs sources like gasoline additives, organic solvents, and household products were common contaminants observed in drinking water (US Environmental Protection Agency, 2008).

1.7. References:

Anderson, R. A., Thomson, I., & Harland, W. A. (1979). The importance of cyanide and organic nitriles in fire fatalities. *Fire and Materials, 3*(2), 91-99. doi: 10.1002/fam.810030207

Ashley, D. L., Bonin, M. A., Cardinali, F. L., McCraw, J. M., Holler, J. S., Needham, L. L., & Patterson, D. G. (1992). Determining volatile organic compounds in human blood from a large sample population by using purge and trap gas chromatography/mass spectrometry. *Analytical Chemistry, 64*(9), 1021-1029. doi: 10.1021/ac00033a011

Atlas, E. (1993). Alkyl nitrates, nonmethane hydrocarbons, and halocarbon gases over the equatorial Pacific Ocean during saga 3. *J. Geophys. Res., 98*, 16933-16947.

Bellamy, L., Casas, J.-P., Hingorani, A. D., & Williams, D. (2009). Type 2 diabetes mellitus after gestational diabetes: a systematic review and meta-analysis. *The Lancet, 373*(9677), 1773-1779.

Bellar, T. A., Lichtenberg, J. J., & Kroner, R. C. (1974). The Occurrence of Organohalides in Chlorinated Drinking Waters. *American Water Works Association, 66*(12), 4.

Blake, D. R., Smith, T. W., Chen, T. Y., Whipple, W. J., & Rowland, F. S. (1994). Effects of biomass burning on summertime nonmethane hydrocarbon concentrations in the Canadian wetlands. *Journal of Geophysical Research: Atmospheres, 99*(D1), 1699-1719. doi: 10.1029/93JD02598

Bond, T., Huang, J., Templeton, M. R., & Graham, N. (2011). Occurrence and control of nitrogenous disinfection by-products in drinking water – A review. *Water Research, 45*(15), 4341-4354. doi: http://dx.doi.org/10.1016/j.watres.2011.05.034

Centers for Disease Control and Prevention. National diabetes fact sheet: national estimates and general information on diabetes and prediabetes in the United States, A., GA: U.S. Department of Health and Human Services, Centers for Disease Control and Prevention, 2011. (2011). *Centers for Disease Control and Prevention. National diabetes fact sheet: national estimates and general information on diabetes and prediabetes in the United States, 2011. Atlanta, GA*.

Colman, J. J., Swanson, A. L., Meinardi, S., Sive, B. C., Blake, D. R., & Rowland, F. S. (2001). Description of the Analysis of a Wide Range of Volatile Organic Compounds in Whole Air Samples Collected during PEM-Tropics A and B. *Analytical Chemistry, 73*(15), 3723-3731. doi: 10.1021/ac010027g

Derwent, R. G., Hester, R. E., & Harrison, R. M. (1995). Sources, distributions, and fates of VOCs in the atmosphere *Volatile Organic Compounds in the Atmosphere* (Vol. 4, pp. 1-16): The Royal Society of Chemistry.

Dunemann, L., & Hajimiragha, H. (1993). Development of a screening method for the determination of volatile organic compounds in body fluids and environmental samples using purge and trap gas chromatography—mass spectrometry. *Analytica Chimica Acta, 283*(1), 199-206. doi: http://dx.doi.org/10.1016/0003-2670(93)85223-7

Fiehn, O. (2008). Extending the breadth of metabolite profiling by gas chromatography coupled to mass spectrometry. *TrAC Trends in Analytical Chemistry, 27*(3), 261-269. doi: http://dx.doi.org/10.1016/j.trac.2008.01.007

Filipiak, W., Sponring, A., Filipiak, A., Ager, C., Schubert, J., Miekisch, W., . . . Troppmair, J. (2010). TD-GC-MS Analysis of Volatile Metabolites of Human Lung Cancer and Normal Cells *In vitro*. *Cancer Epidemiology Biomarkers & Prevention, 19*, 182-195.

Finlayson-Pitts, B. J., & Pitts Jr, J. N. (2000) *Chemistry of the Upper and Lower Atmosphere* (pp. 1-969). San Diego: Academic Press.

Galassetti, P. R., Novak, B., Nemet, D., Rose-Gottron, C., Cooper, D. M., Meinardi, S., . Blake, D. R. (2005). Breath Ethanol and Acetone as Indicators of Serum Glucose Levels: An Initial Report. *Diabetes Technology & Therapeutics, 7*(1), 9. doi: 10.1089/dia.2005.7.115.

Golfinopoulos, S. K., Lekkas, T. D., & Nikolaou, A. D. (2001). Comparison of methods for determination of volatile organic compounds in drinking water. *Chemosphere, 45*(3), 275-284. doi: http://dx.doi.org/10.1016/S0045-6535(00)00553-1

Graedel, T. E., Bates, T. S., Bouwman, A. F., Cunnold, D., Dignon, J., Fung, I., . . . Veldt, C. (1993). A compilation of inventories of emissions to the atmosphere. *Global Biogeochemical Cycles, 7*(1), 1-26. doi: 10.1029/92GB02793

Greiter, M. B., Keck, L., Siegmund, T., Hoeschen, C., Oeh, U., & Paretzke, H. G. (2010). Differences in exhaled gas profiles between patients with type 2 diabetes and healthy controls. *Diabetes Technology & Therapeutics, 12*(6), 9. doi: doi:10.1089/dia.2009.0181.

Haagen-Smit, A. J., Bradley, C. E., & Fox, M. M. (1953). Ozone Formation in Photochemical Oxidation of Organic Substances. *Industrial & Engineering Chemistry, 45*(9), 2086-2089. doi: 10.1021/ie50525a044

Halbritter, S., Fedrigo, M., Ho, V., Szymczak, W., Maier, J. M., Ziegler, A.-G., & Hummel, M. (2012). Human Breath Gas Analysis in the Screening of Gestational Diabetes Mellitus. *Diabetes Technology & Theraputics, 14*(10), 9. doi: 10.1089/dia.2012.0076

Han, X., M. Holtzman, D., W. McKeel, D., Kelley, J., & Morris, J. C. (2002). Substantial sulfatide deficiency and ceramide elevation in very early Alzheimer's disease: potential role in disease pathogenesis. *Journal of Neurochemistry, 82*(4), 809-818. doi: 10.1046/j.1471-4159.2002.00997.x

Heikes, D. L., Jensen, S. R., & Fleming-Jones, M. E. (1995). Purge and Trap Extraction with GC-MS Determination of Volatile Organic Compounds in Table-Ready Foods. *Journal of Agricultural and Food Chemistry, 43*(11), 2869-2875. doi: 10.1021/jf00059a018

Houeto, P., Borron, S. W., Marlière, F., Baud, F. J., & Levillain, P. (2001). Development of a Method for Measuring Volatile Organic Compounds in the Blood of Fire Victims Using'Purge and Trap' Gas Chromatography. *Indoor and Built Environment, 10*(2), 62-69. doi: 10.1177/1420326X0101000202

Kim, S.-H., Yang, S.-O., Kim, H.-S., Kim, Y., Park, T., & Choi, H.-K. (2009). 1H-nuclear magnetic resonance spectroscopy-based metabolic assessment in a rat

model of obesity induced by a high-fat diet. *Analytical and Bioanalytical Chemistry, 395*(4), 1117-1124. doi: 10.1007/s00216-009-3054-8

Kopelman, P. G. (2000). Obesity as a medical problem. *Nature, 404*(6778), 635-643.

Krasner, S. W., Weinberg, H. S., Richardson, S. D., Pastor, S. J., Chinn, R., Sclimenti, M. J., Thruston, A. D. (2006). Occurrence of a New Generation of Disinfection Byproducts†. *Environmental Science & Technology, 40*(23), 7175-7185. doi: 10.1021/es060353j

Kuo, P. P. K., Chian, E. S. K., DeWalle, F. B., & Kim, J. H. (1977). Gas stripping, sorption, and thermal desorption procedures for preconcentrating volatile polar water-soluble organics from water samples for analysis by gas chromatography. *49*(7).

Lacaux, J. P., Brustet, J. M., Delmas, R., Menaut, J. C., Abbadie, L., Bonsang, B., . . . Helas, G. (1995). Biomass burning in the tropical savannas of Ivory Coast: An overview of the field experiment Fire of Savannas (FOS/DECAFE 91). *Journal of Atmospheric Chemistry, 22*(1-2), 195-216. doi: 10.1007/BF00708189

Lee, J., Ngo, J., Blake, D., Meinardi, S., Pontello, A. M., Newcomb, R., & Galassetti, P. R. (2009). Improved predictive models for plasma glucose estimation from multi-linear regression analysis of exhaled volatile organic compounds. *J Appl Physiol, 107*(1), 155-160. doi: 10.1152/japplphysiol.91657.2008

Leonard, C., Liu, H.-F., Brewer, S., & Sacks, R. (1998). High-Speed Gas Extraction of Volatile and Semivolatile Organic Compounds from Aqueous Samples. *Analytical Chemistry, 70*(16), 3498-3504. doi: 10.1021/ac980153t

Lepine, L., & Archambault, J. F. (1992). Parts-per-trillion determination of trihalomethanes in water by purge-and-trap gas chromatography with electron capture detection. *Analytical Chemistry, 64*(7), 810-814. doi: 10.1021/ac00031a020

Matz, G., Kibelka, G., Dahl, J., & Lennemann, F. (1999). Experimental study on solvent-less sample preparation methods: Membrane extraction with a sorbent interface, thermal membrane desorption application and purge-and-trap. *Journal of Chromatography A, 830*(2), 365-376. doi: http://dx.doi.org/10.1016/S0021-9673(98)00853-X

Minh, T. D. C., Oliver, S. R., Flores, R. L., Ngo, J., Meinardi, S., Carlson, M. K., . . . Blake, D. R. (2012). Noninvasive Measurement of Plasma Triglycerides and Free Fatty Acids from Exhaled Breath. *Journal of Diabetes Science and Technology, 6*(1), 6.

Moore, R. M., & Blough, N. V. (2002). A marine source of methyl nitrate. *Geophysical Research Letters, 29*(15), 27-21-27-24. doi: 10.1029/2002GL014989

Niri, V. H., Bragg, L., & Pawliszyn, J. (2008). Fast analysis of volatile organic compounds and disinfection by-products in drinking water using solid-phase microextraction–gas chromatography/time-of-flight mass spectrometry. *Journal of Chromatography A, 1201*(2), 222-227.

Novak, B. J., Blake, D. R., Meinardi, S., Rowland, F. S., Pontello, A., Cooper, D. M., & Galassetti, P. R. (2007). Exhaled methyl nitrate as a noninvasive marker of hyperglycemia in type 1 diabetes. *Proceedings of the National Academy of Sciences, 104*(40), 15613-15618. doi: 10.1073/pnas.0706533104

O'Neill, H. J., Gordon, S. M., O'Neill, M. H., Gibbons, R. D., & Szidon, J. P. (1988). A computerized classification technique for screening for the presence of breath biomarkers in lung cancer. *Clinical Chemistry, 34*, 6. doi: http://www.clinchem.org/content/34/8/1613.full.pdf+html

Paschke, K. M., Mashir, A., & Dweik, R. A. (2010). Clinical applications of breath testing. *F1000 Medicine Reports, 2*(56), 6. doi: http://www.ncbi.nlm.nih.gov/pmc/articles/PMC2990505/pdf/medrep-02-56.pdf

Pasikanti, K. K., Ho, P. C., & Chan, E. C. Y. (2008). Gas Chromatography/Mass Spectrometry in Metabolic Profiling of Biological Fluids. *Journal of Chromatography B, 871*(2), 202-211.

Pauling, L., Robinson, A. B., Teranishi, R., & Cary, P. (1971). Quantitative Analysis of Urine Vapor and Breath by Gas-Liquid Partition Chromatography. *Proceedings of the National Academy of Sciences of the United States of America, 68*(10), 2374-2376.

Peoples, A. J., Pfaffenberger, C. D., Shafik, T. M., & Enos, H. F. (1979). Determination of volatile purgeable halogenated hydrocarbons in human adipose tissue and blood serum. *Bulletin of Environmental Contamination and Toxicology, 23*(1), 244-249. doi: 10.1007/bf01769950

Phillips, M. (1992). Breath Tests in Medicine. *Scientific American, 267*(1), 6.

Phillips, M., Cataneo, R., Ditkoff, B., Fisher, P., Greenberg, J., Gunawardena, R., . . . Wong, C. (2006). Prediction of breast cancer using volatile biomarkers in the breath. *Breast Cancer Research and Treatment, 99*(1), 19-21. doi: 10.1007/s10549-006-9176-1

Phillips, M., Cataneo, R. N., Cummin, A. R. C., Gagliardi, A. J., Gleeson, K., Greenberg, J., Row, W. N. (2003). Detection of Lung Cancer With Volatile Markers in the Breath. *Chest, 123*, 2115-2123.

Phillips, M., Cataneo, R. N., Ditkoff, B. A., Fisher, P., Greenberg, J., Gunawardena, R., Wong, C. (2003). Volatile Markers of Breast Cancer in the Breath. *The Breast Journal, 9*(3), 184-191.

Phillips, M., Gleeson, K., Hughes, J. M. B., Greenberg, J., Cataneo, R. N., Baker, L., & McVay, W. P. (1999). Volatile organic compounds in breath as markers of lung cancer: a cross-sectional study. *The Lancet, 353*(9168), 1930-1933. doi: Doi: 10.1016/s0140-6736(98)07552-7

Piccot, S. D., Watson, J. J., & Jones, J. W. (1992). A global inventory of volatile organic compound emissions from anthropogenic sources. *Journal of Geophysical Research: Atmospheres, 97*(D9), 9897-9912. doi: 10.1029/92JD00682

Sato, A., & Nakajima, T. (1987). Pharmacokinetics of organic solvent vapors in relation to their toxicity. *Scand J Work Environ Health, 13*(2), 13.

Simpson, I. J., Meinardi, S., Blake, D. R., Blake, N. J., Rowland, F. S., Atlas, E., & Flocke, F. (2002). A biomass burning source of C1–C4 alkyl nitrates. *Geophysical Research Letters, 29*(24), 2168. doi: 10.1029/2002GL016290

Spagou, K., Theodoridis, G., Wilson, I., Raikos, N., Greaves, P., Edwards, R., . . . Klapa, M. I. (2011). A GC–MS metabolic profiling study of plasma samples from mice on low- and high-fat diets. *Journal of Chromatography B, 879*(17–18), 1467-1475. doi: http://dx.doi.org/10.1016/j.jchromb.2011.01.028

Swinnerton, J. W., Linnenbom, V. J., & Cheek, C. H. (1962). Determination of Dissolved Gases in Aqueous Solutions by Gas Chromatography. *Analytical Chemistry, 34*(4), 483-485. doi: 10.1021/ac60184a010

US Environmental Protection Agency, U. (2008). Basic Information – Organic Gases (Volatile Organic Compounds – VOCs), US Environmental Protection Agency, USA, 2008, . from http://www.epa.gov/iaq/voc.html

Wang, C., Kong, H., Guan, Y., Yang, J., Gu, J., Yang, S., & Xu, G. (2005). Plasma Phospholipid Metabolic Profiling and Biomarkers of Type 2 Diabetes Mellitus Based on High-Performance Liquid Chromatography/Electrospray Mass Spectrometry and Multivariate Statistical Analysis. *Analytical Chemistry, 77*(13), 4108-4116. doi: 10.1021/ac0481001

Wang, J.-L., & Chen, W.-L. (2001). Construction and validation of automated purge-and-trap–gas chromatography for the determination of volatile organic compounds. *Journal of Chromatography A, 927*(1–2), 143-154. doi: http://dx.doi.org/10.1016/S0021-9673(01)01074-3

Ward, D. E., Susott, R. A., Kauffman, J. B., Babbitt, R. E., Cummings, D. L., Dias, B., Setzer, A. W. (1992). Smoke and fire characteristics for cerrado and deforestation burns in Brazil: BASE-B Experiment. *Journal of Geophysical Research: Atmospheres, 97*(D13), 14601-14619. doi: 10.1029/92JD01218

Warner, J. M., & Beasley, R. K. (1984). Purge and trap chromatographic method for the determination of acrylonitrile, chlorobenzene, 1,2-dichloroethane, and ethylbenzene in aqueous samples. *Analytical Chemistry, 56*(11), 1953-1956. doi: 10.1021/ac00275a045

Willett, W. C., Dietz, W. H., & Colditz, G. A. (1999). Guidelines for Healthy Weight. *New England Journal of Medicine, 341*(6), 427-434. doi: doi:10.1056/NEJM199908053410607

Wills, M. R., & Savory, J. (1981). Biochemistry of renal failure. *Annals of Clinical & Laboratory Science, 11*(4), 292-299.

Yuan, K., Kong, H., Guan, Y., Yang, J., & Xu, G. (2007). A GC-based metabonomics investigation of type 2 diabetes by organic acids metabolic profile. *Journal of Chromatography B, 850*(1–2), 236-240. doi: http://dx.doi.org/10.1016/j.jchromb.2006.11.035

Chapter 2: Methods

2.1. Canister Preparation

2.1.1. Sampling Canister Sterilization

Sample collection was done with evacuated 1.9 L stainless steel canisters (Weldtec, Lake Forest, CA), which were electropolished both inside and out. Each canister had a Swagelok metal bellows valve SS-4B6 (Swagelok Company, Solon, OH) linking to a Swagelok port connecter (Swagelok Company, Solon, OH) welded on the canister lid. Sampling canisters were baked before use in an oven at 150 °C for 24 hours with their Swagelok metal bellows valves opened, except for the canisters used for the collection of ambient room air. In order to prevent loss of gases on the canister wall, a humid environment was maintained (Sive, 1998a). A stream of house air, passing through deionized water contained in an Erlenmeyer flask, was directed into the oven in ¼ ” OD stainless steel tubing during the entire baking process . Details of building canisters and canister maintenance were included in Sive’s work (1998b).

2.1.2. Pump and Flush for All Sampling Canisters

Before each sampling time, canisters were cleaned via evacuation and helium dilution at the pump-flush manifold. The pump-flush manifold was composed of six Edwards pumps (Edwards E2M-12, Wilmington, MA), six Edwards ACT-E thermocouples gauges, one 1000 torr and one 10,000 torr Baratron® capacitance manometers (MKS, Andover, MA). Canisters were first evacuated to 10^{-2} torr to remove original contents. Then, canisters were pressurized to 200 torr with ultra high purity (UHP) helium (Matheson, Newark, CA) for the dilution of the remaining contents. Each

of the pumps was individually connected to a six-foot long U tube before connecting to the pump-flush manifold. All six-foot long U tubes were always immersed in liquid nitrogen. This step prevented possible back diffusion of pump oil. Then, the canisters were evacuated to 10^{-2} torr again and the metal bellows valves of the canisters were closed to maintain vacuum. Evacuated canisters were considered ready for sample collection.

2.2. Breath Sample Collection

For exhaled breath collection, a three-way Swagewlok Ultra-Torr® tee (Solon, OH) was connected to the Swagelok port connector of a sampling canister via the middle end. Six-inch long ¼" inch OD Teflon® (Nalgene, Rochester, NY) tubing was inserted to one end of the Ultra-Torr® tee and the remaining end was left open/closed depending on whether the breath sample was being collected. Before the collection of breath samples, subjects took a deep breath and held it for a few seconds for the exchange of gas at the alveoli. When the subject started breathing into the tubing, the far end of the Ultra-Torr® tee was left open for two seconds to allow any dead space air to vent to the room. Dead space air was the air that did not or barely exchanged gases at the alveoli, which included the air originally in the tubing, the Ultra-Torr® tee, the mouth and the airway. The sampler (usually me), wearing a latex glove, then closed the vent end of the Ultra-Torr® tee by covering the end with the sampler's thumb. Meanwhile, the Swagelok metal bellows valve on the canister was opened to collect exhaled breath samples as shown in Figure 2.1 (Gorham et al., 2009). Breath samples were collected until the canister was full or until subjects could not breathe out any further. In both cases, collected exhaled

breath was enough for gas content analysis. An ambient room air sample was collected every time a breath sample was collected. Corresponding room air samples reflected background air composition. Exhaled breath samples were compared after the room background was subtracted.

Figure 2.1: Breath Sample Collection Scheme (Gorham et al., 2009)

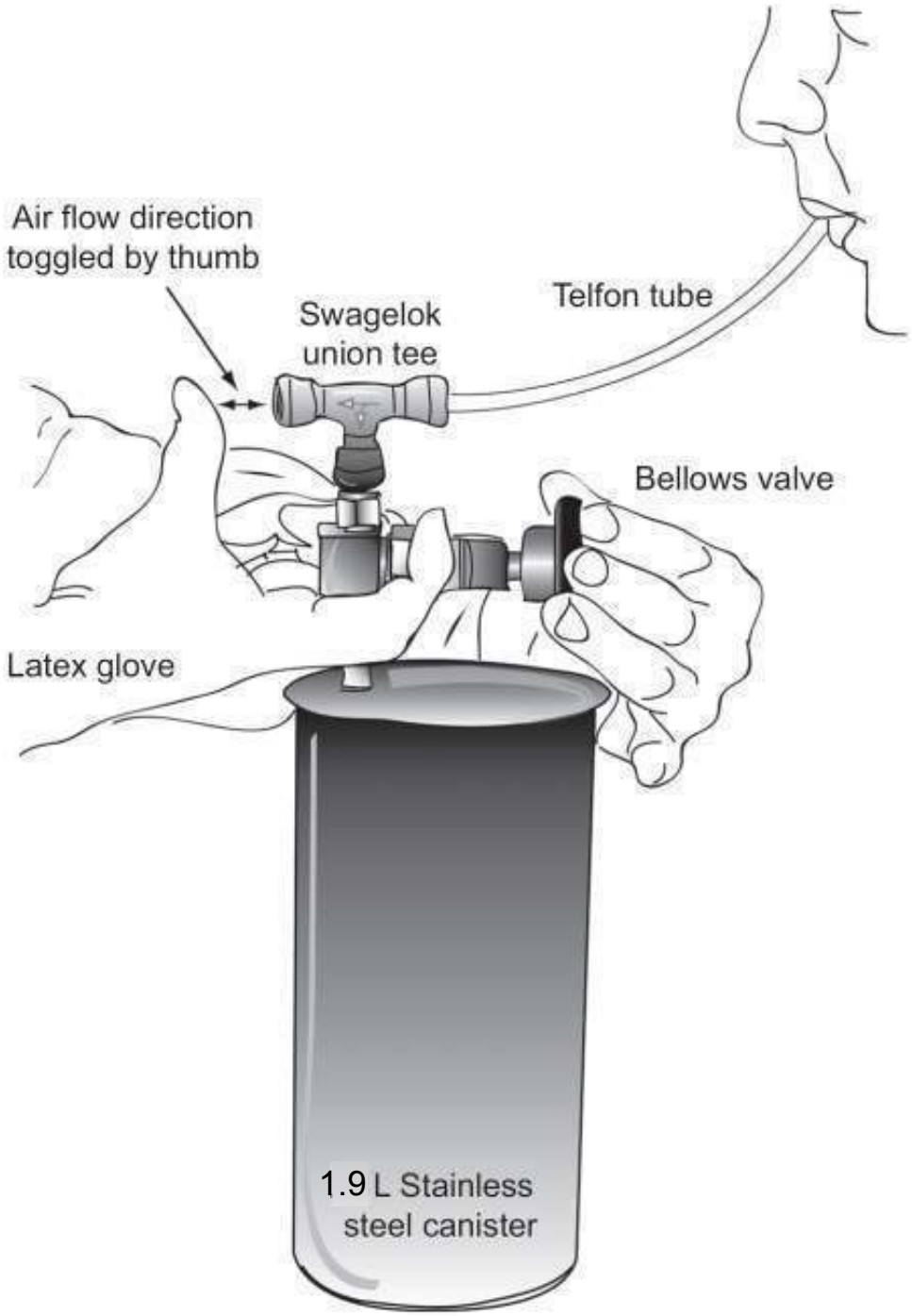

2.3. Purging Glass Vessel

Degassed samples were collected by purging specimen (water or plasma) with UHP helium in a customized purging device. The purging glass vessel in this project was adapted from the pioneering work done in the Rowland-Blake Group (Kamboures, 2006; Lee, 2011). The glass vessel had two parts: a cap and a bottom as seen in Figure 2.2. Three purging vessels used were made by the UC Irvine Glass Shop. A Viton® O-ring was placed in between the cap and the bottom and held together with a Thomas® spherical joint pinch clamp. The cap had two ¼" OD glass tubes. The left glass tube introduced UHP helium into the glass vessel. At the end of that glass tubing was a two-cm glass frit, which created the micro bubbles to purge gases from fluids of interest. On the right side of the glass vessel cap was a short glass tube, which directed purged gases to the canister for collection. The bottom part of the purging vessel had a glass tube that was sealed by a PhenoRed^{TM}-400 $^{3}/_{8}$" diameter septum (Phenomenex, Torrance, CA) and a polypropylene open-top cap (Fisher Scientific, Houston, TX), where the fluid sample was injected by syringe (with the cap removed). The capacities of the three glass vessels used were 203.0 ± 0.4, 208.0 ± 1.0, and 203.0 ± 1.0 ml at room temperature respectively.

Figure 2.2: Purging Glass Vessel.

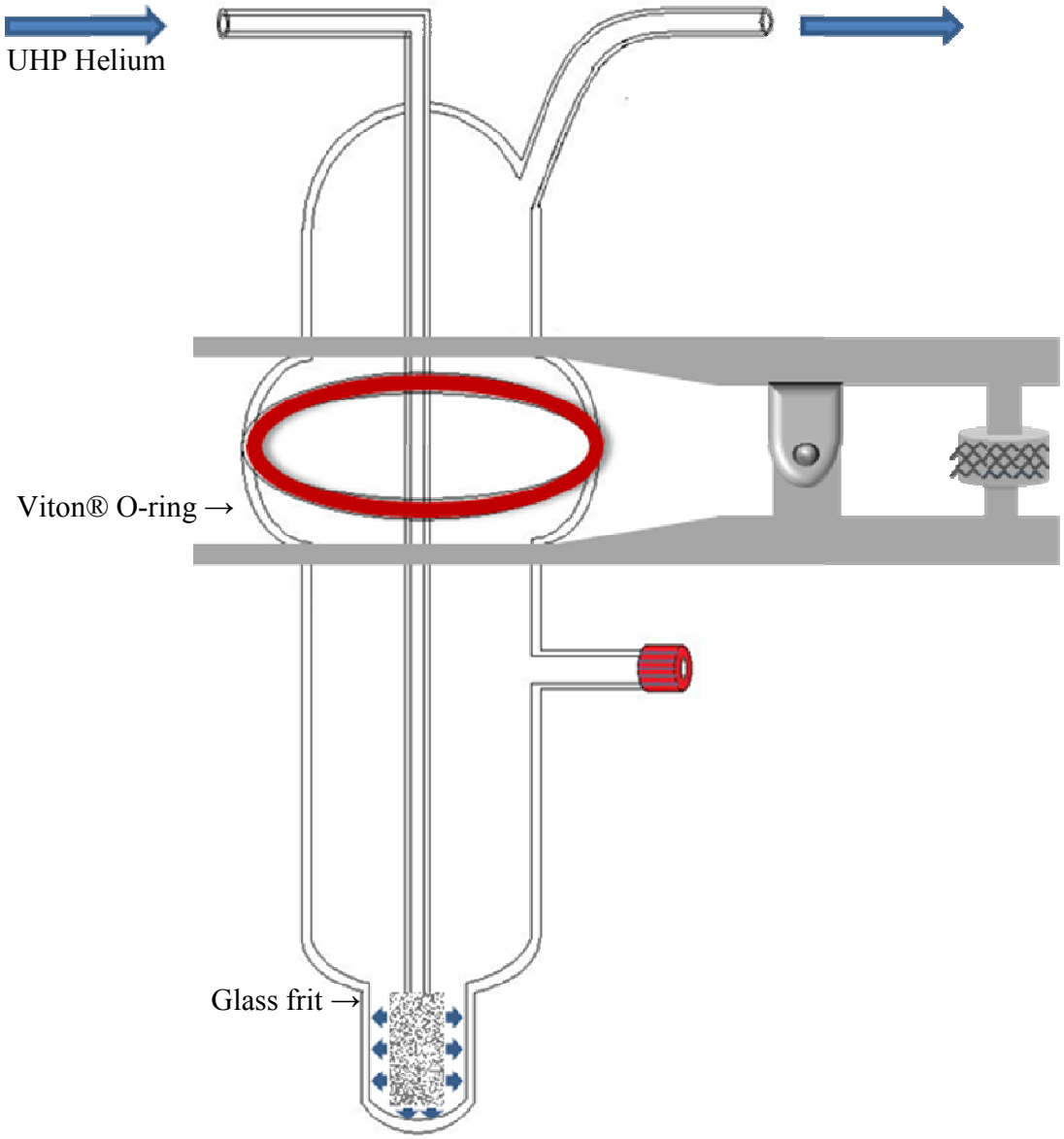

2.4. Purging Manifold

The purging manifold was adapted from Novak's design (Lee, 2011; Novak, 2007). The purging manifold had an Edwards ACT-E thermocouple gauge, a 1000 torr Baratron® capacitance manometer, two Brooks 5850 mass flow controllers (MFC) (Brooks, Hatfield, PA), and an Edwards E2M-12 pump. The pump was connected to a three-foot long U tube, which was immersed in a liquid nitrogen filled dewar to negate back diffusion of pump oil from the pump to the vacuum line. Ultra high purity helium was passed though a 5A molecular sieve trap also contained in the liquid nitrogen filled dewar. Before each purging experiment, the manifold including the glass vessel and connection line were flushed with UHP helium for ten-minute with both MFCs set at 80 ml/min. This step helped remove and dilute the original gas contents within the purging manifold and glass vessel. When the ten-minute helium flush was completed, the purging glass vessel was pressurized to 760 torr with UHP helium. Then, nine ml of the fluid sample of interest was injected via the septum into the heat-sterilized glass vessel with a new 20 ml Becton Dickinson syringe (BD, Franklin Lakes, NJ). After the injection, UHP helium flow purged VOCs from the fluid sample within the glass vessel. Meanwhile, the evacuated 1.9 L stainless canister was open for degas sample collection. For blood samples, MFCs were set at eight ml/min for 38 minutes resulting in 120 torr of degas sample collection. For water samples, MFCs were set at 80 ml/min for about 24 min and 760 torr of degas sample was collected. The glass vessel was heat-sterilized at 150 °C between each purging experiment.

Figure 2.3: Purging Manifold

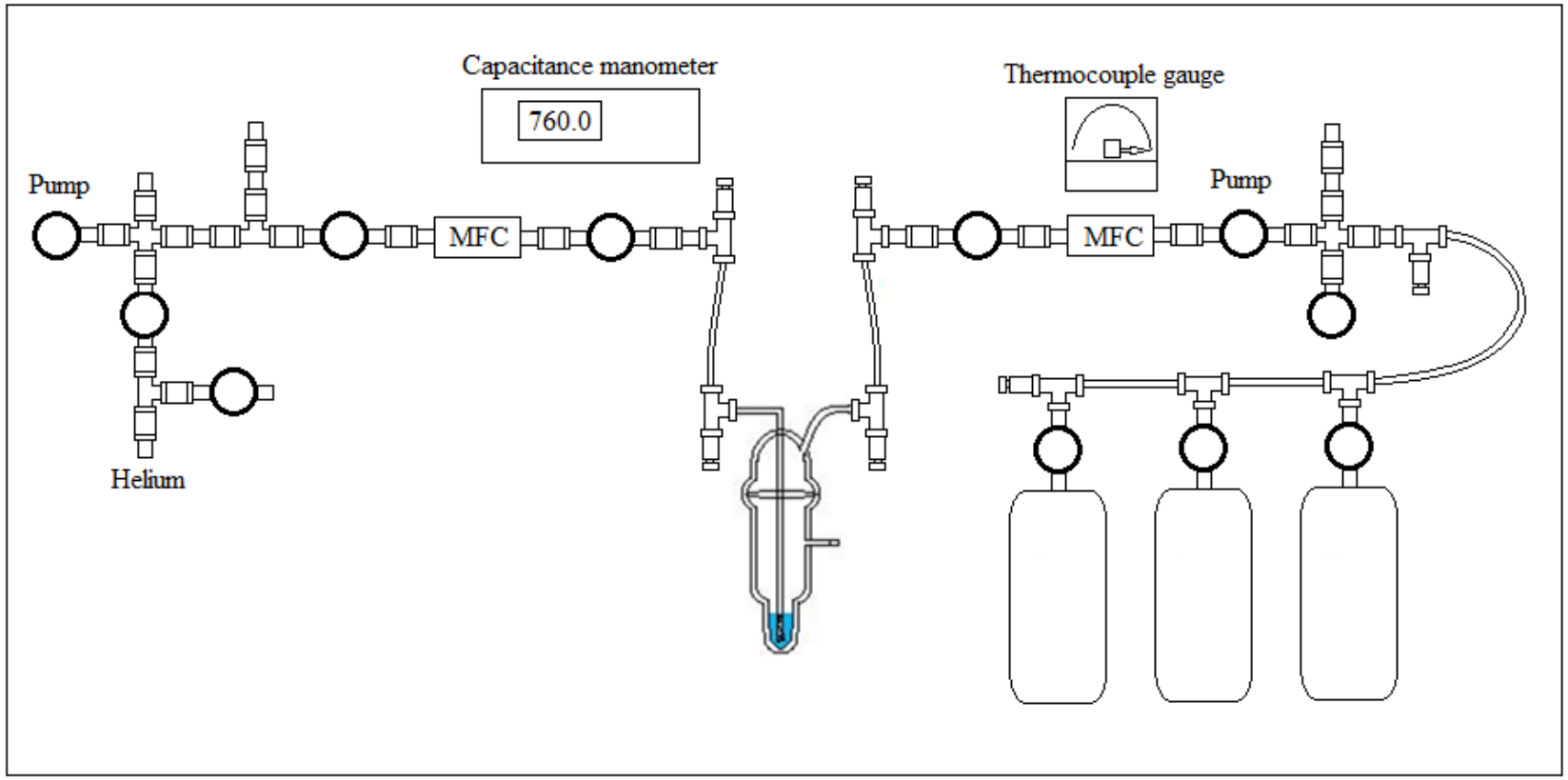

Figure 2.4: Photo of Degas Cart

2.5. Analytical Systems

All gas samples were analyzed for nonmethane hydrocarbons (NMHC) on the analytical systems in the Rowland-Blake Group. Exhaled breath and corresponding room air samples were analyzed for carbon monoxide (CO), carbon dioxide (CO_2), and methane (CH_4) in the Rowland-Blake Group as well.

2.5.1. CO/CO_2 System

The CO/CO_2 system is composed of two HP 5890 GCs (HP, Palo Alto, CA). The CO/CO_2 system manifold is composed of one CO loop (volume = 17 ml), one CO_2 loop (volume = 2.3 ml), a 1500 torr capacitance manometer (Wallace and Tiernan, INC., Belleville, NJ), and an Edwards E2M-12 pump (as shown in Figure 2.5). Helium was used for carrier gas for the CO/CO_2 system. For room samples, the CO loop was loaded with 500 torr (11 ml at S.T.P) and the CO_2 loop was loaded with 500 torr (1.52 ml at STP) of sample respectively. For breath samples, the CO and CO_2 loops were loaded with 500 torr (91 ml at STP) and 20 torr (0.061 ml at STP) of sample, because breath samples had high CO_2 concentration (3-7 %) (Gartner, 2011; Kamboures, 2006). The CO_2 loop was connected to a three-meter column (molecular sieve 5A packed) paired with a thermal conductor detector (TCD). Column and oven parameters are listed in Table 2.1 (Gartner, 2011).

The gas sample contained in the CO loop was injected into a two-meter column (Carbosphere^{TM}, 80/100 mesh packed). The initial part of the eluent was vented to ambient air, because the catalyst, Chromosorb® G coated with 2% nickel, could be oxidized by oxygen and deactivated. After oxygen was vented to the room, CO was sent

to the nickel catalyst, which catalyzed the reduction of CO to CH_4 by H_2 (Equantion 2.1). CH_4 generated in the previous step was analyzed by the flame ionization detector (FID). Analysis of the methane generated from CO was followed by a helium backflush of the column, because a nickel catalyst could also catalyze the reduction of CO_2 by hydrogen. Helium backflush prevented possible interference of CO analysis. Both TCD and FID signals output to Chromeleon® Chromatography Data Analysis Software.

Equation 2.1

$$\mathbf{CO + 3H_2} \xrightarrow{\text{Ni Catalyst, 375 ℃}} \mathbf{CH_4 + H_2O}$$

Figure 2.5: Schematic Diagram of CO/CO_2 System

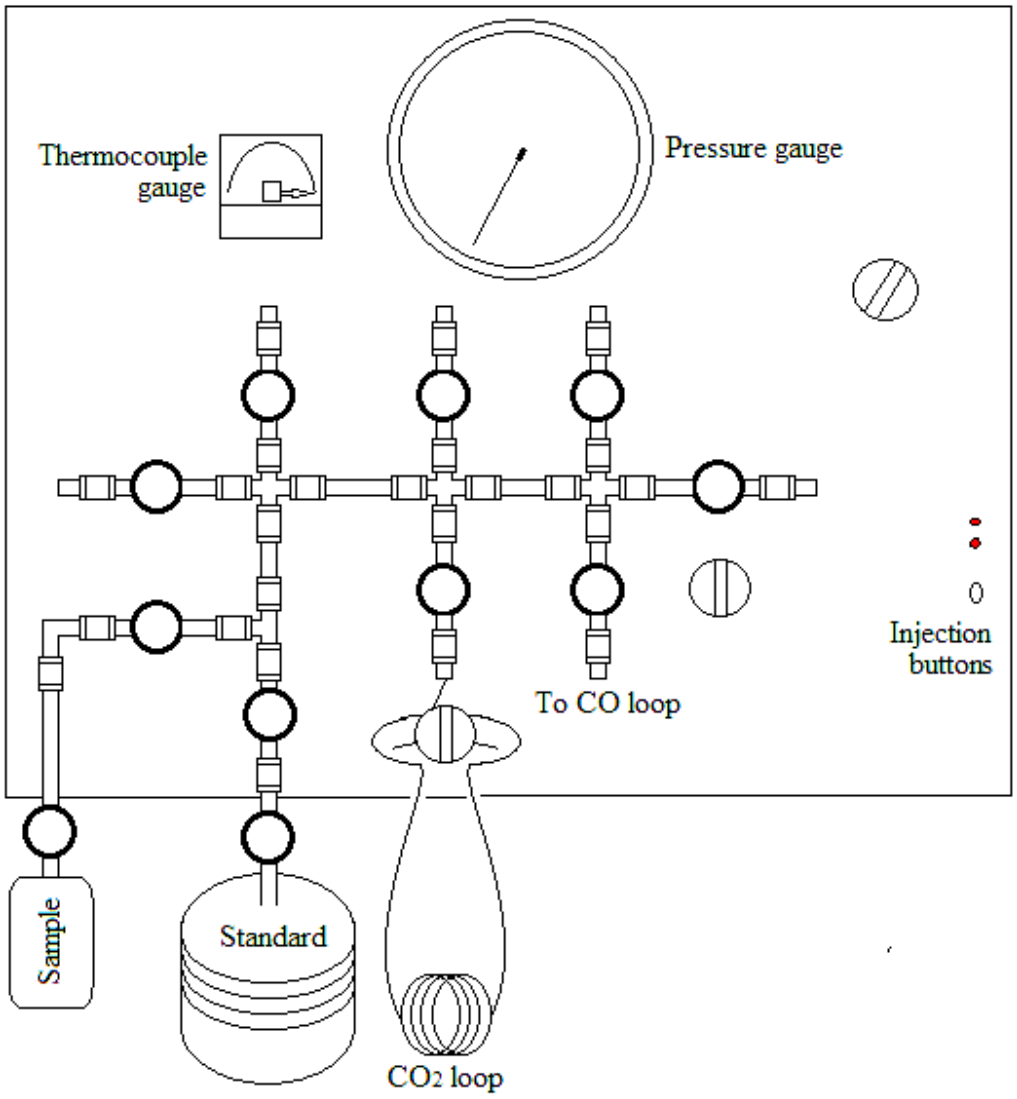

Table 2.1: CO/CO_2 and Methane System Parameters (Barletta et al., 2002; Simpson, Rowland, Meinardi, & Blake, 2006)

	CO	CO_2	CH_4
Column	3 m	2 m	0.9 m
	0.125" OD	0.125" OD	0.125" OD
	80/ 100 mesh 5A molecular sieve	80/100 mesh Carbosphere	80/100 mesh Spherocarb molecular sieve
Carrier Gas	Helium	Helium	Nitrogen
Detector	FID	TCD	FID
	T (°C) = 250	T (°C) = 250	T (°C) = 230
Temperature	T_i (°C) = 60	T_i (°C) = 150	T_i (°C) = 85
Setup	T_f (°C) = 110	T_f (°C) = 220	T_f (°C) = 85
	Run time (mins) = 7.42	Run time (mins) = 8.0	Run time varied
LOD	5 ppbv	10 ppmv	20 ppbv
Precision	4 ppbv	5 ppmv	1 ppbv

2.5.2. CO/CO_2 Mixing Ratio Calculation

Mixing ratios were calculated by comparing the manually integrated peak area from chromatograms of the target gas in the sample with the working standards with known CO and CO_2 concentrations. Working standards were run between every eight gas samples. For room air samples, the working standard contained 192 ppbv CO and 364 ppmv CO_2, calibrated with standards from the National Bureau of Standards (NBS). Working standards prepared for breath samples were 192 ppbv CO and 5 % CO_2 (calibrated with a standard from the NBS). The average peak areas of CO in the working standard were divided by the CO concentration in the working standard, which was defined as the response factor for CO (RF_{CO}). The mixing ratio of CO in the sample was derived by dividing the integrated area of CO peak by RF_{CO} (as shown in Equation 2.2 and 2.3). Concentrations of CO_2 in gas samples were derived in the same manner.

Equation 2.2

$$RF_{CO} = \frac{Average\ Area_{CO\ in\ working\ standard}}{Concentration_{CO\ in\ working\ standard}}$$

Equation 2.3

$$Mixing\ ratio_{CO} = \frac{Area_{CO\ in\ gas\ sample}}{RF_{CO}}$$

An actual example of CO mixing ratio calculation

$RF_{CO} = 42622 \pm 1199 / 192 = 220 \pm 6\ ppbv^{-1}$

CO mixing ratio in a room sample = 82005 / 221 = 370 ± 10 ppbv

2.5.3. Methane System

The methane (CH_4) system is composed of one HP 5890 GC, an Edwards pump (Edwards, Wilmington, MA), a Wallace and Tiernan 1500 torr capacitance manometer, and a loop. To analyze CH_4 concentration, 400 torr (2.6 ml at STP) of gas sample was loaded to the loop (volume = 5 ml) (Figure 2.6). After injection, the sample was carried by nitrogen to the GC system, consisting of a 0.9 m 80/100 mesh Spherocarb^{TM} packed column, and output to an FID. The FID signal was recorded and integrated by a Spectra-Physics® 4400 integrator (Santa Clara, CA) (Blake, 1984). Working standard (1.77 ppmv, calibrated with standard from NBS) was analyzed between every eight samples. The average methane peak area from methane standard was divided by the methane concentration to determine RF_{CH4}. The methane mixing ratios in gas samples were calculated by dividing the methane integrated area of each sample with RF_{CH4}. Detailed GC parameters are listed in Table 2.1.

Figure 2.6: Schematic Diagram of Methane System

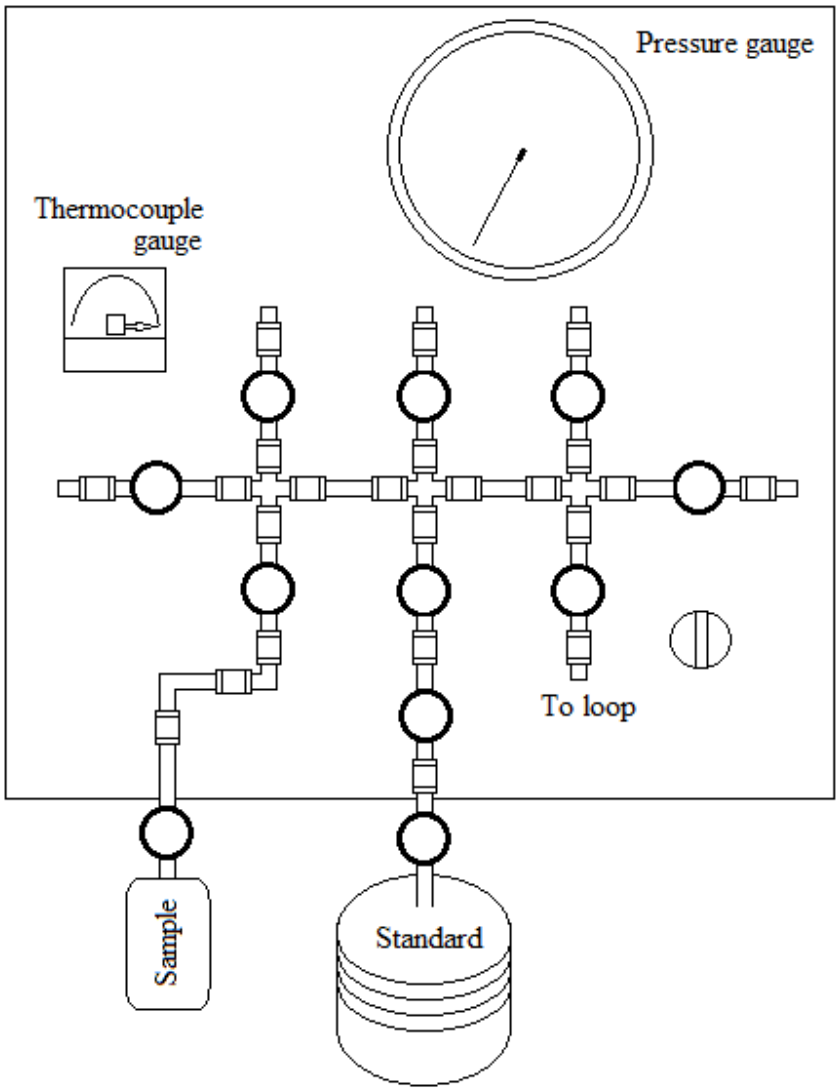

2.5.4. Nonmethane Hydrocarbons System

The nonmethane hydrocarbons (NMHC) analytical system in the Rowland-Blake Laboratory consisted of two Edwards E2M-12 pumps, one capacitance monometer (Arocel pressure sensor 622AB), one Edwards TC-1 thermocouple gauge, one six-port switching valve, one splitter box, and three HP 6890 gas chromatographs (GCs) (HP, Palo Alto, CA). The three GCs were abbreviated as GC-1, GC-2, and GC-3. Fabrication and validation of the analytical capability of the system were previously discussed by Sive (1998a) and Colman et. al. (2001).

GC-1 had two column-detector combinations: the DB-5 column coupled with a Restek 1701 column paired with an ECD, and the DB-5ms coupled with a mass selective detector (MSD). The DB-5 column consisted of 5 % phenyl-methylpolysiloxane and 95 % dimethylpolysiloxane. The DB-5 column with the ECD detected C_1-C_2 halocarbons, C_1-C_5 alkyl nitrates (Figure 2.7). DB-5ms had the same composition as a DB-5 column, but had an improved signal-to-noise level. The MSD had two detection modes: scan mode and selected ion monitoring (SIM) mode. When in scan mode, the MSD can detect a range of ion masses. If any ion mass was found important, the MSD ion mass database can provide suggestions of proper candidates. To determine which correct candidate species was the one, dilution of pure gas of the candidate was analyzed. Retention time of the candidate on each column can be used to verify results. In SIM mode, the MSD was set to determine known compounds. Therefore, the MSD was useful for the detection of known and ambiguous compounds.

Figure 2.7: Chromatogram of DB-5/ECD

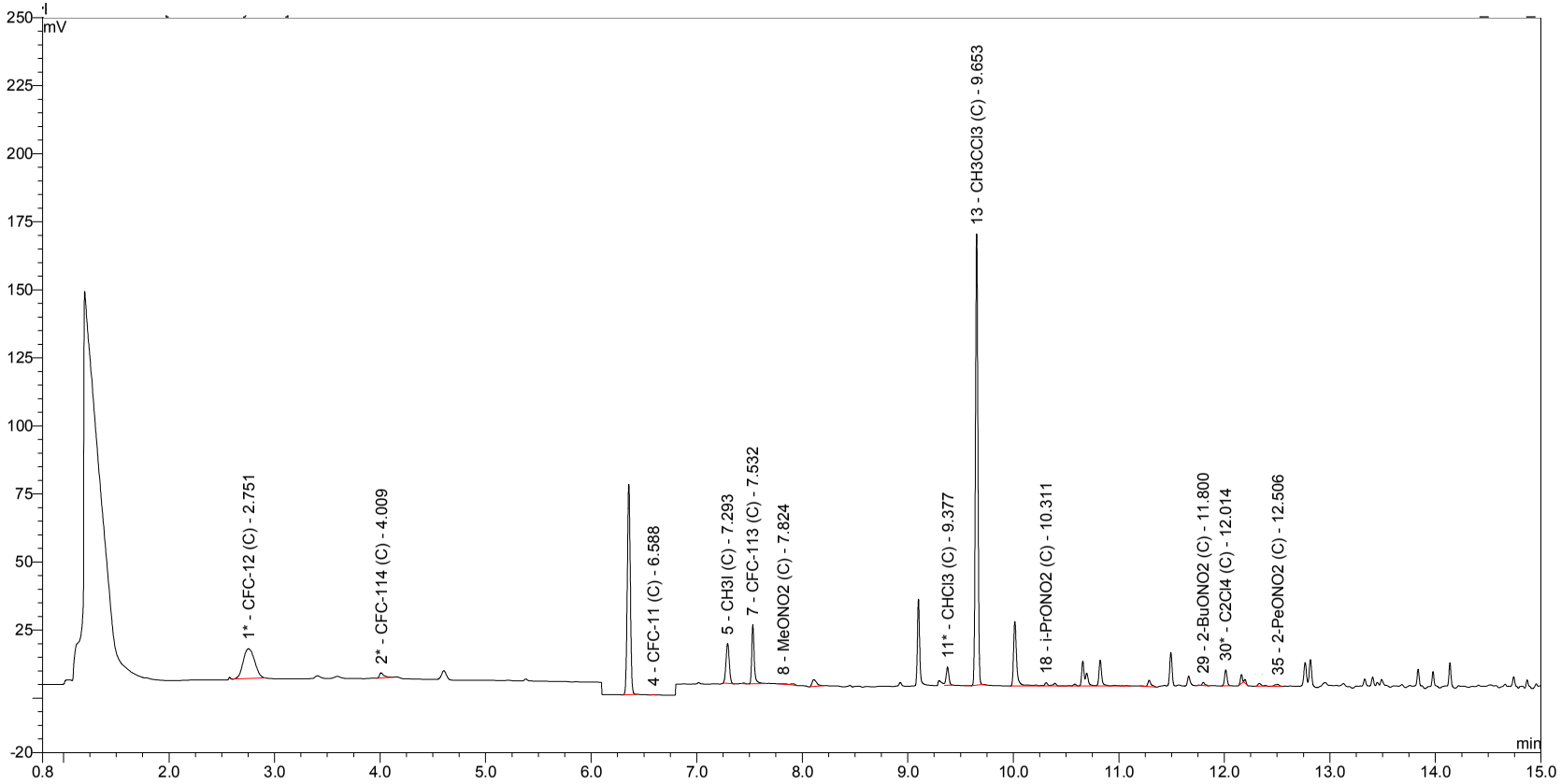

Table 2.2: Some of the Compounds Measured in the Rowland-Blake Group by DB-5/ECD

Compound name (Chemical formula)		
CFC-11 ($CFCl_3$)	Trichloromethane ($CHCl_3$)	Tetrachloroethene (C_2Cl_4)
CFC-12 (CF_2Cl_2)	Bromodichloromethane (CH_2BrCl)	Methyl nitrate (CH_3ONO_2)
Methyl bromide (CH_3Br)	Dibromochloromethane ($CHBr_2Cl$)	Ethyl nitrate ($C_2H_5ONO_2$)
Methyl chloride (CH_3Cl)	Carbon tetrachloride (CCl_4)	*i*-Propyl nitrate ($C_3H_7ONO_2$)
Methyl iodide (CH_3I)	Trichloroethene (C_2HCl_3)	2-Butyl nitrate ($C_4H_9ONO_2$)

Table 2.3: Some of the Compounds Measured in the Rowland-Blake Group by DB-5ms/MS

Compound name (Chemical formula)		
t-2-Butene (C_2H_4)	CFC-12 (CCl_2F_2)	Acetone (C_2H_6O)
c-2-Butene (C_2H_4)	Bromomethane (CH_3Br)	Butanone (C_4H_8O)
i-Pentane (C_5H_{12})	Chloromethane (CH_3Cl)	2-Pentanone ($C_5H_{10}O$)
Isoprene (C_5H_8)	Iodomethane (CH_3I)	3-Pentanone ($C_5H_{10}O$)
Benzene (C_6H_6)	Dibromomethane (CH_2Br_2)	Methyl nitrate (CH_3ONO_2)
Toluene (C_7H_8)	Dichloromehtane (CH_2Cl_2)	Ethyl nitrate ($C_2H_5ONO_2$)
o-Xylene (C_8H_{10})	Tribromomethane ($CHBr_3$)	*i*-Propyl nitrate ($C_3H_7ONO_2$)
m/p-Xylene (C_8H_{10})	Trichloromethane ($CHCl_3$)	*n*-Propyl nitrate ($C_3H_7ONO_2$)
α-Pinene ($C_{10}H_{16}$)	Tetrachloromethane (CCl_4)	2-Butyl nitrate ($C_4H_9ONO_2$)
β-Pinene ($C_{10}H_{16}$)	Tetreachloroethene (C_2Cl_4)	Acetaldehyde (C_2H_4O)
1,2,4-trimethylbenzene (C_9H_{12})	Trichloroethene (C_2HCl_3)	Butanal (C_4H_8O)
1,3,5-trimethylbenzene (C_9H_{12})	Chloroethene (CH_2CHCl)	Benzealdehyde (C_7H_6O)
2-Ethyltoluene (C_9H_{12})	Trichloroethane (CH_3CCl_3)	Methacrolein (C_4H_6O)
3-Ethyltoluene (C_9H_{12})	Methanol (CH_3OH)	Methyl vinyl ketone (C_4H_6O)
4-Ethyltoluene (C_9H_{12})	Ethanol (C_2H_5OH)	Carbon disulfide (CS_2)
CFC-11 (CCl_3F)	*i*-propanol (C_3H_7OH)	Dimethyl disulfide ($CH_3S_2CH_3$)

GC-2 had a DB-1 column made of 100% dimethylpolysiloxane (J&W Scientific, Folsom, CA). The DB-1 column was paired with a flame ionization detector (FID), which detected C_3-C_{10} hydrocarbons, some oxygenates (methanol, ethanol, acetone, 2-butanone, etc), and some sulfides (dimethyl sulfide and dimethyl disulfide) (as shown in Figure 2.8). The DB-1 pared with the FID also had the advantage of good linear response versus carbon number (Colman et al., 2001).

GC-3 had two column-detector combinations. The first combination was a Restek®-1701 column, which was composed of 14 % cyanopropyl-methylpolysiloxane and 86 % dimethylpolysiloxane (Restek Corporation, Bellefonte, PA), and was paired with an ECD and detected halocarbons and alkyl nitrates (Figure 2.9). The second column-detector combination was a GS-Alumina Porous Layer Open Tubular (PLOT) column coupled with a DB-1 column. The PLOT/DB-1 column output to a FID demonstrated good separation power of C_2-C_6 hydrocarbons (Figure 2.10).

Figure 2.8: DB-1/FID Chromatogram (a) 3.5 to 12 min (b) 12 to 17.5 min

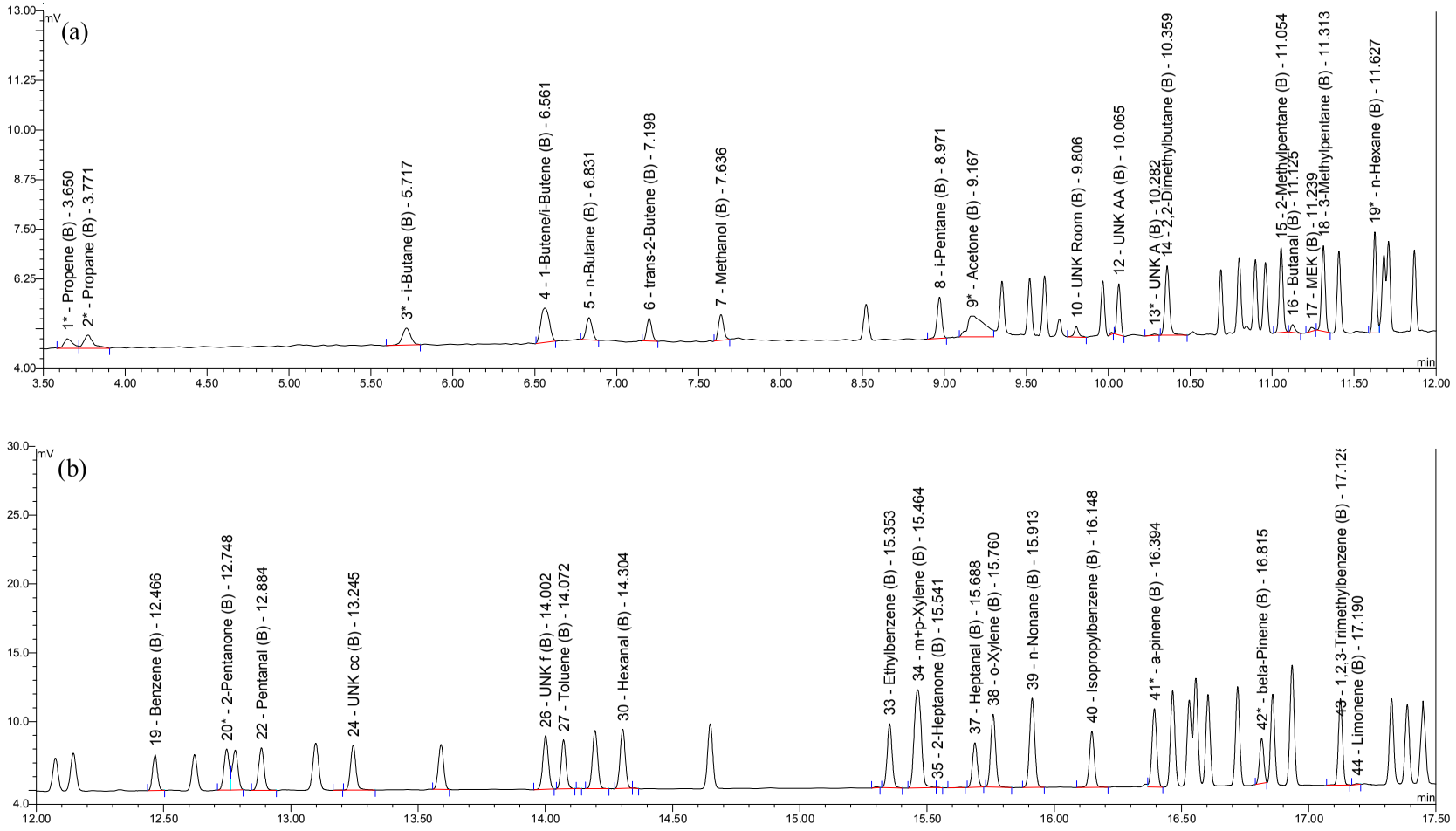

Table 2.4: Some of the Compounds Measured in the Rowland-Blake Group by DB-1/FID.

Compound name (Chemical formula)		
Ethane (C_2H_6)	Isoprene (C_5H_8)	1,2,4-Trimethylbenzene (C_9H_{12})
Propane (C_3H_8)	2-Methylpentane (C_6H_{14})	1,3,5-Trimethylbenzene (C_9H_{12})
Propene (C_3H_6)	3-Methylpentane (C_6H_{14})	α-Pinene ($C_{10}H_{16}$)
n-Butane (C_4H_{10})	Benzene (C_6H_6)	β-Pinene ($C_{10}H_{16}$)
i-Butane (C_4H_{10})	Toluene (C_7H_8)	Methanol (CH_3OH)
cis-2-Butene (C_4H_8)	*m/p* -Xylene (C_8H_{10})	Ethanol (C_2H_5OH)
1/*i*-Butene (C_4H_8)	*o*-Xylene (C_8H_{10})	Acetone (C_3H_6O)
trans-2-Butene (C_4H_8)	Ethylbenzene (C_8H_{10})	Butanone (C_4H_8O)
1,3-Butadiene (C_4H_6)	*m*-Ethyltoluene (C_9H_{12})	Acetaldehyde (CH_3CHO)
n-Pentane (C_5H_{12})	*o*-Ethyltoluene (C_9H_{12})	Dimethyl sulfide (CH_3SCH_3)
i-Pentane (C_5H_{12})	*p*-Ethyltoluene (C_9H_{12})	Dimethyl trisulfide (CH_3SSSCH_3)

Figure 2.9: Restek® 1701/ECD Chromatogram

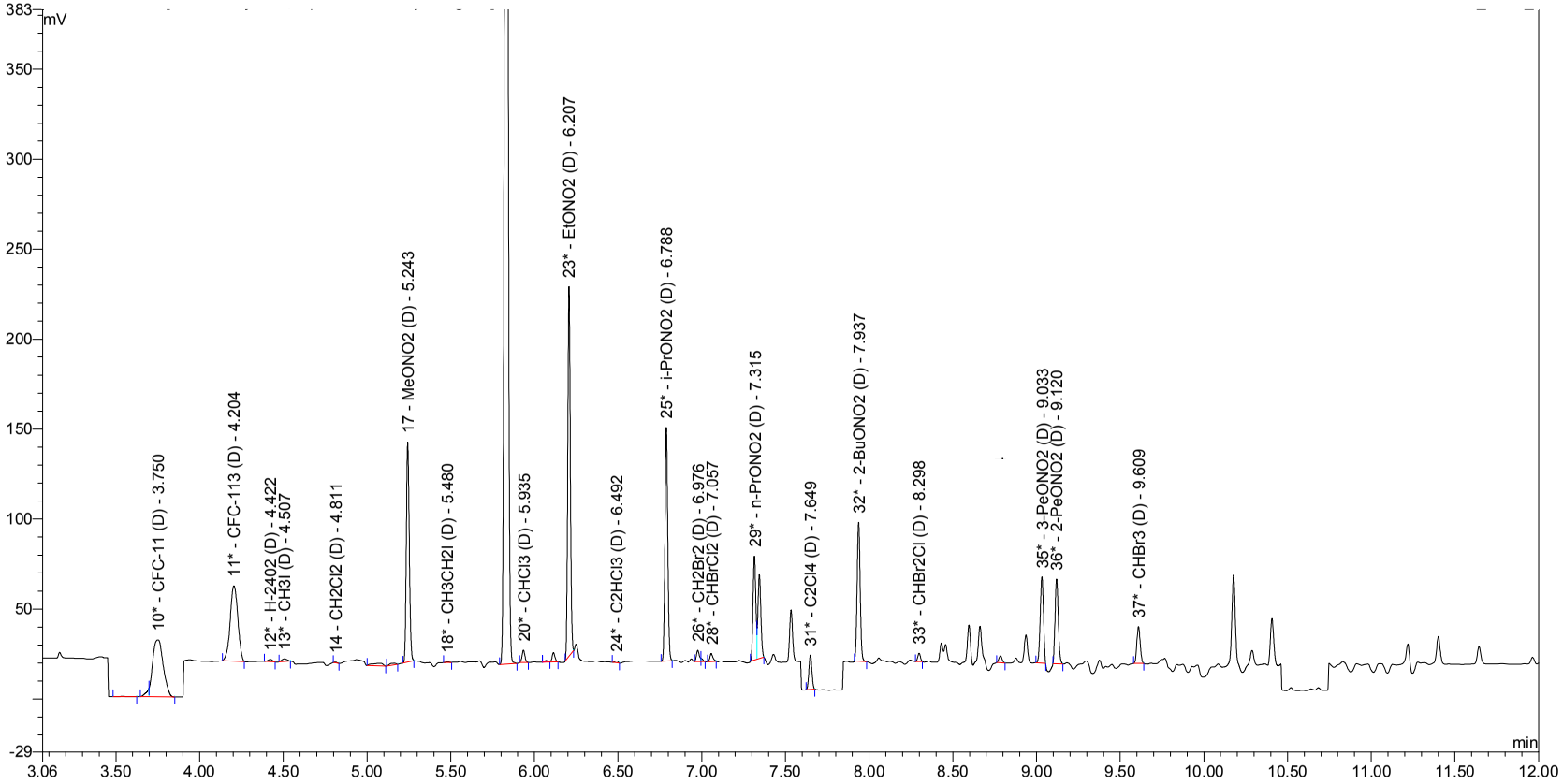

Table 2.5: Some of the Compounds Routinely Measured in the Rowland-Blake Group by Restek® 1701/ECD.

Compound name (Chemical formula)		
CFC-11 ($CFCl_3$)	Trichloromethane ($CHCl_3$)	Tetrachloroethene (C_2Cl_4)
CFC-113 (CF_2Cl_2)	Bromodichloromethane (CH_2BrCl)	Methyl nitrate (CH_3ONO_2)
Methyl bromide (CH_3Br)	Dibromochloromethane ($CHBr_2Cl$)	Ethyl nitrate ($C_2H_5ONO_2$)
Methyl chloride (CH_3Cl)	Carbon tetrachloride (CCl_4)	*i*-Propyl nitrate ($C_3H_7ONO_2$)
Methyl iodide (CH_3I)	Trichloroethene (C_2HCl_3)	*n*-Propyl nitrate ($C_3H_7ONO_2$)

Figure 2.10: PLOT/DB-1/FID

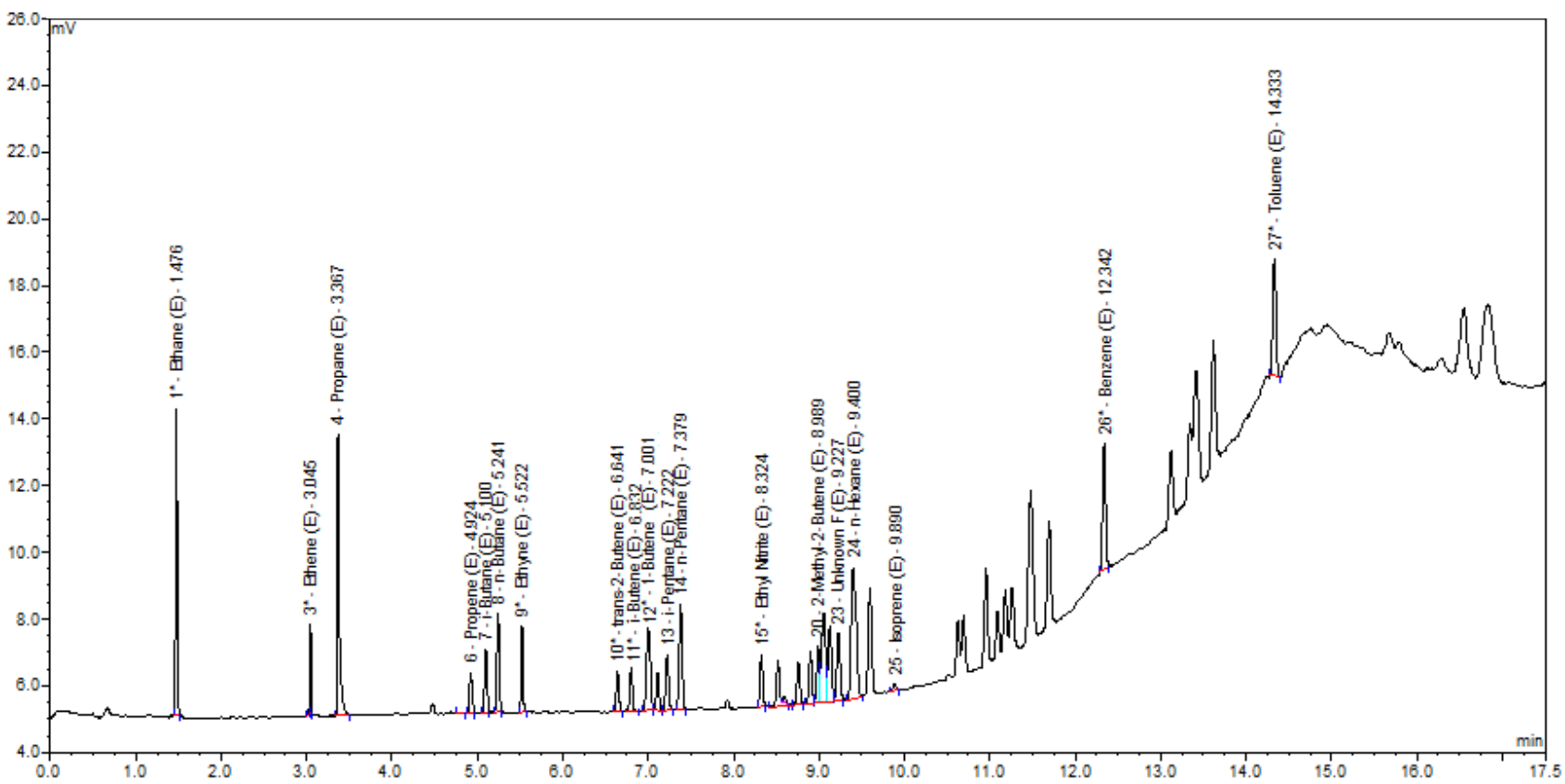

Table 2.6: Some of the Compounds Routinely Measured in the Rowland-Blake Group by PLOT/DB-1/FID

Compound name (Chemical formula)	
Ethane (C_2H_6)	1-Butene (C_4H_8)
Ethene (C_2H_4)	*i*-Butene (C_4H_8)
Ethyne (C_2H_2)	*n*-Pentane (C_5H_{12})
Propane (C_3H_8)	*i*-Pentane (C_5H_{12})
Propene (C_3H_6)	Isoprene (C_5H_8)
n-Butane (C_4H_{10})	*n*-Hexnae (C_6H_{14})
i-Butane (C_4H_{10})	Benzene (C_6H_6)
trans-2-Butene (C_4H_8)	Toluene (C_7H_8)

The VOCs analysis was completed by all the five columns simultaneously. In many cases, the same compounds could be detected by more than one detector, which helped improve the measurement precision. Sometimes co-elution of two gases was observed on one column, but a separation of the same gases was successful on another column.

For the analysis of VOCs, 100 torr of each gas sample (exhaled breath, ambient room, and helium-purged sample of plasma) was cryogenically trapped in the preconcentration loop (filled with glass beads, volume = 5 ml) before injection, which equaled to 229 ml at standard temperature and pressure (STP). Water purging samples were very clean. Therefore, 500 torrs (1145 ml at STP) were trapped from each of them. The preconcentration loop was cooled by liquid nitrogen (77K). The desired amount of sample cryogenically trapped in the loop was pumped for one minute after trapping ended to remove volatile gases like oxygen, nitrogen, and argon while less volatile compounds remained condensed. The six-port switching valve was turned to "bypass," where the trapped VOCs were isolated. Before the gas sample was injected into three GCs, the loop was immersed in 80 ˚C water to re-volatilize VOCs. Before each injection, GC-1 and GC-2 were cryogenic cooled to -60 °C and GC-3 were cooled to -20 °C. The switching valve was turned to "inject" 20 seconds after the three GCs were cooled to programmed initial temperatures. A stream of helium gas then carried the injected gas samples into a slitter box, which split the eluent into five streams. Each stream entered an individual column/detector combination. Oven temperatures were programmed to increase to desired temperature for the separation. Table 2.2 details columns and temperatures of the NMHC system.

Figure 2.11 Schematic Diagram of the NMHC System in Rowland-Blake Group

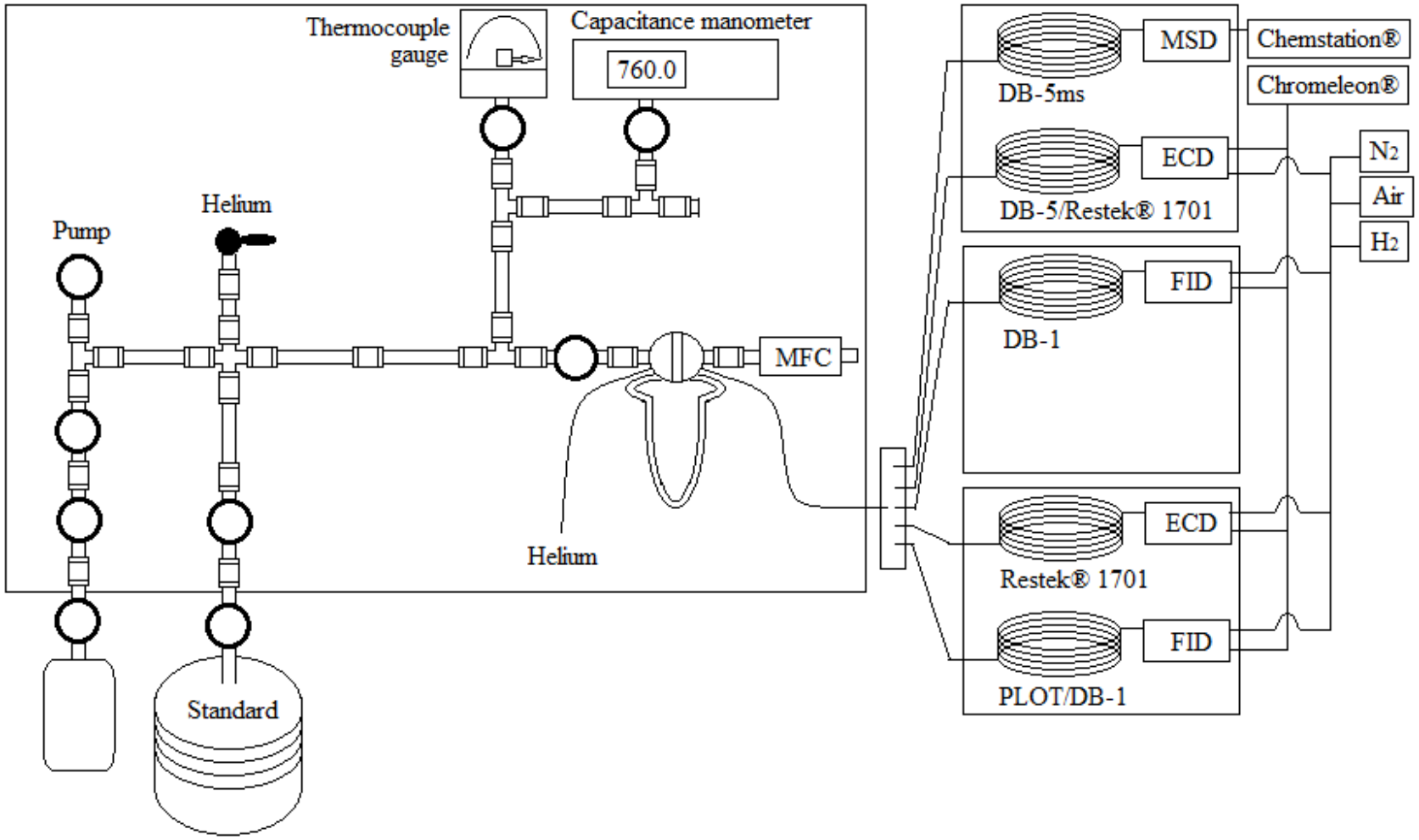

Table 2.7 Column and Oven Details of the NMHC Analytical System in the Rowland-Blake Group

	GC-1		GC-2	GC-3	
Column	DB-5/Restek 1701	DB-5ms	DB-1	Restek 1701	PLOT/DB-1
Detector	ECD	MSD	FID	ECD	FID
Analytical Specialty	C_1-C_2 halocarbons, C_1-C_5 alkylnitrates	Known and unknown compounds	C_3-C_{10} hyrocarbons, some oxygenates (methanol, ethanol, isopropanol, acetone, 2-butanone), DMDS	C_1-C_2 halocarbons, C_1-C_5 alkylnitrates	C_2-C_6 hydrobons
Temperature Programs					
T_i (°C)	-60		-60	-20	
Time at T_i (min)	1.5		1.5	1.5	
Ramp rate to T_1 (°C/min)	15		10	30	
T_1 (°C)	110		0	60	
Time at T_1 (min)	0		0	0	
Ramp rate to T_2 (°C/min)			17		
T_2 (°C)			145		
Time at T_2 (min)			0		
Ramp rate to T_f (°C/min)	29		65	14	
T_f (°C)	220		200	220	
Time at T_f (min)	0.95		0.7	3.8	
Run time (min)	17.5		18	17.5	

Table 2.8 Column and Oven Details of the NMHC Analytical System in the Rowland-Blake Group Continued.

	Column: Length (m)	Inner Diameter (mm)
GC-1	DB-5 column: 30 Restek-1701 column: 5	0.25 0.25
GC-1	DB-5ms column: 60	0.25
GC-2	DB-1 column: 60	0.32
GC-3	Restek-1701 column: 60	0.25
GC-3	GS-Alumina PLOT column: 30 DB-1 column: 5	0.53 0.53

2.6 Quantification of VOCs Measured on the NMHC System

Each ECD and FID signal of the NMHC system was output to Chromeleon® (Dionex, Sunnyvale, CA). The resulting chromatograms were manually integrated for peak area of each gas. The MSD signal was output to Chemstation® (Hewlett-Packard, Sunnyvale, CA) and manually integrated for peak area for each compound. Commercially available cylinders of known mixing ratio hydrocarbons (Scott-Marrin, San Bernardino, CA) and alkyl nitrates cylinder prepared by Atlas Group (Elliot Atlas, University of Miami) were used to make working standards.

The working standard container, called a pontoon, was evacuated to 10^{-2} torr and doped with 20 torr of water, which prevent the loss of hydrocarbons on the container wall according to previous study (Sive, 1998a). Then, the desired amount of gases was carefully transferred from cylinders with hydrocarbons or alkyl nitrates to the pontoon. California White Mountain Research Station (CWMRS) air was transferred to the pontoon to a final pressure around 300 psi. Mixing ratios for compounds in pontoons were calculated according to Equation 2.4.

Equation 2.4:

$$P_1V_1 = P_2V_2$$

Working standards with a range of mixing ratios were prepared and compared with a diluted hydrocarbon standards to confirm mixing ratios. The diluted hydrocarbon standard was made by transferring a desired amount from a Scott hydrocarbon cylinder to a 20 torr water-doped 2 L canister and diluted with UHP helium to desired mixing ratios. Alkyl nitrate mixing ratios in the working standards were confirmed by the Atlas Group

(Elliot Atlas, University of Miami). Each sample running day, two junk samples (WMRS air) and one standard were run before running samples. A standard was also run between every eight samples to monitor possible instrumental drift. During airborne projects, multiple standards were run between samples. Inter laboratory comparisons have shown great consistency between our results and other groups' results (Colman et al., 2001; Sive, 1998a).

Average peak area of each compound included in standards were divided by their individual concentration, which results in response factors (RF) for each compound (Equation 2.2) For compounds included in standards, integrated peak area of each compound from gas samples was divided with RF to calculate mixing ratio (Equation 2.3).

Those compounds that were not contained in the standards were not able to be quantified, except for those on the DB-1/FID. The linearity between RFs and effective carbon numbers (ECN) for compounds detected on DB-1/FID allowed the quantification of compounds that were not included in our standards (Sive, 1998a). For gas y, which represents a gas that is detected on the FID while not included in the standards, RF_y equals ECN_y times $RF_{Propane}$ divided by three (effective carbon number of propane) (Equation 2.5). The mixing ratios of gas y in samples are calculated by dividing area for gas y with RF_y as in Equation 2.6.

Equation 2.5:

$$RF_y = ECN_y \frac{RF_{Propane}}{3}$$

2.7 Water Sample Purging Efficiency The purging efficiency for methyl and *i*-propyl nitrates was determined by continuously purging a nine ml water sample until five 760 torr degassed samples were collected at room temperature (four repetitions). Also, purging efficiency for both nitrates was determined by purging a nine ml water sample until three 760 torr degassed samples were collected at 78 – 82 ℃ were collected (four repetitions). The results (Figures 2.12 – 2.13) showed that the increased temperature had no effect on the recovery of the three alkyl nitrates and therefore all subsequent studies were conducted at room temperature. These data suggest that purging at room temperature was sufficient to obtain quantitative results of the three alkyl nitrates.

Estimation of purging efficiency of methyl nitrate, and *i*-propyl nitrate

= (mixing ratio in the first degassed sample) / (sum of mixing ratio from all three degas samples at 78-82 °C) x100%

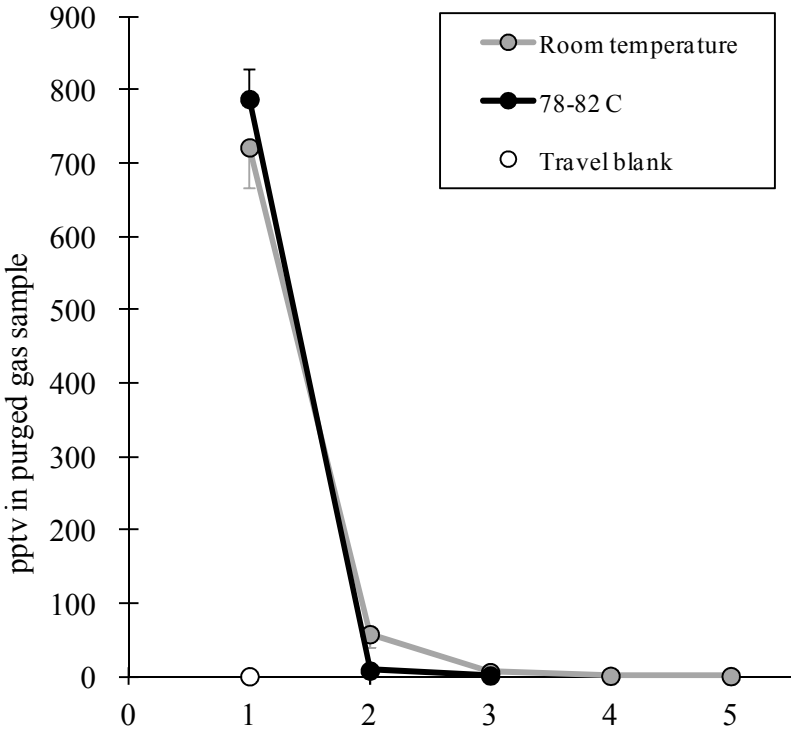

Figure 2.12: Continuous Purge of Water Samples for Methyl Nitrate.

Grey: UVP continuously purged until five 760 torr degassed samples collected at room temperature. Black: UVP continuously purged until three 760 torr degassed samples collected at 78-82 °C. White: travel blank purged once at room temperature. X-axis is the number of helium-purged sample.

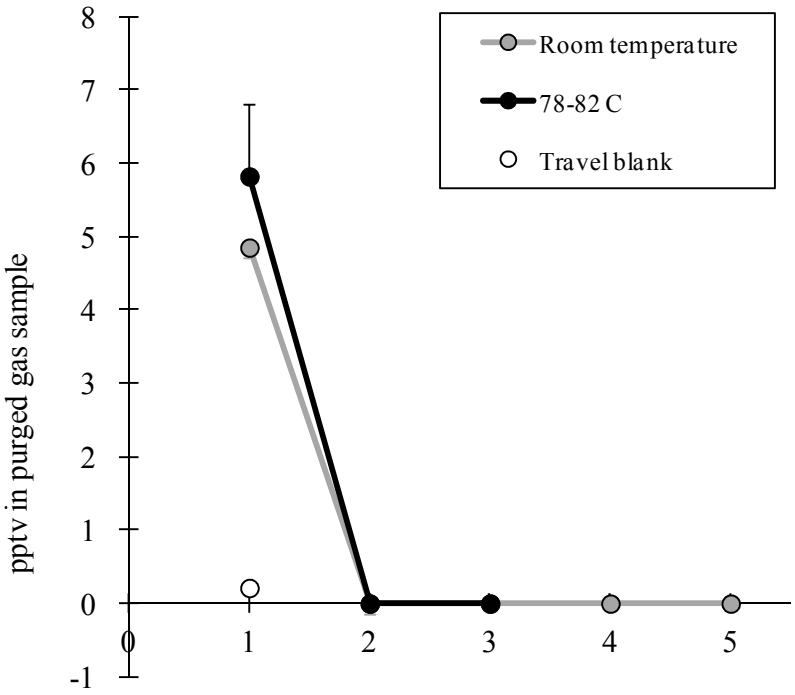

Figure 2.13: Continuous Purge of Water Samples for *i*-Propyl Nitrate.

Grey: UVP continuously purged until five 760 torr degassed samples collected at room temperature. Black: UVP continuously purged until three 760 torr degassed samples collected at 78-82 °C. White: travel blank purged once at room temperature. X-axis is the number of helium-purged sample.

2.8. Plasma Purging Efficiency

Plasma purging efficiency was estimated by purging a nine ml plasma sample continuously and collected in three canisters. The same procedure was repeated three times, with plasma collected from the same subject at the same time. Usually, purging time and the amount collected in our experiment design has a relationship as Figure 2.15.

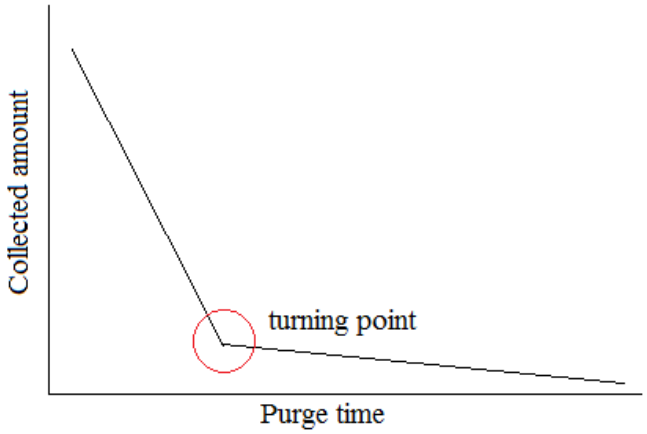

Figure 2.14: Detected Amount versus Purging Time

In the plasma purging efficiency experiments, foaming limited the purging time. Foaming has been a consistent problem when purging plasma. Therefore, the efficiency of plasma purging is estimated by our continuous purging data and an estimation of total amount of each monitored substance. Assuming the total amount is the sum of concentration from the three collected purged samples and the calculated concentration at helium purge time = 60 minute. According to our data, 60 minute is very close to the collection of most of the gas (Figure 2.16).

A total of 120 torr (about 38 min collection time) of the plasma degas sample was collected for each visit of a subject. The plasma purge efficiency estimation is as follows.

Purging efficiency estimation

= normalized accumulated amount at 38 min/ normalized accumulated amount at 60 min.

An example of isoprene of a plasma degas sample (trend: [isoprene] = 0.0271x purge time + 0.6168, accumulated [isoprene] at 38 and 60 min were calculated.)

= 1.64 (ng/l) / 2.10 (ng/l) = 78%.

Because the purging precision was fairly good we are able to use the 38 minute purge and correct thus yielding reliable results.

Figure 2.15: Normalized Purged Amount versus Purge Time

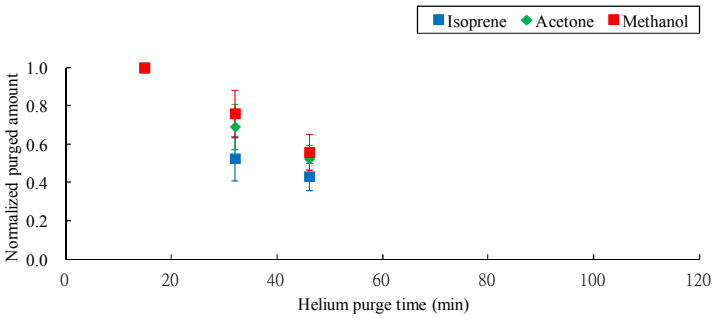

Figure 2.16 Normalized Accumulated Collected Amount versus Time

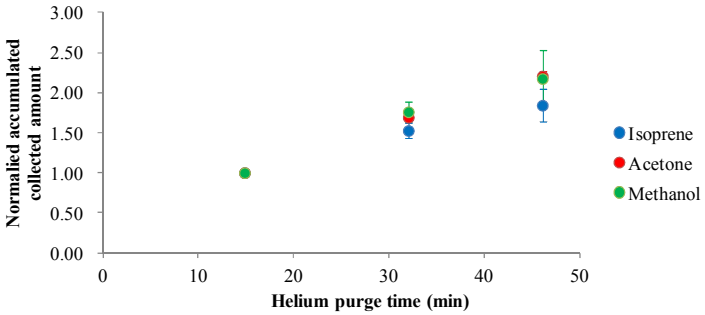

2.9. References:

Barletta, B., Meinardi, S., Simpson, I. J., Khwaja, H. A., Blake, D. R., & Rowland, F. S. (2002). Mixing ratios of volatile organic compounds (VOCs) in the atmosphere of Karachi, Pakistan. *Atmospheric Environment, 36*(21), 3429-3443. doi: http://dx.doi.org/10.1016/S1352-2310(02)00302-3

Blake, D. R. (1984). *Increasing concentrations of atmospheric methane, 1979-1983.* (Ph.D), University of California, Irvine.

Colman, J. J., Swanson, A. L., Meinardi, S., Sive, B. C., Blake, D. R., & Rowland, F. S. (2001). Description of the Analysis of a Wide Range of Volatile Organic Compounds in Whole Air Samples Collected during PEM-Tropics A and B. *Analytical Chemistry, 73*(15), 3723-3731. doi: 10.1021/ac010027g

Gartner, M. D. (2011). *Exhaled Breath Analysis of Emergency Room Patients with Diabetes and Respiratory Diseases.* (Ph.D.), University of California, Irvine, Ann Arbor. (849723656)

Gorham, K. A., Sulbaek Andersen, M. P., Meinardi, S., Delfino, R. J., Staimer, N., Tjoa, T., Blake, D. R. (2009). Ethane and n-pentane in exhaled breath are biomarkers of exposure not effect. *Biomarkers, 14*(1), 17-25. doi: doi:10.1080/13547500902730680

Kamboures, M. A. (2006). *The gas chromatographic analysis of breath as a means to assess pathology and physiology in individuals with cystic fibrosis and other diseases.* (Ph. D.), University of Californai, Irvine.

Lee, H. J. (2011). *Breath analysis on end-stage renal disease patients during hemodialysis treatment [electronic resource] / by Hyun Ji Lee*. Irvine, Calif. University of California, Irvine.

Novak, B. J. (2007). *Non-invasive monitoring of metabolism, diabetes, and oxidative stress using exhaled human breath.* (Ph. D.), University of California, Irvine. (LD 791.9 .C45 2007 N68)

Simpson, I. J., Rowland, F. S., Meinardi, S., & Blake, D. R. (2006). Influence of biomass burning during recent fluctuations in the slow growth of global tropospheric methane. *Geophysical Research Letters, 33*(22), L22808. doi: 10.1029/2006GL027330

Sive, B. C. (1998a). *Atmospheric nonmethane hydrocarbons : analytical methods and estimated hydroxyl radical concentrations.* (Ph.D), University of California, Irvine. (LD 791.9 .C45 1998 S58)

Sive, B. C. (1998b). *Atmospheric nonmethane hydrocarbons : analytical methods and estimated hydroxyl radical concentrations.* (Ph. D., Chemistry), University of California, Irvine. (LD 791.9 .C45 1998 S58)

Chapter 3: Volatile Organics in OCWD Water Samples

3.1. Introduction

Water is one of the most precious natural resources on our planet. Therefore, establishing stable and economically sound sustainable substitutional water sources, such as recycled water, is important in addressing ever-increasing water demand. Reclamation at state of the art water facilities demonstrates the ability to provide quality water economically. According to a recent survey (Newton et al., 2011), reclaimed water in the U.S. is mostly used for irrigation (agriculture, golf courses, landscaping), ground water recharge, and the food production industry. The Orange County Water District (OCWD) has provided recycled water for the seawater intrusion barrier and ground water recharge in Orange County since the mid-1970s. The OCWD recycles secondary wastewater from the Orange County Sanitation District (OCSD), by coupling multiple advanced purification techniques, including microfiltration, reverse osmosis (RO), and UV/H_2O_2 based ultraviolet advanced oxidation process (UVAOP) (Figure 3.1). The secondary wastewater is treated by screens, settling, biological organic compound consumption, and chlorination in the OCSD. Though water treatment facilities aim to provide the public with water that is safe to drink and use, it is found that some disinfection by-products (DBPs) are generated in water treatment processes. There have been extensive studies and applications of recycled water, however, how chemicals are removed or generated within water treatment processes is still not clear (Linge et al., 2013). To study how water dissolved VOCs change through RO and UV/H_2O_2 based UVAOP, water samples collected at various stages of the purification process were collected. These samples were purged with purified ultra high purity helium in our UCI laboratory.

3.1.1. Purification Process at OCWD

The OCWD purifies secondary wastewater from the OCSD with microfiltration, reverse osmosis, and UV/H_2O_2 based UVAOP (Figure 3.1). The first step of the water treatment process at the OCWD is microfiltration with tiny straw-like polypropylene hollow fibers (0.2 micrometer pores) (Siemens CMF-S Microfiltration System).

Figure 3.1 Schematic of the Purification Process and Water Sample Collection at the OCWD for Phase 1 Study

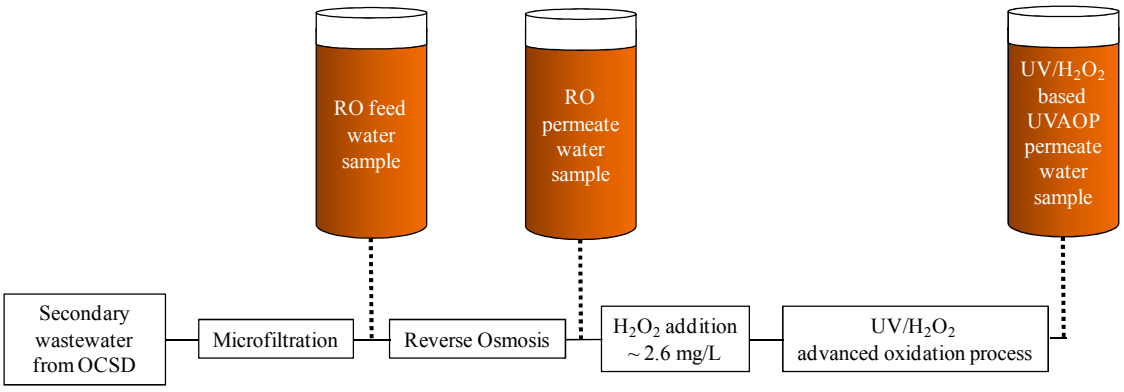

Sodium hypochlorite (NaOCl) is added before microfiltration to prevent accumulation and growth of organisms on microfiltration fibers. Some of the water samples had five mg sodium thiosulfate ($Na_2S_2O_3$) added to each to reduce residual hypochlorite and hypochlorous acid (Equation 3.1-3.4). Later on these samples will be referred to as quenched or with quencher.

Equation 3.1 $$NaOCl + H_2O \rightarrow Na^+ + OH^- + HOCl$$

Equation 3.2 $$HOCl \rightleftharpoons H^+ + OCl^-$$

Equation 3.3 $$Na_2S_2O_3 \rightarrow 2Na^+ + S_4O_6^{2-}$$

Equation 3.4 $$2\,S_2O_3^{2-} + 2OCl^- + H^+ \rightarrow S_4O_6^{2-} + 2Cl^- + OH^-$$

Polypropylene fibers are housed in cylinder cartridges, which contain a total of 237 million polypropylene microfiltration fibers. A pump generated pressure (~10 lb/in^2) was applied to pull the water entering the microfiltration cells, only water passes the microfiltration tube through 2x10^{-7} m holes. Particles with a diameter larger than 2x10^{-7} m are removed. For example, bacteria diameters range from 2x10^{-7} to 2x10^{-5} m (Alcamo, 1995), thus microfiltration can remove most of the bacteria contained in the reclaimed water. The microfiltration is capable of producing 82 million gallons of effluent per day.

Later, the filtered water is transferred into a two million gallon break tank. The effluent is first treated with sulfuric acid (H_2SO_4) and anti-fouling agent to prevent RO membranes from being adhered to or clogged by organisms. Treated water is then filtered again to ensure no physical objects enter the RO system to prevent physical damage of RO membranes. Then, the effluent is sent to the RO process, where water passes through

the thin-film composite polyamide RO membranes (Hydranautics ESPA-2), which are contained in pressure vessels. Each RO membrane sheet is positioned in between a spacer sheet and a water collector sheet. All the layers in the same vessel connect to a pipe (with holes in the sides) and circle around the pipe. Influent enters one end of the RO pressure vessels, where spacer layers create room for influent water to enter the membrane composite. Semi-permeable polyamide RO membranes allow pure water to permeate and reject salts, minerals, organic compounds, viruses, and bacteria when pressure (~ 150 lb/in^2) is applied. The RO effluent enters the collector layer. Effluent is sent to the permeate pipe and drained from the far end. The RO system has 2,250 pressure vessels and each of them holds seven RO membrane composites, which together produce 70 million gallons of RO permeate per day. The rejected water is released to the ocean.

The RO permeate is then sent to the UV/H_2O_2 based UVAOP facility, where hydrogen peroxide (H_2O_2) (~2.6 mg/L) is first added. Secondly, the mixture of RO permeate and H_2O_2 is treated by UV irradiation in reaction chambers. Each UV lamp is inside an independent quartz sleeve, which isolates the lamp from the water being treated. Each vessel has 72 UV lamps (λ_{max} = 254 nm, 257 watt). The UV/H_2O_2 based UVAOP produces 70 million gallons permeate per day.

The UV/H_2O_2 based UVAOP removes solutes by OH radical reactions and photolysis induced reactions. The H_2O_2 cleaves into two hydroxyl radicals (HO·) upon UV irradiation (Equation 3.5) (Legrini, Oliveros, & Braun, 1993).

Equation 3.5 $$H_2O_2 \xrightarrow{hv} 2HO\cdot$$

Reactions generated by hydroxyl radicals include the following.

(1) Hydrogen abstraction: a hydoxyl radical abstracts a hydrogen atom from a hydrocarbon molecule. The reaction produces water and a radical intermediate, which quickly reacts with oxygen in an aerobic environment. (Equations 3.6 and 3.7).

Equation 3.6 $$RH + HO\cdot \rightarrow R\cdot + H_2O$$

Equation 3.7 $$R\cdot + O_2 \rightarrow \cdot RO_2$$

(2) Addition to unsaturated carbon (Equation 3.8).

Equation 3.8 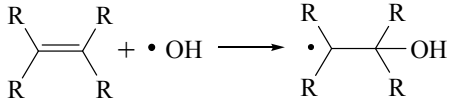

(3) Electron transfer to hydroxyl radicals: as shown in Equation 3.9.

Equation 3.9 $$HO\cdot + RX \rightarrow RX\cdot^{+} + OH^{-}$$

Reactions associated with UV irradiation is photolysis of contaminants can proceed in two pathways: (1) Equation 3.10 – 3.11; (2) Equation 3.12 (Legrini et al., 1993).

Equation 3.10 $$RH \overset{hv}{\rightarrow} RH^{*}$$

Equation 3.11 $$RH^{*} + O_2 \rightarrow RH\cdot^{+} + \cdot O_2^{-}$$

Equation 3.12 $$R - X \overset{hv}{\rightarrow} R\cdot + X\cdot$$

The UV/H_2O_2 based UVAOP serves as an efficient backup for the purification/disinfection process because of its remarkable ability to remove contaminants such as N-nitrosodimethylamine (NDMA), which are difficult to remove

by other disinfection or purification processes. N-nitrosodimethylamine is a nitrogenated DBP, which is removed by the UV/H_2O_2 based UVAOP twice as efficiently as the RO process in the OCWD (Plumlee, López-Mesas, Heidlberger, Ishida, & Reinhard, 2008).

3.1.2. Water Sample Collection

There are two phases of experiments in this study. Phase I studies how dissolved VOCs change through the RO process and the UV/H_2O_2 based UVAOP. Therefore, water samples were collected before and after the RO process (RO feed and RO permeate), and after the UV/H_2O_2 based UVAOP (UVAOP permeate). Once influent water enters the RO process, water remains in the flow line until it leaves the UV/H_2O_2 based UVAOP facility. When water samples were collected from a faucet or a fountain on each site, water samples were exposed to ambient air. To take into consideration the exposure to ambient air, travel blanks were collected. Travel blanks are MilliQ® water collected in advance and transferred to new vials on each site before water sample collection (with or without quencher).

In between the water pipes of the OCWD purification process are faucets/fountains that enable the OCWD staff to collect instant samples for monitoring purposes. Water samples for the Phase I study were collected from the faucets/fountains for RO feed, RO permeate, and UVAOP permeate in 40 ml amber vials with open-top caps (VWR International, LLC, Brisbane, CA) at the OCWD facility (Figure 3.2). On each sampling day, a total of 18 water samples were collected. First, two travel blanks (one with quencher and one without quencher) and four water samples from the RO feed faucet (two with quencher and two without quencher) were collected by filling 40 ml amber vials all the way to the top and sealing them with caps.

Two travel blanks (one with and one without quencher), and four from the RO permeate faucet (two with and two without quencher) were collected. Lastly, two travel blanks (one with quencher and one without quencher) and four water samples from the UVAOP permeate fountain (two with quencher and two without quencher) were collected.

The same experiment (Figure 3.2) was conducted on three different dates (Set 1: 10/14/12, Set 2: 12/19/12, and Set 3: 12/26/12).

Figure 3.2: Sample Types in the Phase I Study

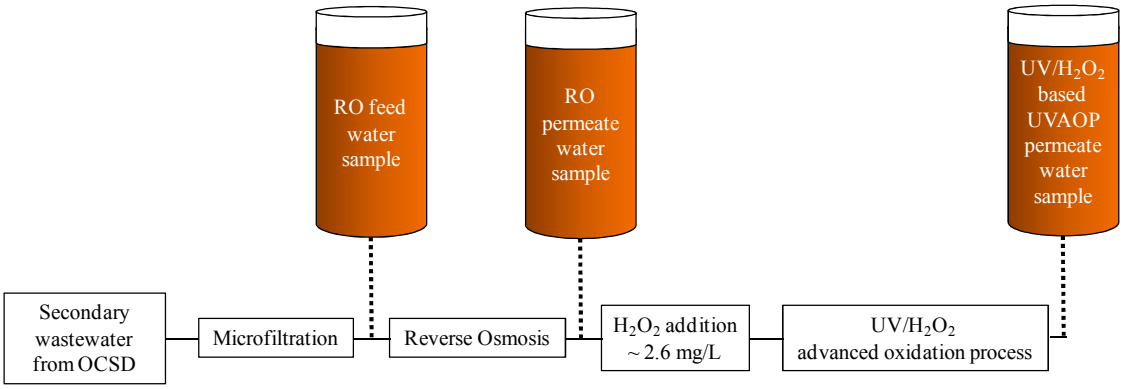

Results from the Phase I study showed that five DBPs monitored are well below suggested levels and two alkyl nitrates of interest (methy- and *i*-propyl nitrate) remained at similar levels before and after reverse osmosis, but a significant increase of these gases was observed after UV/H_2O_2 based UVAOP on one of three experiment dates.

The UV/H_2O_2 based UVAOP is conducted in two steps: (1) addition of hydrogen peroxide and (2) UV ray irradiation. Therefore, three types of water samples, RO permeate, UV/H_2O_2 based UVAOP feedwater, and UV/H_2O_2 based UVAOP permeate, were chosen in the Phase II study to further investigate where the alkyl nitrates increase (Figure 3.3).

Figure 3.3 Sample Types in the Phase II Study

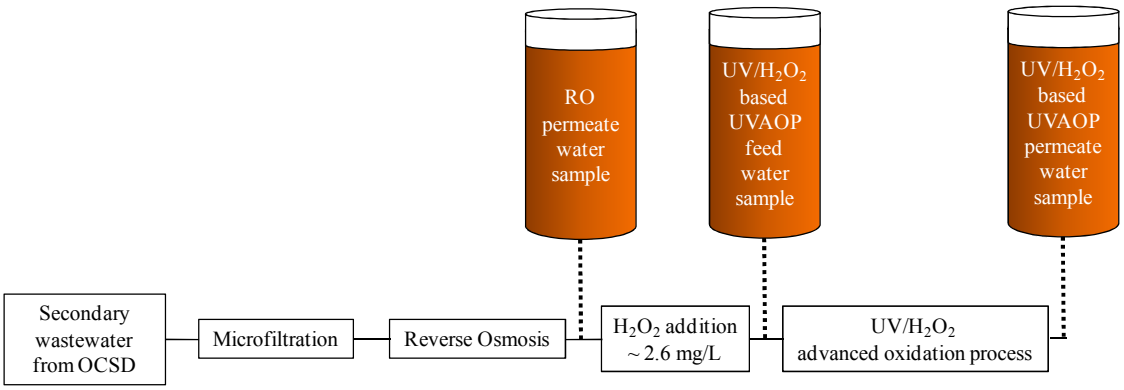

In the Phase II study (04/22/13), a total of 15 water samples were collected. Water sample types include travel blank, RO permeate, UV/H_2O_2 based UVAOP feedwater, and UV/H_2O_2 based UVAOP permeate. First, one travel blank and four water samples from the RO permeate faucet were collected as previously described. Previous results for the two alkyl nitrates of interest had similar trends for water samples with and without quencher. Thus, quencher was not used in the Phase II study. Additionally, one travel blank and four water samples from the UV/H_2O_2 based UVAOP feedwater fountain were collected. Finally, one travel blank and four water samples from UV/H_2O_2 based UVAOP permeate fountain were collected.

3.1.3. Degas Sample Collection

The purging glass vessel was flushed with purified ultra high purity helium (UHP helium) for 10 minutes (flow rate = 80 ml/min) before each sample collection. The glass vessel was then pressurized with UHP helium to 760 torr (collection time ~24 min). Nine ml of water sample was injected into the glass vessel and flushed with UHP helium (80 ml/min) until 760 torr of purged helium was collected in the 1.9L canister.

3.2. Results and Discussion

More than 60 gases were identified from the purged samples, but the most interesting change was observed in the methyl- and *i*-propyl nitrate concentrations between the RO and UVAOP processes. Meanwhile, five known DBPs, including chloromethane (CH_3Cl), tribromomethane ($CHBr_3$), trichloromethane ($CHCl_3$), and bromodichloromethane ($CHBrCl_2$) dibromochloromethane ($CHBr_2Cl$), were observed as well. This chapter focuses on the change of the two alkyl nitrates and the five DBPs. Results from the same type of water samples collected on the same date were averaged. Data are presented as average values ± one standard deviation, except for Figure 3.12 (a)−(c). For example, the average and standard deviation of the two RO feed samples collected on 10/14/12 yields 110±7 ppt CH_3Cl (Table 3.4). Figure 3.12 (a)−(c) show concentrations for each of the samples collected on 04/22/13. Concentrations of water samples are in ppt, which approximately equals to nanogram per liter.

3.2.1. Chloromethane

Results for chloromethane are given in Table 3.1 and Figure 3.4. RO permeate without quencher has the highest amounts of CH_3Cl. RO feed (with and without quencher), UV/H_2O_2 based UVAOP permeate (with and without quencher), and RO permeate with quencher, have similar amounts of CH_3Cl.

The fact that RO permeate with no quencher had increased amounts of chloromethane reflects the residual chlorine reacts with some compounds and produce chloromethane. The question would be what happened in the RO process.

For small compounds with high affinity to polyamide membranes, adsorption on the RO membranes surface can happen (Group, 2008). Because of the strong affinity between RO membranes and certain solutes, accumulation of these compounds on membrane surface is possible. When a certain compound is low in feed water, RO membranes may release the compound back into the effluent or permeate (Group, 2008). Though the above effect could exist, it still can hardly explain the reagent(s) source for the production of chloromethane in unquenched RO permeate.

Another observation is that RO permeate samples with no quencher also showed a significant difference between different dates (10/19/12: 580±20 ppt and 12/26/12: 290±20 ppt). It is known that halogenated DBPs are products of disinfectants and dissolved organics. Therefore, the observation is likely a result of the difference in dissolved organic substances on the two days.

Table 3.1: Chloromethane Concentrations (ppt) in RO Feed, RO Permeate and UV/H_2O_2 based UVAOP Permeate in Phase I study.

	TB* (RO feed site)	TB (RO permeate site)	TB (UVAOP site)	RO feed	RO permeate	UVAOP permeate
With quencher		n=1			n=2	
Set 1	50	28	29	110±7	88±20	110±2
Set 2	31	32	44	71±10	83±3	92±10
Set 3	59	59	27	64±4	77±3	110±10
No quencher		n=1			n=2	
Set 1	51	49	59	130±10	580±20	130±6
Set 2	43	52	49	120±20	430±40	110±10
Set 3	101	130	37	140±10	290±20	130±4
average ± 1 standard deviation						

* TB: travel blank

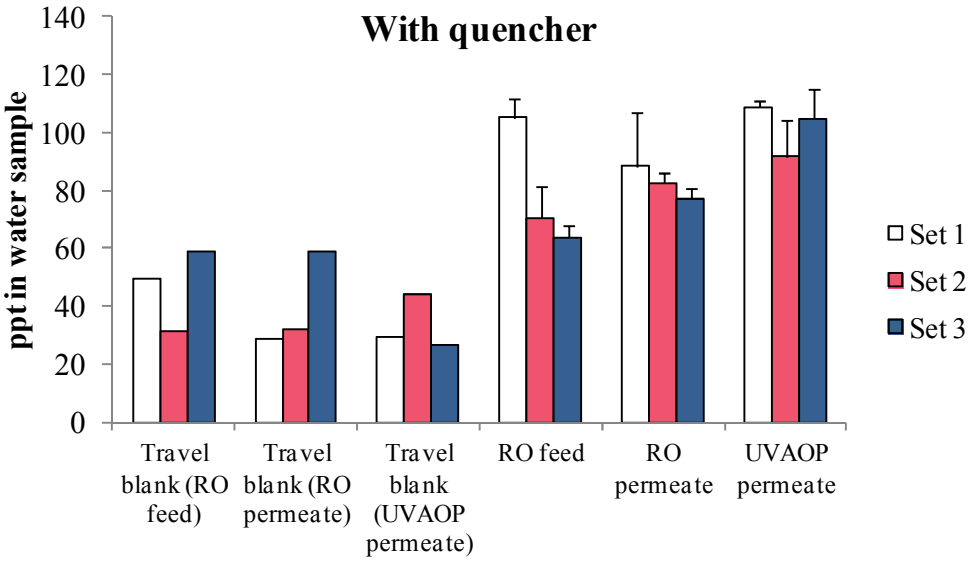

(a)

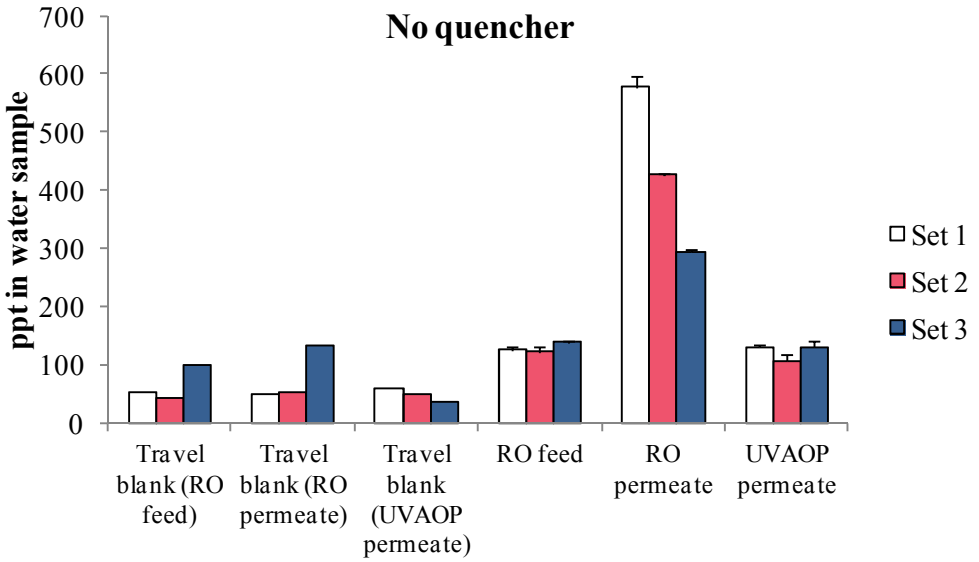

(b)

Figure 3.4 (a) and (b): Phase I Chloromethane Concentrations in Travel Blank, RO Feed, RO Permeate, and UV/H_2O_2 based UVAOP Permeate with and without Quencher.

3.2.2. Tribromomethane

A significant reduction of tribromomethane ($CHBr_3$) (Table 3.2 and Figure 3.5) in the RO and UV/H_2O_2 based UVAOP is observed in water samples with and without quencher. Tribromomethane was not detected in travel blanks with and without quencher.

The average removal efficiency of tribrimomethane is 36±6 − 51±4 % (quenched samples) and 43±24 − 59±5 % (non-quenched samples). In comparison to CH_3Cl (50.5 g/mole), $CHBr_3$ has higher molecular weight (252.7 g/mole) and larger size. Polyamide RO membranes used in the OCWD have a better rejection for large molecules (MW > 150 g/mole) and non-polar molecules (Group, 2008), which implies RO procedure may remove $CHBr_3$ better than CH_3Cl.

The UV/H_2O_2 based UVAOP removed $CHBr_3$ well. From previous studies (Jo, 2008; Nicole, De Laat, Dore, Duguet, & Suty, 1991), $CHBr_3$ was removed quickly by direct photolysis by λ=254nm compared to chlorinated THMs, which is consistent with our results.

Table 3.2: Tribromomethane Concentrations (ppt) in RO Feed, RO Permeate and H_2O_2 based UVAOP Permeate in Phase I Study.

	TB* (RO feed site)	TB (RO permeate site)	TB (UVAOP site)	RO feed	RO permeate	UVAOP permeate
With quencher		n=1			n=2	
Set 1	BDL**	BDL	BDL	58±2	29±1	5±1
Set 2	BDL	BDL	BDL	28±2	16±2	3±0.3
Set 3	BDL	BDL	BDL	15±1	10±0.5	2±0.1
No quencher		n=1			n=2	
Set 1	BDL	BDL	BDL	69±3	28±1	4±0.3
Set 2	BDL	BDL	BDL	29±6	17±1	3±1
Set 3	BDL	BDL	BDL	19±1	9±0.4	2±0.1
average ± 1 standard deviation						

* TB: travel blank
**BDL: below detection limit

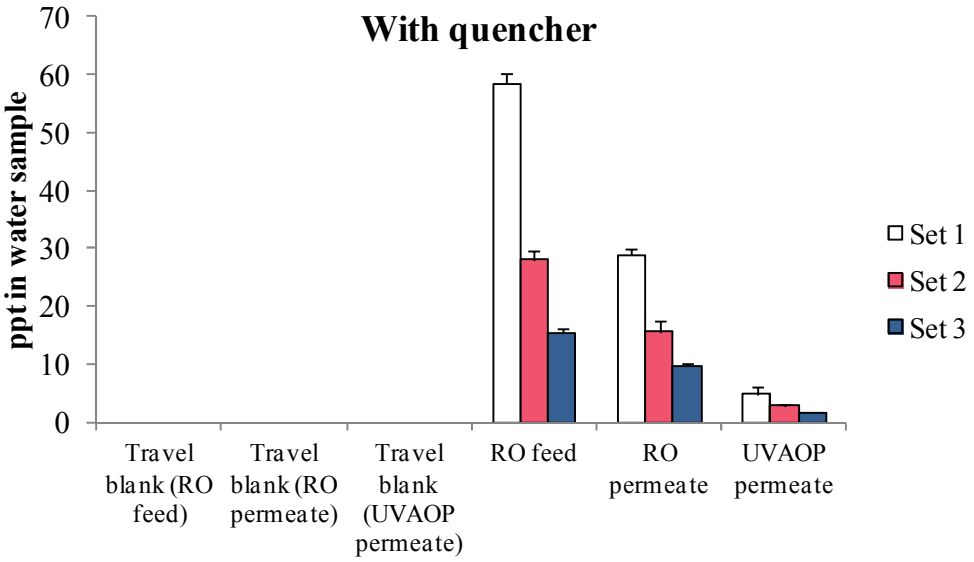

(a)

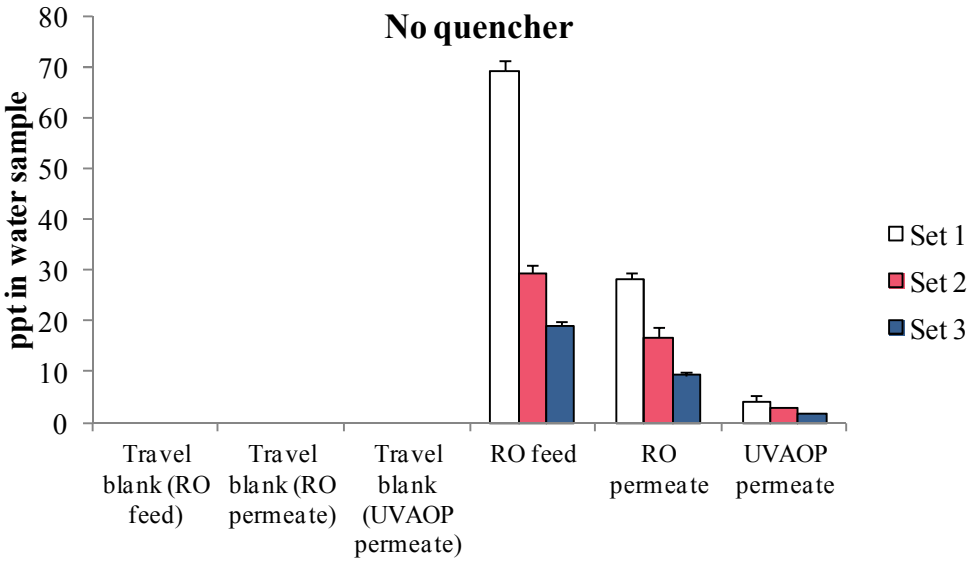

(b)

Figure 3.5 (a) and (b): Phase I Tribromethane Concentrations in Travel Blank, RO Feed, RO Permeate, and UV/H_2O_2 based UVAOP Permeate with and without Quencher.

3.2.3. Trichloromethane

Trichloromethane ($CHCl_3$) is between 22 − 27 ppt in travel blanks with and without quencher. RO feed water has the highest amount of $CHCl_3$. The removal efficiency of $CHCl_3$ is 49±3 − 60±2 % (quenched samples) and 56±4 − 64±3 % (non-quenched samples). The UV/H_2O_2 based UVAOP does not remove much $CHCl_3$. Similar observation is made for water samples with and without quencher.

The rejection of $CHBr_3$ and $CHCl_3$ by the RO process is very close. This is reasonable since $CHBr_3$ and $CHCl_3$ have similar molecular shape, size polarity, and partition between water and octanol.

However, the UV/H_2O_2 based UVAOP have very little removal of $CHCl_3$ compared to $CHBr_3$.

It has been proposed that brominated and chlorinate methane removal by UV/H_2O_2 based UVAOP is mainly by direct photolysis initiated by C−X cleavage (X = Cl, Br) (Jo, 2008). The postulation is based on comparisons of bond energies, molar adsorption coefficients (ε), removal by UV/H_2O_2 based UVAOP.

Equation 3.13 $$CHX_3 \overset{hv}{\rightarrow} \cdot CHX_2 + \cdot X \quad (X = Cl, Br)$$

Tribromomethane has lager removal by UVAOP, smaller C−X bond dissociation energy (Table 3.3), and higher ε at 254 nm than trichloromethane (Jo, 2008). Also CBr_4 is removed faster than $CHBr_3$ (Jo, 2008). The same result was observed for CCl_4 and $CHCl_3$, indicating H abstraction by OH radical is not significant in the removal mechanism by UV/H_2O_2 based UVAOP (Jo, 2008; Legrini et al., 1993).

Table 3.3: List of Bond Dissociation Energies.

	Bond Dissociation Energy (kJ/mol)
$H-CCl_3$	400[1]
$H-CBr_3$	402[1]
$Cl-CHCl_2$	322[2]
$Br-CHBr_2$	274[1]

[1] (McGivern, Derecskei-Kovacs, North, & Francisco, 1999)

[2] (Won, 2007)

Table 3.4: Trichloromethane Concentrations (ppt) in RO Feed, RO Permeate and UV/H_2O_2 in based UVAOP Permeate in Phase I Study.

	TB* (RO feed site)	TB (RO permeate site)	TB (UVAOP site)	RO feed	RO permeate	UVAOP permeate
With quencher		n=1			n=2	
Set 1	25	22	22	2300±50	1200±20	990±300
Set 2	23	23	27	2500±50	1000±20	1000±60
Set 3	26	24	22	1600±100	770±20	820±40
No quencher		n=1			n=2	
Set 1	23	24	23	2700±100	1200±30	1100±20
Set 2	33	23	27	2800±100	1100±20	1000±60
Set 3	26	26	23	2000±60	730±10	800±10
average ± 1 standard deviation						

* TB: travel blank

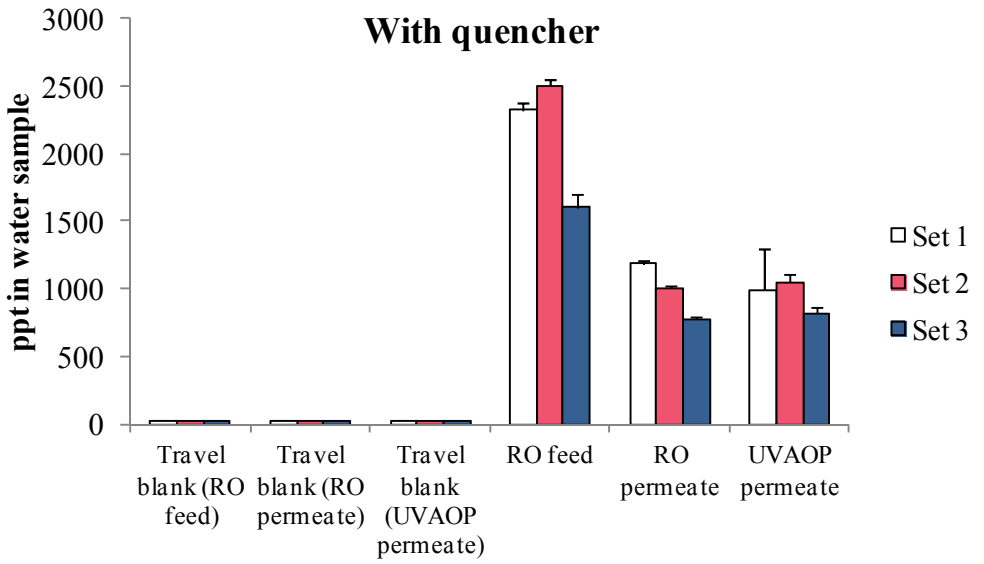

(a)

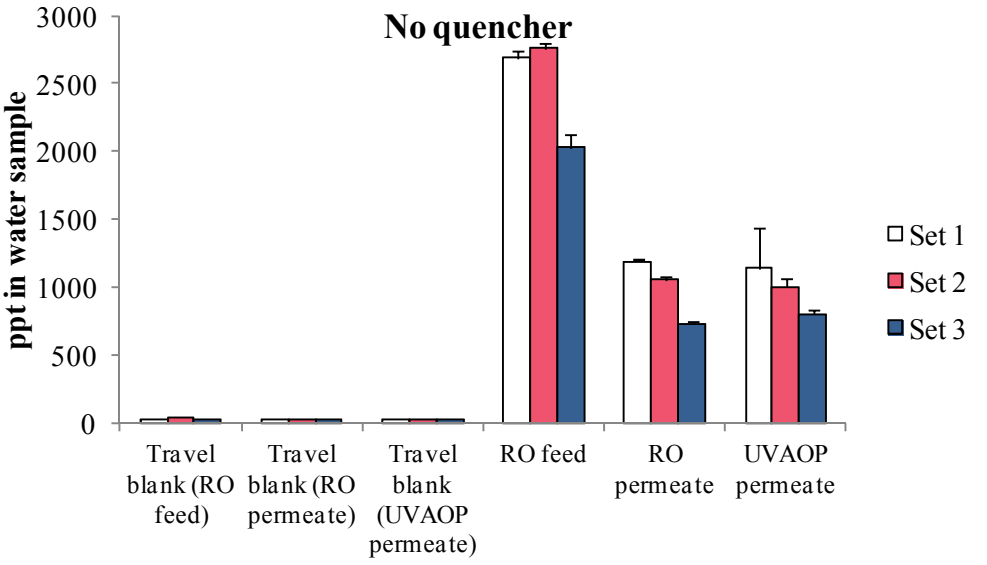

(b)

Figure 3.6 (a) and (b): Phase I Trichloromethane Concentrations in Travel Blank, RO Feed, RO Permeate, and UV/H_2O_2 Based UVAOP Permeate with and without Quencher.

3.2.4. Bromodichloromethane

Bromodichloromethane ($CHBrCl_2$) is below the detection limit for travel blank (RO feed, RO permeate, and UVAOP permeate) with and without quencher. Bromodichloromethane is at similar levels in RO permeate and UVAOP permeate, which are slightly lower than $CHBrCl_2$ in RO feed water both with and without quencher.

As discussed earlier, the removal of $CHBrCl_2$ by RO process is expected to be similar to $CHBr_3$ and $CHCl_3$, because the polarity and membrane affinity for $CHBrCl_2$, $CHBr_3$, and $CHCl_3$ are close. However, the observed removal of $CHBrCl_3$ is smaller than $CHBr_3$ and $CHCl_3$ in this study. Similar phenomena are observed for $CHBr_2Cl$. The RO removal efficiency demonstrates a correlation with $CHBr_2Cl$ concentration. Maybe at low $CHBrCl_2$, RO removal becomes smaller as well.

The removal of $CHBrCl_2$ by UV/H_2O_2 based UVAOP is about 15 % on 10/14/12, and not significant on the other two experiment dates. Smaller removal by UV/H_2O_2 based UVAOP compared to $CHBr_3$ is as expected.

The $CHBrCl_2$ removal becomes insignificant when its concentration is below 20 pptv for both RO and UV/H_2O_2 based UVAOP. This may imply the solute removal threshold for both techniques used in OCWD.

Table 3.5: Bromodichloromethane Concentrations (ppt) in RO feed, RO Permeate and UV/H_2O_2 Based UVAOP Permeate in Phase I Study.

	TB* (RO feed site)	TB (RO permeate site)	TB (UVAOP site)	RO feed	RO permeate	UVAOP permeate
With quencher		n=1			n=2	
Set 1	BDL**	BDL	BDL	43±5	40±1	34±1
Set 2	BDL	BDL	BDL	16±1	14±1	13±1
Set 3	BDL	BDL	BDL	28±9	19±1	18±1
No quencher		n=1			n=2	
Set 1	BDL	BDL	BDL	51±3	40±1	33±1
Set 2	BDL	BDL	BDL	19±1	13±1	13±0.5
Set 3	BDL	BDL	BDL	25±1	19±1	18±1
average ± 1 standard deviation						

* TB: travel blank
** BDL: below detection limit

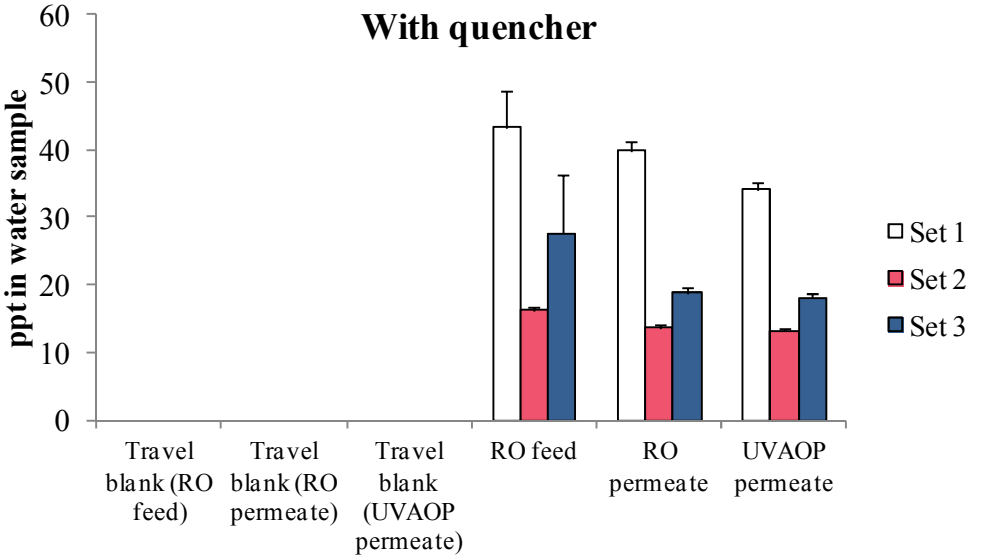

(a)

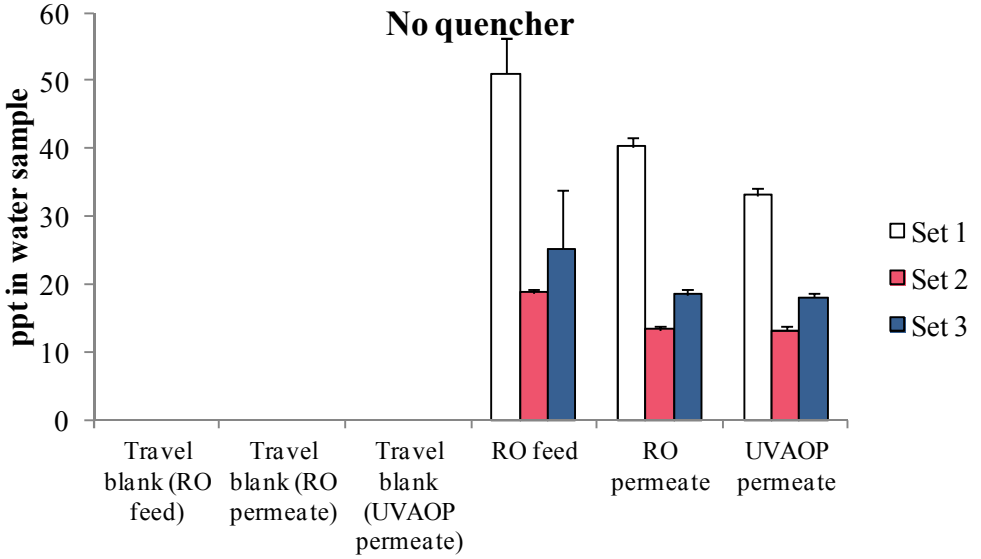

(b)

Figure 3.7 (a) and (b): Phase I Bromodichloromethane Concentrations in Travel Blank, RO Feed, RO Permeate, and UV/H_2O_2 based UVAOP Permeate with and without Quencher.

3.2.5. Dibromochloromethane

The amount of dibromochloromethane ($CHBr_2Cl$) decreases steadily through the RO and UVAOP processes and is below detection limit in travel blanks with and without quencher.

The removal of $CHBr_2Cl$ by RO demonstrates a positive correlation with concentration (Table 3.6). The correlation may be the explanation for the higher removal for $CHCl_3$ than $CHBrCl_2$ and $CHBr_2Cl$, since the later two are much lower in concentration than $CHCl_3$.

The removal of $CHBr_2Cl$ by UV/H_2O_2 based UVAOP is more than that of $CHBrCl_2$, likely because it has one more bromine. Our result is consistent with the proposed removal mechanism.

Table 3.6: Dibromochloromethane Concentrations (ppt) in RO Feed, RO Permeate and UV/H_2O_2 based UVAOP Permeate in Phase I Study.

	TB* (RO feed site)	TB (RO permeate site)	TB (UVAOP site)	RO feed	RO permeate	UVAOP permeate
With quencher		n=1			n=2	
Set 1	BDL**	BDL	BDL	45±0.5	39±0.4	30±0.3
Set 2	BDL	BDL	BDL	38±1	31±0.4	20±1
Set 3	BDL	BDL	BDL	22±0.2	18±0.4	10±0.3
No quencher		n=1			n=2	
Set 1	BDL	BDL	BDL	49±0.5	39±0.4	29±0.3
Set 2	BDL	BDL	BDL	39±0.4	31±1	20±0.4
Set 3	BDL	BDL	BDL	24±0.2	18±0.3	10±0.2
average ± 1 standard deviation						

* TB: travel blank
** BDL: below detection limit

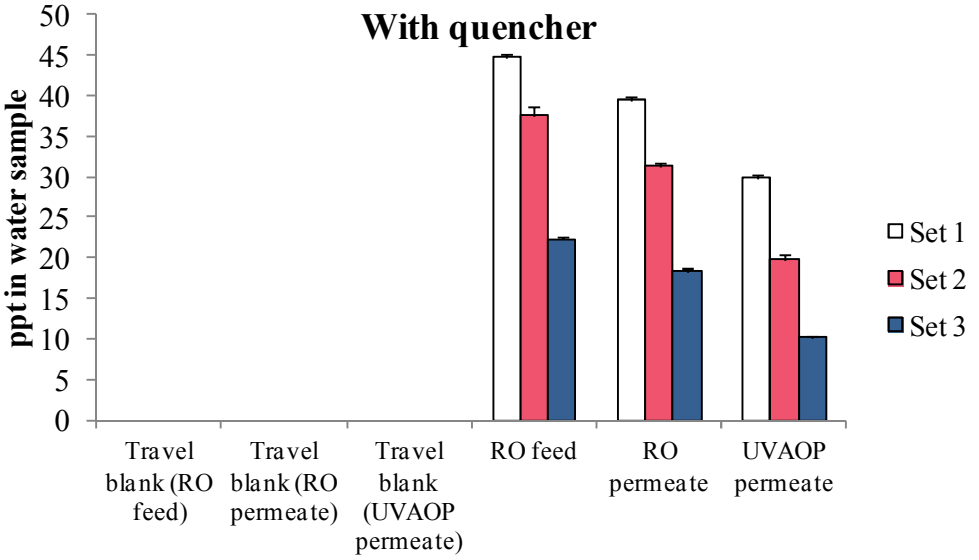

(a)

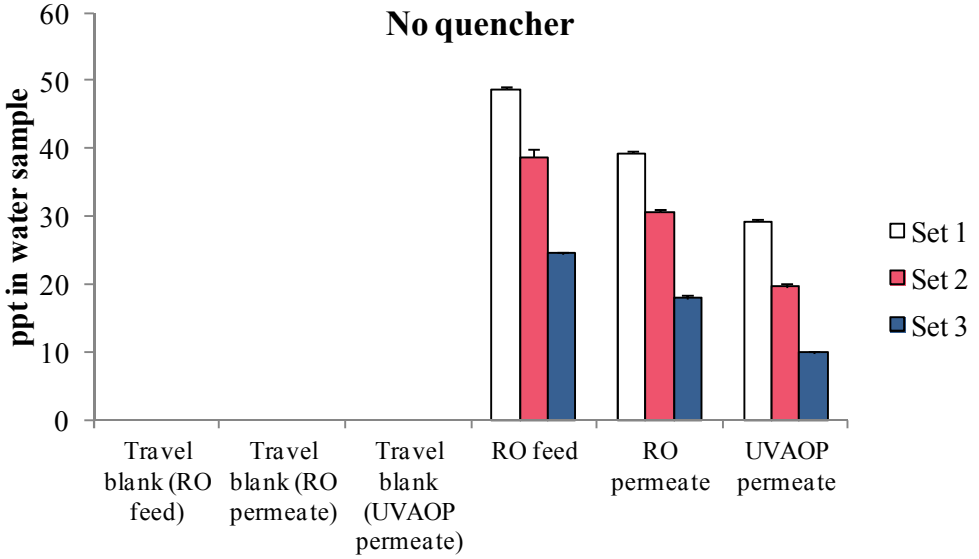

(b)

Figure 3.8 (a) and (b): Phase I Dibromochloromethane Concentrations in Travel Blank, RO Feed, RO Permeate, and UV/H_2O_2 based UVAOP Permeate with and without Quencher.

Out of more than 600 DBPs that have been reported since mid-1970s, halogenated DBPs (mainly mono-, di-, trihalomethanes, haloacetic acids, haloketones, and haloaldehydes) and nitrogenerous DBPs (mainly haloacetonitriles, haloacetamides, cyanogen halides, halonitromethanes, and nitrosamines) compose most of the DBPs (Bond, Huang, Templeton, & Graham, 2011; Krasner et al., 2006).

According to the International Agency for Research on Cancer (IARC), $CHCl_3$ and $CHBrCl_2$ may have carcinogenic effects on humans, while current studies for the other two THMs cannot conclude their carcinogenic effects (IARC, 2012). The sum of the four trihalomethane concentrations in this study is well below the EPA maximum contaminant level (MCL), 80 ppb. The chloromethane concentration in UV/H_2O_2 based UVAOP permeate is around 100 ppt, which is below the healthy advisory for CH_3Cl (30 ppb). Health advisory is the suggested chemical concentration in drinking water, at which there are no foreseeable severe health effect and no carcinogenic effect from long term daily exposure. There is no MCL set by the EPA for CH_3Cl at this point.

Table 3.7: **Chloromethane Concentrations (ppt) and the sum of Trihalomethane Concentrations (ppt) in UVAOP Permeate from Phase I Study**

	$[CH_3Cl]_{UVAOP\ permeate}$		$\Sigma\ [THM_4]_{UVAOP\ permeate}$	
	quencher	no quencher	quencher	no quencher
Set 1	110±2	130±6	1100±400	1200±90
Set 2	90±10	110±10	1100±130	1000±300
Set 3	110±10	130±4	850±70	830±60

THM_4: $CHBr_3$, $CHCl_3$, $CHBrCl_2$, $CHBr_2Cl$

To estimate the impact of the THMs on local air quality, let's assume all the four THMs contained in UVAOP permeate escape to the atmosphere. Using the average production of UVAOP permeate (70 million gallons per day), , we are able to estimate the maximum release amount of each THMs monitored.

Table 3.8: Estimation of Maximum $CHBr_3$, $CHCl_3$, $CHBrCl_2$, and $CHBr_2Cl$ Released from UVAOP Permeate and Global Annual Flux of the Four THMs. (Ordóñez et al., 2012; Watts, Long, & Meek, 2004)

	UVAOP permeate (kg/yr)	Global annual flux (kg/yr)
$CHBr_3$	0.4±0.03	$5.33x10^8$
$CHCl_3$	110±2	$6.6x10^8$
$CHBrCl_2$	3±0.1	$2.26x10^8$
$CHBr_2Cl$	3±0.03	$1.97x10^7$

The results show that the amounts of the four THMs released from UVAOP permeate in OCWD are significantly lower than annual global flux. The impact of air quality by the four THMs should not be a concern.

3.2.6. Methyl Nitrate

Methyl nitrate was not detected in travel blanks both with and without quencher. It ranged around tens of ppt for RO feed and RO permeate (Table 3.10). Methyl nitrate increased to hundreds of ppt after UVAOP (as shown in Table 3.10) for both quenched and non-quenched water samples.

Phase II results demonstrate that methyl nitrates does not change much after the addition of hydrogen peroxide, which indicates that the increase of alkyl nitrates occurs after the mixture of RO permeate and hydrogen peroxide was exposed to UV irradiation.

Possible Cause of Methyl Nitrate Increase

The increase of methyl nitrate did not happen until the mixture of RO permeate and H_2O_2 was in contact with UV irradiation. The UV irradiation produces radicals and initiates serial radical reactions. This implies the increase of alkyl nitrates results from radical reactions.

Dahl et al. (2005; 2003) examined the radical mechanism involving aqueous nitrite, alkanes, oxygen, and irradiation (Table 3.9) in both natural waters and MilliQ® water with UV irradiation. Methyl, ethyl, and *i*-propyl nitrates were successfully generated, thus confirming the feasibility of the alkyl peroxy radical and nitric oxide radical mechanism.

Table 3.9: Alkyl Nitrate Formation Mechanism in Aqueous Solution Proposed by Dahl (2003)

Equation 3.14	$H_2O_2 + hv \rightarrow 2\ HO\cdot$
Equation 3.15	$NO_2^- + H_2O + hv \rightarrow NO\cdot + HO\cdot + OH^-$
Equation 3.6	$R\text{-}H + HO\cdot \rightarrow R\cdot + H_2O$
Equation 3.7	$R\cdot + O_2 \rightarrow RO_2\cdot$
Equation 3.16	$RO_2\cdot + NO\cdot \rightarrow RO + NO_2$
Equation 3.17	$RO_2\cdot + NO\cdot \rightarrow RONO_2$

The source of alkyl radials can be intermediates of photolysis of dissolved organics or reactions of OH radicals and dissolved organics. For example, the proposed mechanism of acetic acid and OH radical reaction in the atmosphere generates methyl radicals and CO_2 (Butkovskaya, Kukui, Pouvesle, & Le Bras, 2004; Vimal & Stevens, 2006).

Equation 3.18 $$CH_3COOH + \cdot OH \rightarrow CH_3COO\cdot + H_2O$$

Equation 3.19 $$CH_3COO\cdot \rightarrow \cdot CH_3 + CO_2$$

It is noteworthy that methane is generated at wastewater treatment processes during reactions of bacteria and dissolved organics (McCarty, 1964).

Equation 3.20 $$CO_2 + 4\,H_2 \rightarrow CH_4 + 2H_2O$$

Equation 3.21 $$CH_3COO^- + H_2O \rightarrow CH_4 + HCO_3^-$$

The dissolved methane concentrations in the effluent from bio oxidation reactor have been reported at the level of ppm (Hartley & Lant, 2006; Souza, 2011). Assuming this is the dissolved methane concentration in the RO influent, and the RO rejection of methane is 99-99.9%, methane concentration in RO permeate is at ppb level. At such levels, dissolved methane can be an important source of methyl radicals.

However, if methane is largely lost to ambient air before entering the RO system, then dissolved methane concentration calculated by Henry's law constant is about 30 ppt (K_H = 1.3 x 10^{-3} M/atm, average atmospheric methane in mid-latitude northern hemisphere in 2011 = 1.874 ppm) ("Advanced Global Atmospheric Gases Experiment (AGAGE) data," ; Mackay & Shiu, 1981). In this case, there must be other methyl radical source(s).

Table 3.10: $MeONO_2$ Concentrations (ppt) in RO Feed, RO Permeate and UV/H_2O_2 based UVAOP Permeate in Phase I Study.

	TB* (RO feed site)	TB (RO permeate site)	TB (UVAOP site)	RO feed	RO permeate	UVAOP permeate
With quencher		n=1			n=2	
Set 1	BDL**	BDL	BDL	18±2	15±1	640±60
Set 2	BDL	BDL	BDL	12±1	10±1	470±40
Set 3	BDL	BDL	BDL	11±1	18±2	590±60
No quencher		n=1			n=2	
Set 1	BDL	BDL	BDL	40±4	16±1	620±60
Set 2	BDL	BDL	BDL	18±2	11±1	450±50
Set 3	BDL	BDL	BDL	20±2	16±2	550±60
average ± one standard deviation						

* TB: travel blank
** BDL: below detection limit

Table 3.11: Phase II Methyl Nitrate Concentrations (ppt) in RO Permeate, UV/H_2O_2 based UVAOP Feed, and UV/H_2O_2 based UVAOP Permeate (No Quencher) (04/22/13).

	TB* (RO permeate)	TB (UVAOP feed)	TB (UVAOP permeate)	RO permeate	UVAOP feed	UVAOP permeate
		n=1			n=4	
$MeONO_2$	BDL**	BDL	BDL	38±4	29±9	1000±100

* TB: travel blank
**BDL: below detection limit

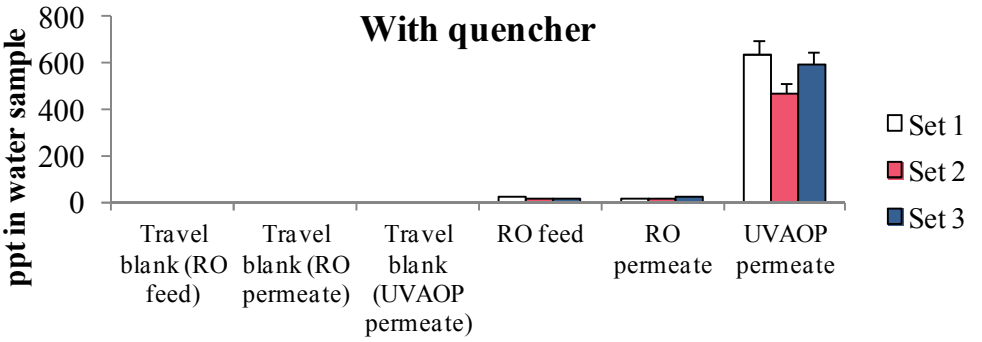

(a)

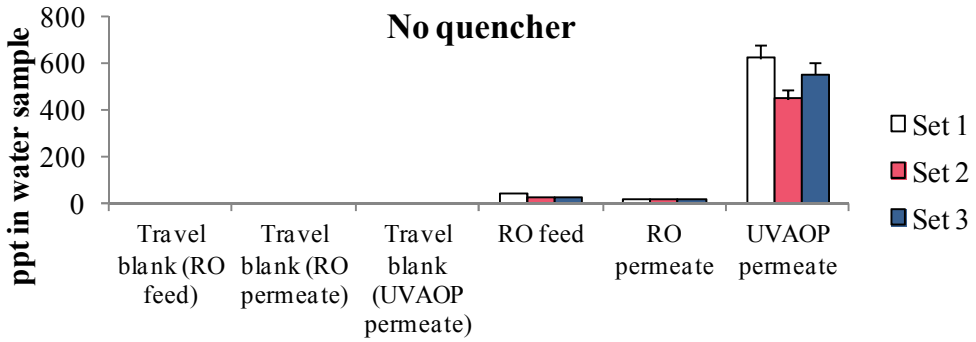

(b)

Figure 3.9 (a) and (b): Phase I Methyl Nitrate Concentrations in Travel Blank, RO Feed, RO Permeate, and UV/H_2O_2 Based UVAOP Permeate with and without Quencher.

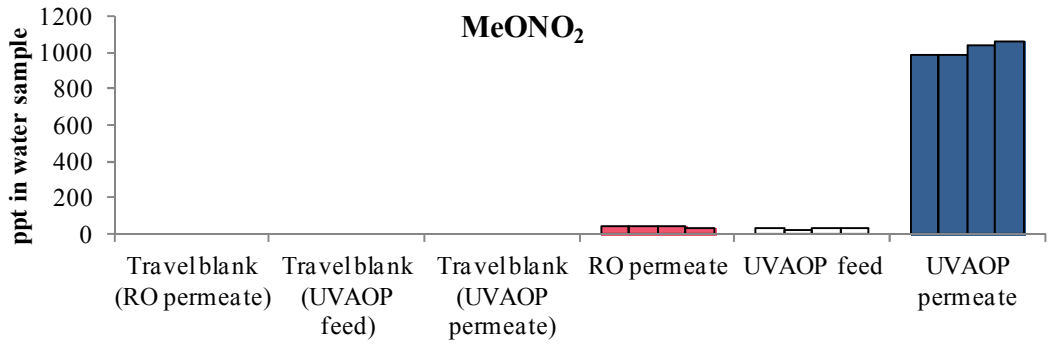

Figure 3.10: Phase II Methyl Nitrate in Travel Blank, RO Permeate, UV/H_2O_2 based UVAOP Feed, and UV/H_2O_2 based UVAOP Permeate without Quencher.

3.2.7. *i*-Propyl nitrate

i-Propyl nitrate (Figure 3.11 (a) and (b)) was below detection limit in travel blank. In the RO process, *i*-propyl nitrate concentrations show a significant decrease (Table 3.12). After UV/H_2O_2 based UVAOP, *i*-propyl nitrate concentrations show a significant increase (Table 3.12).

The source of *i*-propyl nitrate can be oxidation product of dissolved organics, such as *i*-butanal (Finlayson-Pitts & Pitts Jr, 2000). The i-propyl radical soon combines with oxygen. The *i*-propyl peroxy radical reacts with NO and produces *i*-propyl nitrate.

Equation 3.22 $$i\text{-}C_3H_7CHO + \cdot OH \rightarrow i\text{-}C_3H_7CO\cdot + H_2O$$

Equation 3.23 $$i\text{-}C_3H_7CO\cdot + O_2 \rightarrow i\text{-}C_3H_7CO_3\cdot$$

Equation 3.24 $$i\text{-}C_3H_7CO_3\cdot + \cdot NO \rightarrow i\text{-}C_3H_7CO_2 + NO_2$$

Equation 3.25 $$\rightleftharpoons i\text{-}C_3H_7CO_3NO$$

Equation 3.26 $$i\text{-}C_3H_7CO_2 \rightarrow i\text{-}C_3H_7\cdot + CO_2$$

Table 3.12: *i*-$PrONO_2$ Concentrations (ppt) in RO Feed, RO Permeate and UV/H_2O_2 based UVAOP Permeate in Phase I Study.

	TB* (RO feed site)	TB (RO permeate site)	TB (UVAOP site)	RO feed	RO permeate	UVAOP permeate
With quencher		n=1			n=2	
Set 1	BDL**	BDL	BDL	8±2	3±0.4	11±2
Set 2	BDL	BDL	BDL	6±1	2±0.3	7±1
Set 3	BDL	BDL	BDL	4±1	2±0.2	7±1
No quencher		n=1			n=2	
Set 1	BDL	BDL	BDL	15±2	3±0.5	10±1
Set 2	BDL	BDL	BDL	8±1	2±0.3	7±1
Set 3	BDL	BDL	BDL	7±1	1±0.3	7±1

average ± 1 standard deviation

* TB: travel blank
**BDL: below detection limit

Table 3.13: Phase II *i*-Propyl Nitrate Cconcentrations (ppt) in ROPermeate, UV/H_2O_2 based UVAOP Feed, and UV/H_2O_2 based UVAOP Permeate (04/22/13).

	TB* (RO permeate)	TB (UVAOP feed)	TB (UVAOP permeate)	RO permeate	UVAOP feed	UVAOP permeate
No quencher		n=1			n=4	
i-$PrONO_2$	BDL	BDL	BDL	3±1	2±1	9±2

average ± 1 standard deviation

* TB: travel blank
**BDL: below detection limit

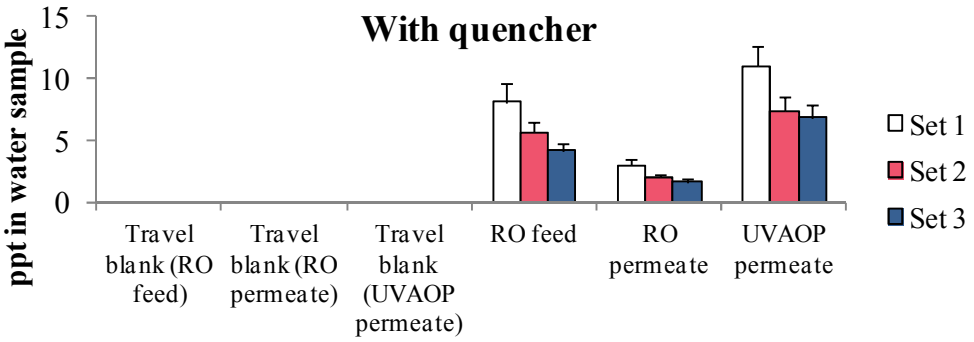

(a)

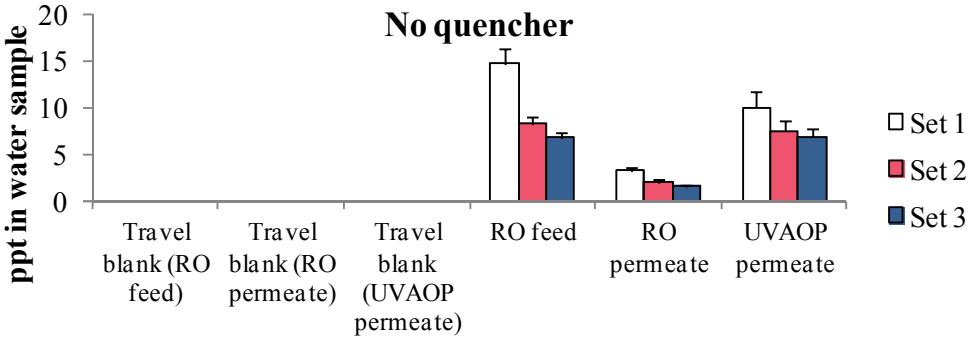

(b)

Figure 3.11 (a) and (b): Phase I *i*-Propyl Nitrate concentrations in Travel Blank, RO Feed, RO Permeate, and UV/H_2O_2 Based UVAOP Permeate with and without Quencher.

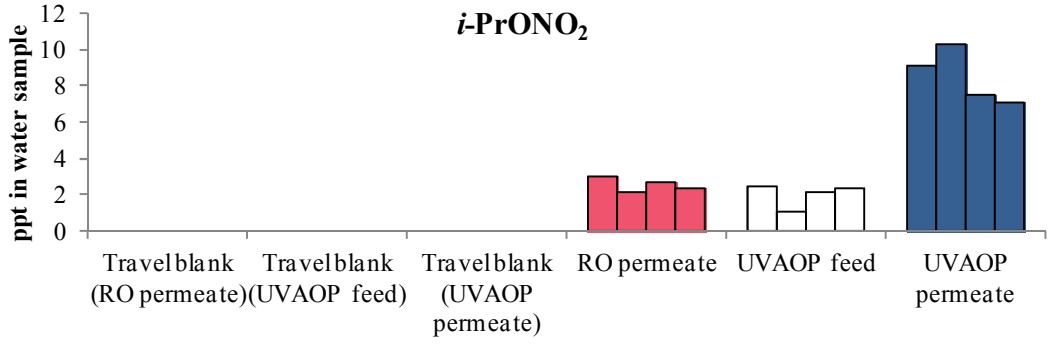

Figure 3.12: Phase II *i*-Propyl Nnitrate in Travel Blank, RO Permeate, UV/H_2O_2 based UVAOP Feed, and UV/H_2O_2 based UVAOP Permeate without Quencher.

3.3. Conclusion

The concentration of CH_3Cl in OCWD treated water is below the healthy advisory. The four trihalomethanes ($CHCl_3$, $CHBr_3$ $CHBr_2Cl$, and $CHBrCl_2$) in this study are also well below maximum contaminant limit. The possible release of the four THMs from UV/H_2O_2 based UVAOP permeate should not impact the air quality according to our estimation. Quack et al. proposed that the effect of anthropogenic sources of trihalomethanes may be considerably significant around the sources (Quack & Wallace, 2003). Quack et al.'s estimation of anthropogenic trihalomethane effect on the atmosphere of the entire planet is trivial (Quack & Wallace, 2003).

The significant increase of methyl nitrate is an important finding for the effect of current purification process in the OCWD. Though various nitrogenerous DPBs are reported (Bond et al., 2011; Roccaro, Vagliasindi, & Korshin, 2011), the generation of alkyl nitrates from the UV/H_2O_2 based UVAOP has not been reported.

Assuming all the methyl nitrate in UVAOP permeate (70 million gallon per day) is released to the ambient air, 97±10 kg of methyl nitrate would be released per year. Compared to methyl nitrate global annual flux: 230 Gg/year, the potential release of methyl nitrate from UVAOP permeate is not significant. It would be interesting to measure the amount of these compounds remaining in the Anaheim basin ground water recharge and seawater barrier injection wells to estimate their potential for environmental impact.

Even though the increase of alkyl nitrates happened after the mixture of H_2O_2 and RO permeate, reaction of UV irradiation and RO permeate without H_2O_2 has not been

investigated. Whether increase of methyl- and *i*-propyl nitrate results from direct photolysis, OH radical reactions, or both of them should be verified. Also, how the OH radical concentrations, UV irradiation intensity, and reaction time effect the alkyl nitrate concentration should be further studied. This would allow the effect of UV/H_2O_2 based UVAOP on reclaimed water to be better assessed.

3.4. References:

Advanced Global Atmospheric Gases Experiment (AGAGE) data.

Alcamo, E. (1995). *The Microbiology Coloring Book*. New York: Addison Wesley.

Bond, T., Huang, J., Templeton, M. R., & Graham, N. (2011). Occurrence and control of nitrogenous disinfection by-products in drinking water – A review. *Water Research, 45*(15), 4341-4354. doi: http://dx.doi.org/10.1016/j.watres.2011.05.034

Butkovskaya, N. I., Kukui, A., Pouvesle, N., & Le Bras, G. (2004). Rate Constant and Mechanism of the Reaction of OH Radicals with Acetic Acid in the Temperature Range of 229−300 K. *The Journal of Physical Chemistry A, 108*(34), 7021-7026. doi: 10.1021/jp048444v

Crittenden, J. C., Hu, S., Hand, D. W., & Green, S. A. (1999). A kinetic model for H2O2/UV process in a completely mixed batch reactor. *Water Research, 33*(10), 2315-2328. doi: http://dx.doi.org/10.1016/S0043-1354(98)00448-5

Crittenden, J. C., Trussell, R. R., Hand, D. W., Howe, K. J., & Tchobanoglous, G. (2012). Reverse Osmosis *MWH's Water Treatment: Principles and Design, Third Edition* (pp. 1335-1414): John Wiley & Sons, Inc.

Dahl, E. E. (2005). *Photochemical production of oceanic alkyl nitrates.* (Ph D), University of California, Irvine.

Dahl, E. E., Saltzman, E. S., & de Bruyn, W. J. (2003). The aqueous phase yield of alkyl nitrates from ROO + NO: Implications for photochemical production in seawater. *Geophysical Research Letters, 30*(6), 1271. doi: 10.1029/2002GL016811

Finlayson-Pitts, B. J., & Pitts Jr, J. N. (2000) *Chemistry of the Upper and Lower Atmosphere* (pp. 1-969). San Diego: Academic Press.

Group, O. C. W. D. R. a. D. (2008). Effects of Molecular and Environmental Properties on Removal of Pharmaceuticals, Endocrine Disruptors and Disinfection Byproducts by Polyamide RO Membranes: US Environmental Protection Agency, Metropolitan Water District of Southern California.

Hartley, K., & Lant, P. (2006). Eliminating non-renewable CO2 emissions from sewage treatment: An anaerobic migrating bed reactor pilot plant study. *Biotechnology and Bioengineering, 95*(3), 384-398. doi: 10.1002/bit.20929

IARC, I. A. f. R. o. C.-. (2012). GENERAL REMARKS *IARC Monographs on the Evaluation of Carcinogenic Risks to Humans* (Vol. 101, pp. 7). 150 Cours Albert Thomas, 69372 Lyon CEDEX 08, France: World Health Organization - WHO.

Jo, C. H. (2008). *Oxidation of Disinfection Byproducts and Algae-related Odorants by UV/H_2O2.* (Ph D), Virginia Polytechnic Institute and State University

Krasner, S. W., Weinberg, H. S., Richardson, S. D., Pastor, S. J., Chinn, R., Sclimenti, M. J., . . . Thruston, A. D. (2006). Occurrence of a New Generation of Disinfection Byproducts†. *Environmental Science & Technology, 40*(23), 7175-7185. doi: 10.1021/es060353j

Legrini, O., Oliveros, E., & Braun, A. M. (1993). Photochemical processes for water treatment. *Chemical Reviews, 93*(2), 671-698. doi: 10.1021/cr00018a003

Linge, K. L., Blythe, J. W., Busetti, F., Blair, P., Rodriguez, C., & Heitz, A. (2013). Formation of halogenated disinfection by-products during microfiltration and reverse osmosis treatment: Implications for water recycling. *Separation and*

Purification Technology, 104(0), 221-228. doi: http://dx.doi.org/10.1016/j.seppur.2012.11.031

Lonsdale, H. K., Merten, U., & Riley, R. L. (1965). Transport properties of cellulose acetate osmotic membranes. *Journal of Applied Polymer Science, 9*(4), 1341-1362. doi: 10.1002/app.1965.070090413

Mackay, D., & Shiu, W. Y. (1981). A critical review of Henry's law constants for chemicals of environmental interest. *Journal of Physical and Chemical Reference Data, 10*(4), 1175-1199. doi: doi:http://dx.doi.org/10.1063/1.555654

McCarty, P. L. (1964). *The methane fermentation, in Heukelekian and Dondero, eds.,: Principles and applications in aquatic microbiology*. New York: John Wiley & Sons, Inc.

McGivern, W. S., Derecskei-Kovacs, A., North, S. W., & Francisco, J. S. (1999). Computationally Efficient Methodology to Calculate C−H and C−X (X = F, Cl, and Br) Bond Dissociation Energies in Haloalkanes. *The Journal of Physical Chemistry A, 104*(2), 436-442. doi: 10.1021/jp993275d

Newton, D., Balgobin, D., Badyal, D., Mills, R., Pezzetti, T., & Ross, H. M. (2011). *RESULTS, CHALLENGES, AND FUTURE APPROACHES TO CALIFORNIA'S MUNICIPAL WASTEWATER RECYCLING SURVEY*.

Nicole, I., De Laat, J., Dore, M., Duguet, J. P., & Suty, H. (1991). Etude de la degradation des trihalo-methanes en milieu aqueux dilue par irradiation UV - determination du rendement quantique de photolyse a 253,7 nm 1. *Environmental Technology, 12*(1), 21-31. doi: 10.1080/09593339109384978

Ordóñez, C., Lamarque, J. F., Tilmes, S., Kinnison, D. E., Atlas, E. L., Blake, D. R., . . . Saiz-Lopez, A. (2012). Bromine and iodine chemistry in a global chemistry-climate model: description and evaluation of very short-lived oceanic sources. *Atmos. Chem. Phys., 12*(3), 1423-1447. doi: 10.5194/acp-12-1423-2012

Plumlee, M. H., López-Mesas, M., Heidlberger, A., Ishida, K. P., & Reinhard, M. (2008). N-nitrosodimethylamine (NDMA) removal by reverse osmosis and UV treatment and analysis via LC–MS/MS. *Water Research, 42*(1–2), 347-355. doi: http://dx.doi.org/10.1016/j.watres.2007.07.022

Quack, B., & Wallace, D. W. R. (2003). Air-sea flux of bromoform: Controls, rates, and implications. *Global Biogeochemical Cycles, 17*(1), 1023. doi: 10.1029/2002GB001890

Roccaro, P., Vagliasindi, F. G. A., & Korshin, G. V. (2011). Quantifying the formation of nitrogen-containing disinfection by-products in chlorinated water using absorbance and fluorescence indexes. *Water Science & Technology, 63*(1), 40-44. doi: 10.2166/wst.2011.006

Sherwood, T. K., Brian, P. L. T., & Fisher, R. E. (1967). Desalination by Reverse Osmosis. *Industrial & Engineering Chemistry Fundamentals, 6*(1), 2-12. doi: 10.1021/i160021a001

Souza, C. L. C., C. A. L. Aquino, S. F. (2011). Quantification of dissolved methane in UASB reactors treating domestic wastewater under different operating conditions. *Water Science & Technology 64*(11), 6.

Vimal, D., & Stevens, P. S. (2006). Experimental and Theoretical Studies of the Kinetics of the Reactions of OH Radicals with Acetic Acid, Acetic Acid-d3 and Acetic

Acid-d4 at Low Pressure. *The Journal of Physical Chemistry A, 110*(40), 11509-11516. doi: 10.1021/jp063224y

Watts, P., Long, G., & Meek, M. E. (2004). Concise International Chemical Assessment Document 58 CHLOROFORM. Geneva: World Health Organization.

Won, Y.-S. (2007). Thermal Stability and Reaction Mechanism of Chloromethanes in Excess Hydrogen Atmosphere. *Journal of Industrial and Engineering Chemistry, 13*(3), 400-405. doi: http://infosys.korea.ac.kr/PDF/JIEC/IE13/IE13-3-0400.pdf

Chapter 4: Breath and Plasma Studies of Overweight and Type 2 Diabetes Mellitus Subjects

4.1. Background

Unlike type 1 diabetes mellitus (T1DM), which happens at a young age due to a deficiency in insulin excretion, type 2 diabetes mellitus (T2DM) is considered a disease correlated with obesity and lack of physical exercise. In other words, it is believed that certain lifestyles can lead to obesity and may gradually develop into T2DM. Thus, studying the characteristics of metabolic status during the development of T2DM may provide insight on ways to better prevent T2DM.

From more than 80 gases monitored, isoprene, acetone, and methanol demonstrate similar variance among groups. Meanwhile, precursors or generation mechanisms of the three gases may be relative to cholesterol, triglycerides, free fatty acids, or glucose. Triglycerides, free fatty acids, and glucose all relate to glucose metabolism in the human body. Diabetic subjects are known for altered glucose mechanism. Correlation between blood indexes and the three gases will be discussed. Breath data is reported by subtracting room air from exhaled breath. To correct possible effects of ambient room air, delta breath, which is breath subtracting room air, was used in this study.

Equation 4.1 $[\text{delta Breath}]_{x\ gas} = [\text{Breath}]_{x\ gas} - [\text{Room}]_{x\ gas}$

4.2. Subject Profiles

T2DM subjects were previously diagnosed. Overweight subjects were defined by body mass index (BMI: weight in kg divided by square of height in meters) > 30. All subjects were non-smokers during this study. T2DM subjects were taking the control medication for diabetes, which they took routinely before joining this study. Methodology was approved by the UCI Institutional Review Board (IRB). Blood sample collection and blood index analysis (glucose level, insulin level, body temperature, weight, height, etc.) were completed in the UCI Institute for Clinical and Translational Science (ICTS) center by professional personnel. Blood degas, exhaled breath, and corresponding ambient room air were analyzed by the Rowland Blake Group.

All subjects fasted overnight before coming to the ICTS center on the day of the study. After subjects rested for about 30 minutes (at time point: -15 min), a first exhaled breath and ambient room air were collected. Meanwhile, a control exhaled breath sample from sampler, which represented a healthy subject, was collected. Fifteen minutes after the first breath sample (at time point: 0 min), a second breath sample, an ambient room air, and a plasma sample were collected. A third exhaled breath sample and a corresponding room sample were collected after another 15 minutes (at time point: +15 min). Helium purged blood degas samples, exhaled breath, and ambient room air were collected in individual 1.9 L stainless canisters.

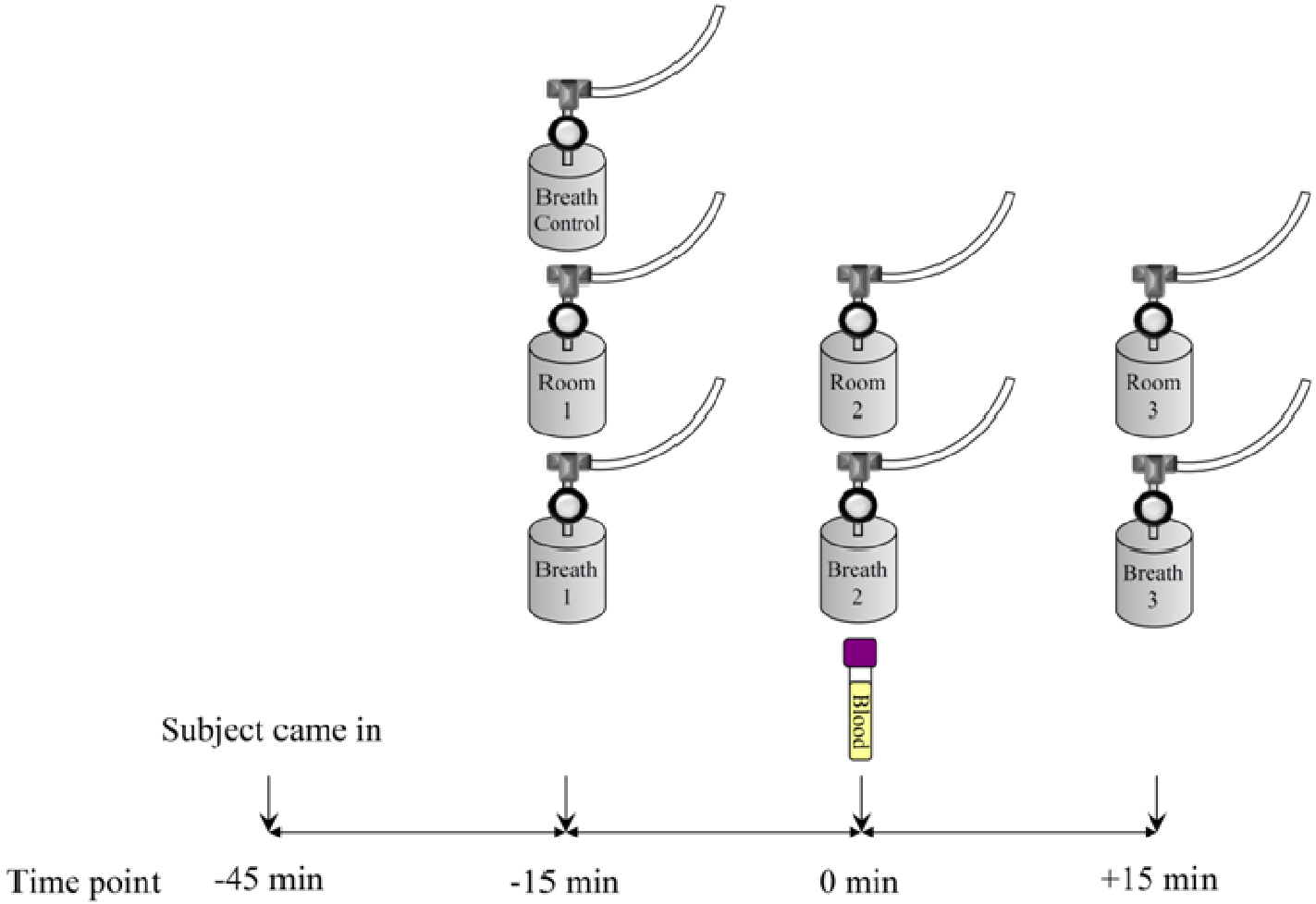

Figure 4.1: Experimental Design of Breath and Plasma of Overweight and T2DM Subjects

Table 4.1: Subject Profiles

Subject	Gender	Age	Type	Visit	BMI	Ins	Glu	TGD	FFAs	HDL-C
1	F	55	OW-F	1	48	12	89	1	823	31
2	M	25	OW-M	1	45	20	92	1	367	22
2	M	25	OW-M	2	45	12	—	1	439	18
3	M	32	OW-M	1	42	14	113	1	409	7
3	M	32	OW-M	2	42	14	108	1	356	13
4	M	39	OW-M	1	43	4	81	2	322	30
4	M	39	OW-M	2	43	5	101	2	576	27
5	M	55	OW-M	1	38	12	125	1	393	24
6	M	23	OW-M	1	38	7	96	1	598	21
7	F	48	T2DM-F	1	44	15	106	1	682	28
8	F	48	T2DM-F	1	34	7	155	2	588	14
8	F	48	T2DM-F	2	34	7	157	2	622	22
8	F	48	T2DM-F	3	35	—	155	—	—	—
9	F	54	T2DM-F	1	26	5	133	2	729	39
9	F	54	T2DM-F	2	26	5	130	4	970	47
10	F	50	T2DM-F	1	42	4	88	1	561	26
11	F	35	T2DM-F	1	40	10	122	2	1013	38
12	F	30	T2DM-F	1	31	3	142	2	1105	28
13	M	50	T2DM-M	1	29	3	106	1	677	34
13	M	50	T2DM-M	2	29	4	121	1	552	27
14	M	33	T2DM-M	1	39	4	97	1	661	31
14	M	33	T2DM-M	2	37	4	87	1	659	36
15	M	58	T2DM-M	1	29	19	302	9	1278	17
15	M	58	T2DM-M	2	29	12	200	6	580	10

BMI: body mass index = body weight in kg / (height in meter)^2.

INS: insulin level in μU/ml.

Glu: glucose level in mg/dl.

TGD: triglyceride level in mmol/dl.

FFA: free fatty acid level in μM

HDL-C: high-density lipoprotein cholesterol in mg/dl.

—: data not available

Table 4.2: Summary of Subject Profiles in Total Amount (OW-F) or in median (min, max) (OW-M, T2DM-F, T2DM-M)

	OW-F	OW-M	T2DM-F	T2DM-M
Age	55	32 (23,55)	48 (30,54)	50 (33,58)
BMI	48	43 (38,45)	34 (26,44)	29 (29,39)
INS (μU/ml)	12	12 (4,20)	5 (3,15)	4 (3,19)
Glucose (mg/dl)	89	99 (81,125)	133 (88,157)	114 (87,302)
Triglycerides (mmol/dl)	1.4	0.9 (0.6,1.8)	2.1 (0.8,3.8)	0.9 (0.5,8.5)
Free fatty acids (μM)	820	400 (320, 600)	680 (560, 1100)	660 (550, 1300)
HDL-C (mg/dl)	31	22 (7,30)	28 (14,47)	29 (10,36)
Subjects	1	5	6	3
Visits	1	8	9	6
Breath samples	3	24	27	18
Plasma samples	1	8	9	6

T2DM females (T2DM-F) and T2DM males (T2DM-M) have higher levels of glucose than our overweight female subject (OW-F) and overweight male subjects (OW-M), indicating poor blood sugar control for T2DM groups. Levels of triglycerides and free fatty acids are also higher for T2DM groups than for OW groups.

4.2.1. Insulin Resistance

In the healthy human body, the pancreas excretes insulin when blood glucose elevates. The released insulin signals muscles and the liver for glucose regulation. The liver can release and store glucose by glucogen synthesis and decomposition. Glucogen is

a branched biopolymer, which is composed of a center protein and branches made up of multiple glucose units. Meanwhile, the liver also decomposes triglycerides for energy production when there is no sufficient carbonhydrates, such as in overnight fasting. Muscle cells also store glucose by synthesizing glucogen. With the release of insulin and elevated blood glucose levels, muscle cells uptake glucose from the blood stream for storage. By increasing the synthesis of glucogen, the liver helps lower blood glucose levels. Triglyceride decomposition by the liver is also reduced, since there is plenty of blood glucose that can be used for energy production.

However, overweight and T2DM subjects have various degrees of insulin resistance. This means the liver and muscle cells do not respond to insulin well and fail to efficiently remove glucose from blood stream (by both muscle cells and the liver), to slow down glucose production (by the liver), and to reduce triglyceride breakdown (by the liver).

T2DM females and males in our study have higher blood glucose, triglyceride, and free fatty acid levels than the overweight female and males in general, indicating T2DM subjects in our study have a higher degree of insulin resistance than overweight subjects.

4.3. Isoprene Generation in the Human Body

Isoprene constitutes up to 70% of the VOCs in expired human breath (Gelmont, Stein, & Mead, 1981). Isoprene generation in the human body is not well understood, though some explanations have been proposed. One is isoprene generation from dimethylallyl pyrophosphate as a by-product of cholesterol synthesis (Stone, Besse, Duane, Dean Evans, & DeMaster, 1993). Another one is isoprene generation via peroxidation of squalene, an intermediate of the cholesterol mevalonate pathway

(McGrath, Patrick, & Silke, 2001; Stein & Mead, 1988). A muscle source of isoprene has also been proposed based on motion correlated increase of expired isoprene and isoprene distribution in venous and arterial blood of pigs (Julian King et al., 2010; Miekisch, Schubert, Vagts, & Geiger, 2001). Bacteria production of isoprene has also been reported as well (Kuzma, Nemecek-Marshall, Pollock, & Fall, 1995).

4.3.1. Breath Isoprene and Plasma Isoprene Levels

Median exhaled isoprene for the OW-F is 46 ppbv (range 46－55 ppbv), for OW-M is 170 ppbv (range 75－270 ppbv), for T2DM-F is 110 ppbv (range 47－210 ppbv), and for T2DM-M is 180 ppbv (range 97－380 ppbv) (Figure 4.2 and Figure 4.4). Breath-born isoprene is generally higher for male overweight and T2DM subjects.

Plasma isoprene for the OW-F is 480 ng/l. Median plasma isoprene for OW-M is 800 ng/l (range 480－1300 ng/l), for T2DM-F is 640 ng/l (range 260－1600 ng/l), and for T2DM-M is 820 ng/l (range 220－2900 ng/l) (Figure 4.3). Plasma isoprene also shows a higher amount for male overweight and T2DM subjects.

4.3.2. Isoprene Studies and Our Results

Previous breath isoprene studies suggested that there is no correlation between age and expired isoprene (Mendis, Sobotka, & Euler, 1994; Taucher et al., 1997), despite the fact that more exhaled isoprene in adults than in children was observed (Kushch et al., 2008; Taucher et al., 1997). In addition, no significant gender difference for exhaled isoprene was observed among healthy subjects (Kushch et al., 2008). However, a significant difference of expired isoprene between the overweight female and male

subjects is observed (p value < 0.001). The same difference is also observed in T2DM subjects (p value < 0.001). Plasma isoprene for OW-F, OW-M, T2DM-F, and T2DM-M subjects is statistically similar.

One possible explanation for the difference between females and males for OW and T2DM groups might be the amount of muscle difference, since King et al. observed isoprene increase relating to physiological motion, and extremely low expired isoprene from muscle dystrophy patients (Julian King et al., 2010; J. King et al., 2012). However, more data from different age groups are needed to validate this presumption.

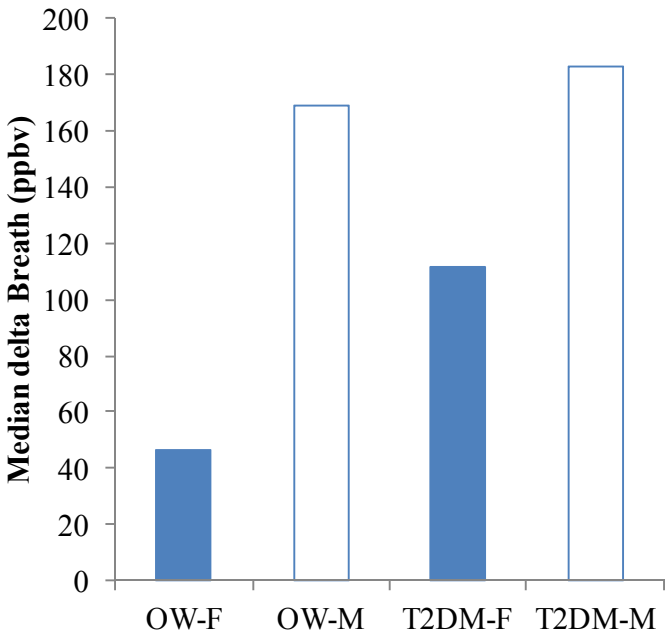

Figure 4.2: Median delta Breath Isoprene of OW-F, OW-M, T2DM-F, and T2DM-M

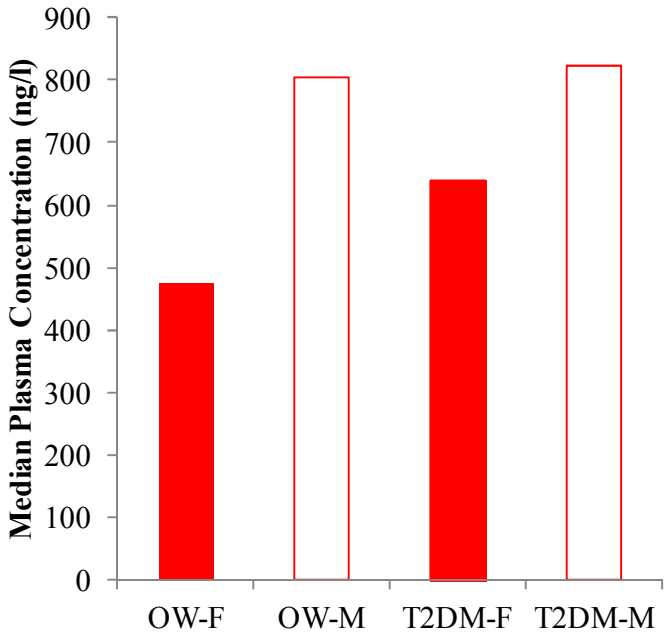

Figure 4.3: Median Plasma Isoprene of OW-F, OW-M, T2DM-F, and T2DM-M

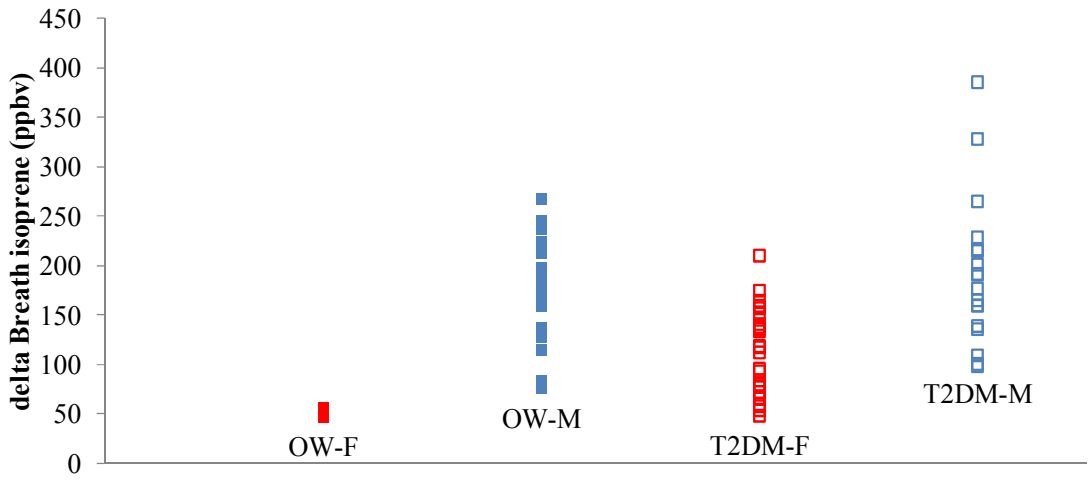

Figure 4.4: delta Breath Isoprene distribution of OW-F, OW-M, T2DM-F, and T2DM-M

4.3.3. Relationship between Isoprene and Triglycerides

All the sampling was conducted after overnight fasting and before the first meal of the sampling day at around eight am, which means all subjects had low carbohydrate levels and triglycerides were the major energy source.

Fatty acids generated from triglyceride hydrolysis are catalyzed by fatty acyl-CoA synthetase. The generated fatty acyl-CoA is further decomposed by enzymes through a four-step cycle: dehydrogenation (two-proton subtraction), hydration, dehydrogenation (one-proton subtraction), and cleavage (Equation 4.2－4.6). The remaining acyl-CoA is further decomposed by the four-step cycle until the entire fatty acid is converted into acetyl-CoA.

Equation 4.2 Hydrolysis of Triglycerides

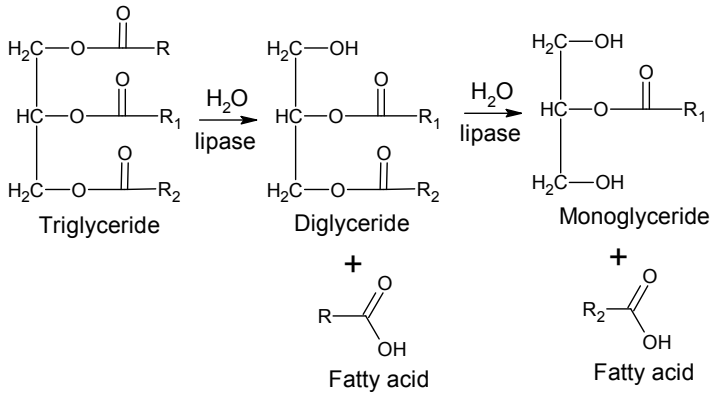

Equation 4.3 Dehydrogenation (two-proton subtraction)

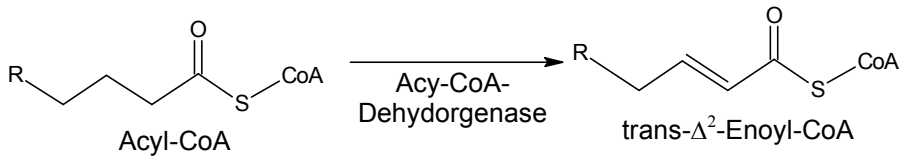

Equation 4.4 Hydration to Carbon Carbon Double Bond

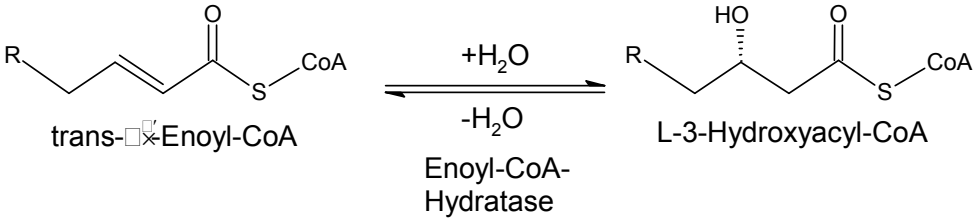

Equation 4.5 Dehydrogenation (one-proton subtraction)

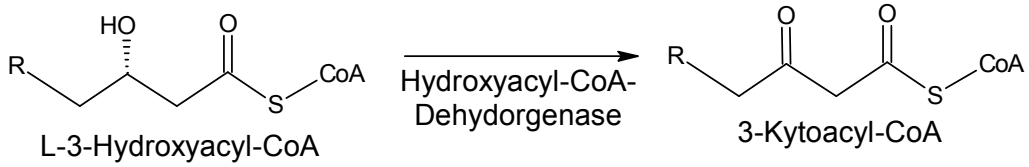

Equation 4.6 Cleavage of acetyl-CoA unit

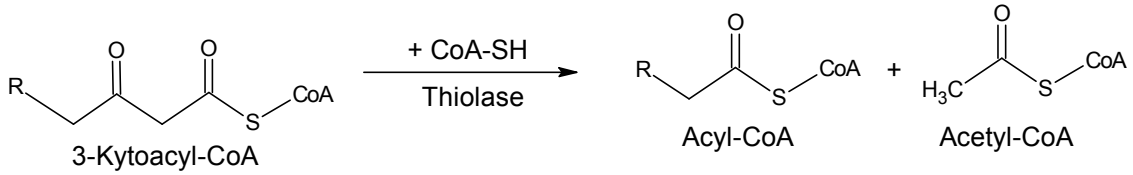

Acetyl-CoA generated during triglyceride metabolism is also precursor for cholesterol synthesis via the mevalonate pathway (Eisenreich, Bacher, Arigoni, & Rohdich, 2004), which also produces the isoprene precursor. In our study, no significant correlation between triglycerides or free fatty acids with plasma isoprene was observed (Figure 4.5), which suggests that isoprene is not directly influenced by triglycerides based on current study groups. Though decrease of isoprene when subjects took cholesterol lowering medication has been reported (Karl et al., 2001; Stone et al., 1993; Zadak et al., 1999) , other studies have also demonstrated no correlation between isoprene and cholesterol (Claire Turner and Patrik Španěl and David, 2006).

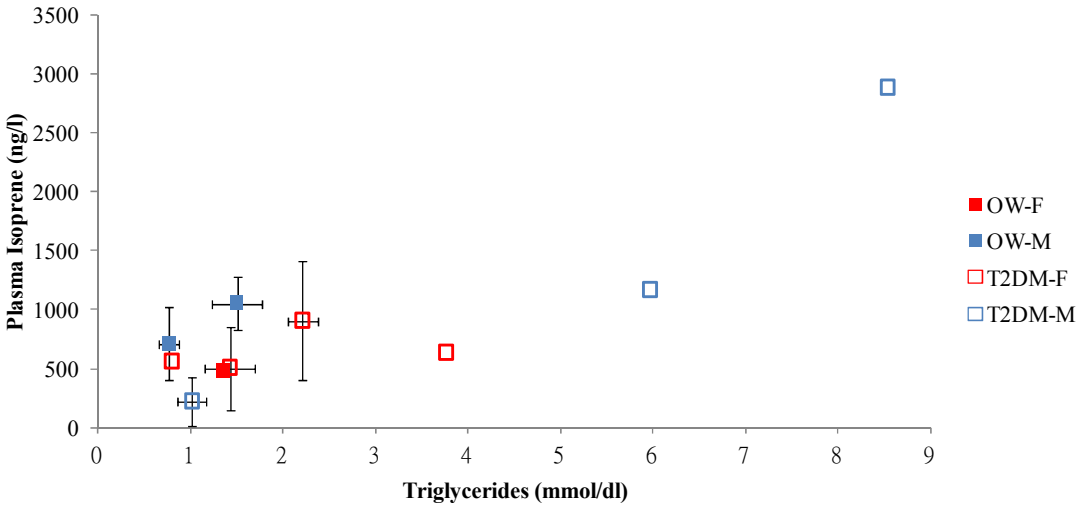

Figure 4.5: Plasma Isoprene (ng/l) versus Triglycerides (mmol/dl). Plasma isoprene is averaged according to triglyceride levels.

4.3.4. Breath Isoprene versus Plasma Isoprene

By averaging plasma and delta breath isoprene according to triglycerides levels (0.5 mmol/dl range), delta breath and plasma isoprene show some correlation; however, there is a data point deviating significantly from the correlation line (Figure 4.6).

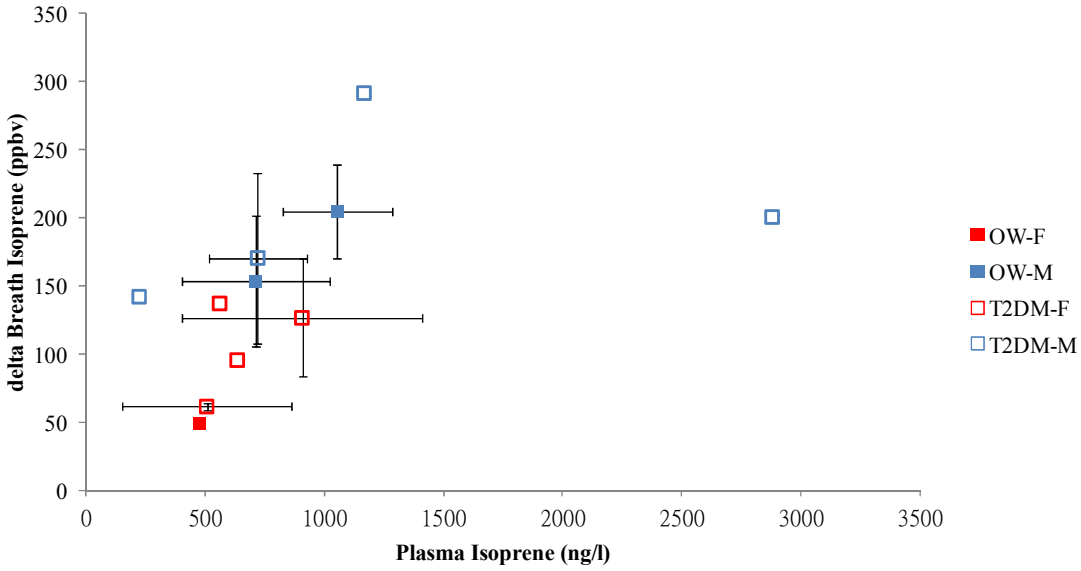

Figure 4.6: Averaged delta Breath Isoprene According to Triglycerides versus Averaged Plasma Isoprene According to Triglycerides.

The outlier in Figure 4.6 is the first visit of subject 15. Table 4.3 shows subject 15 profiles of both visits. Subject 15 had about 1.5 times the glucose, triglycerides, and HDL in his first visit as compared to in his second visit. However, a lower breath isoprene was observed in his first visit. Carbon dioxide levels were similar (~ 5%) for both visits. Therefore, there was no sign of dilution by ambient air.

Table 4.3: Profiles of Subject 15

Subject	Visit	Type	Age	BMI	Insulin	Glucose	TGD	HDL-C	Breath Isoprene (ppbv)	Plasma Isoprene (ng/L)
15	1	T2DM-M	58	29	19	302	8.5	17	200	2900
15	2	T2DM-M	58	29	12	200	6.0	10	290	1200

.

Both T2DM and OW groups seem to follow the trend between delta breath and plasma isoprene. The enormously large plasma and non-comparable breath isoprene values leads to the suggestion that different isoprene sources were being observed. If using the correlation and the delta breath isoprene, the calculated plasma isoprene value is 970 ng/l. The observed plasma value (2900 ng/l) is three times the calculated value for the resting status (970 ng/l). King et al.'s results from exercise triggered breath isoprene increases of three to four times that of resting isoprene values(J King et al., 2009).

In our study, the three breath samples were collected 15 minutes apart. The plasma sample was collected after the breath sample was done. According to the inconsistency between delta breath and plasma isoprene values, and the ratio between observed and calculated plasma isoprene values, it is likely that the plasma sample was collected after subject 15 had some kind of physical motion, such as leg motion or twitching.

Triglycerides did not show a significant effect on observed plasma isoprene and delta breath isoprene. However, averaging delta breath isoprene and plasma isoprene according to triglyceride levels did show a good correlation. It seems that triglycerides somehow effect endogenous isoprene. Both OW and T2DM groups follow the same

correlation. More studies of healthy, OW, and T2DM subjects should be done to elucidate the correlation between delta breath isoprene and plasma isoprene.

4.4. Acetone in OW and T2DM subjects

4.4.1. Acetone Generation and Metabolism in the Human Body

Acetone is generated by decarboxlyation of acetoacetate. During starvation, acetoacetate increases due to the increase of its precursor, acetyl-CoA. Acetoacetate can be converted to β-hydroxybutyrate, a form that can be used for energy generation. Cells can also use acetoacetate to generate energy, which produces acetone as a metabolic waste product. Bloodborne acetone is carried to the liver and exchanged in alveolar cells. Studies of exhaled acetone have shown the ability to monitor blood acetoacetate levels (Musa-Veloso, Likhodii, & Cunnane, 2002; Musa-Veloso et al., 2006), predict blood glucose levels together with expired ethanol (Galassetti et al., 2005), and diagnose diabetes (Deng, Zhang, Yu, Zhang, & Zhang, 2004; Manolis, 1983)

When diabetes patients have poor glucose control or in pre-diabetic subjects, energy generation is mainly from triglycerides and fatty acids. As a result, exhaled acetone elevates. Therefore, breath acetone serves as an important monitoring factor for diabetes subjects (Manolis, 1983).

4.4.2. Breath Acetone and Plasma Acetone Levels

Median exhaled acetone for the OW-F is 220 ppbv (range 210－220 ppbv), for OW-M is 310 ppbv (range 180－1200 ppbv), for T2DM-F is 400 ppbv (range 270－1500 ppbv), and for T2DM-M is 630 ppbv (range 490－1400 ppbv) (Figure 4.7). Breath

acetone is generally higher for male overweight and T2DM subjects. Statistically, delta breath acetone for the OW-F is lower than OW-M ($p = 0.0001$), T2DM-F is lower than T2DM-M ($p = 0.01$), OW-M is lower than T2DM-M ($p = 0.0001$), and OW-F is lower than T2DM-F ($p < 0.0001$). Higher expired acetone during fasting for T2DM subjects suggests a worse control of blood sugar, and insulin resistance. However, expired acetone levels for delta breath acetone for various groups in our study overlap for a considerable range. Therefore, a larger number of subjects can help understand the distribution of expired acetone and the threshold for overweight and diabetic subjects. Acetone in the ambient room samples range from 1.1 to 37 ppbv and the median is 8.0 ppbv. Therefore, room air should not affect the results.

Plasma acetone for the OW-F is 62 μg/l. Median plasma acetone for OW-M is 120 μg/l (range 43－160 μg/l), for T2DM-F is 120 μg/l (range 60－180 μg/l), and for T2DM-M is 160 μg/l (range 42－280 μg/l) (Figure 4.8). Plasma acetone also shows a higher amount for male overweight and T2DM subjects. Though the plasma acetone estimated by our assumption is lower than data previously reported (Kalapos, 2003), the trend still provides insight into OW and T2DM. The difference is likely resulting from the estimation of purge efficiency.

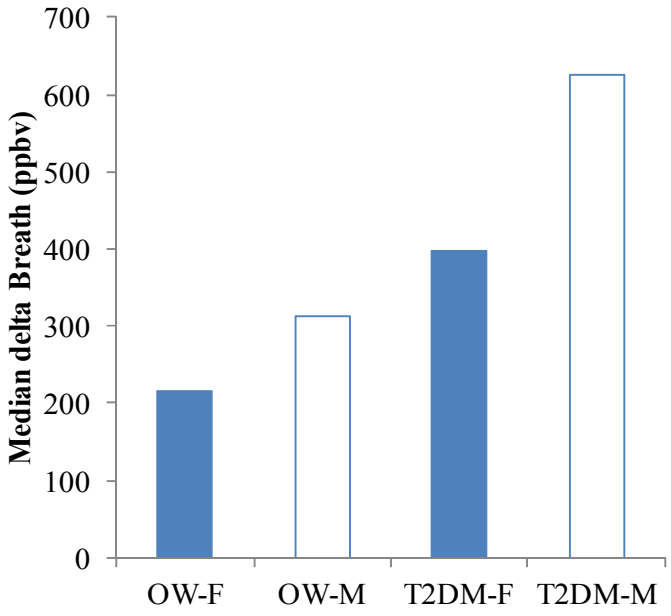

Figure 4.7: Median delta Breath Acetone of OW-F, OW-M, T2DM-F, and T2DM-M

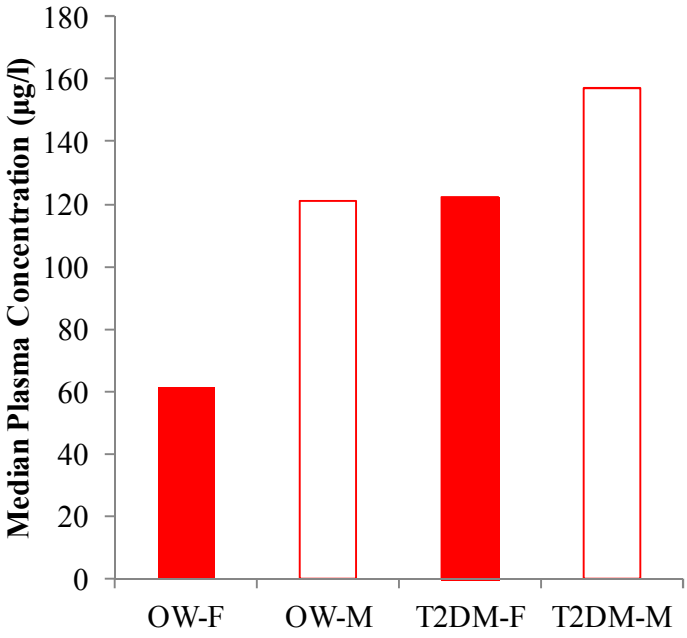

Figure 4.8: Median Plasma Acetone of OW-F, OW-M, T2DM-F, and T2DM-M

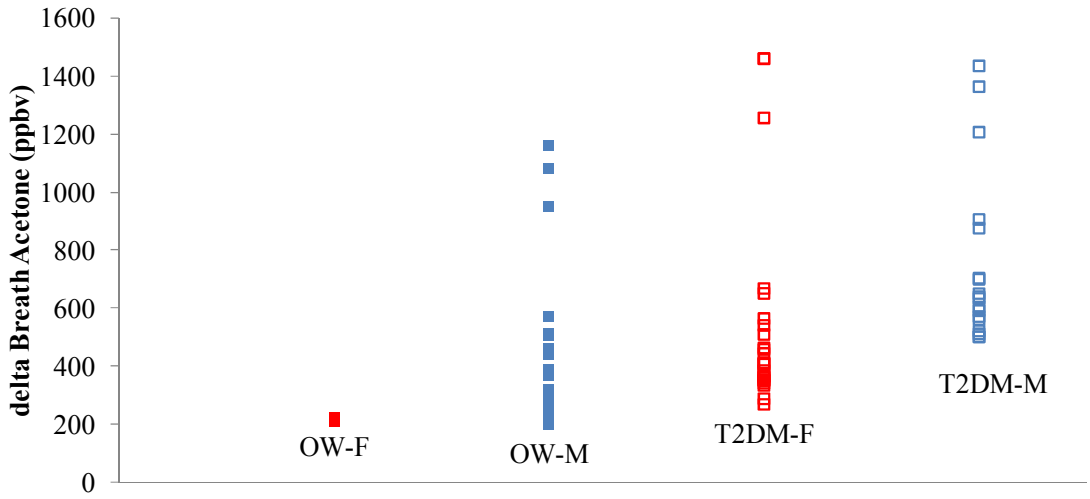

Figure 4.9: delta Breath Acetone Distribution of OW-F, OW-M, T2DM-F, and T2DM-M

Plasma acetone and triglycerides distribution does not show a significant correlation. (Figure 4.10)

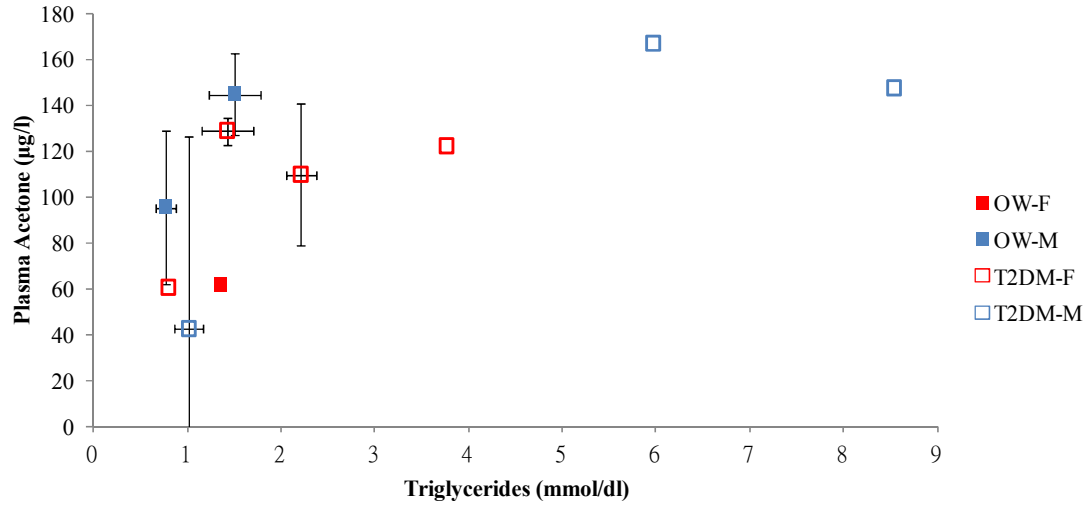

Figure 4.10: Plasma Acetone (µg/l) versus Triglycerides (mmol/dl). Plasma acetone is averaged according to triglyceride levels.

4.4.3. Average according to triglycerides

Similar to isoprene, the averages of delta breath acetone and plasma acetone according to triglycerides demonstrate good correlations indicating triglycerides may have an indirect effect on endogenous acetone (Figure 4.11).

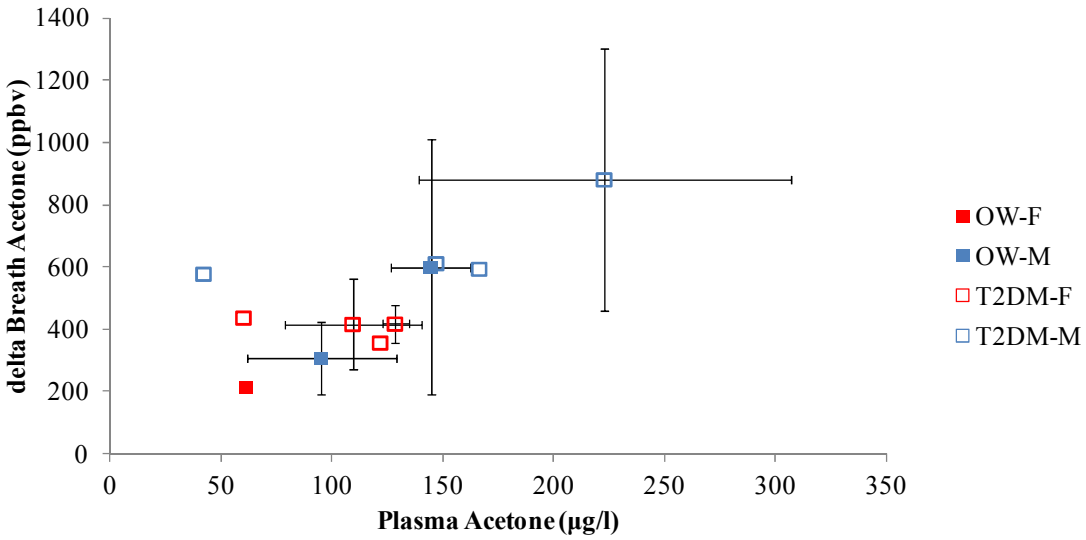

Figure 4.11: Averaged delta Breath Acetone According to Triglycerides versus Averaged Plasma Acetone According to Triglycerides.

4.4.4. Average According to HDL-C (delta Breath versus Plasma acetone)

HDL is a type of lipoprotein, which carries lipids such as cholesterol or triglycerides around cells and the blood stream. HDL-C is cholesterol transported by HDL. Average delta breath and acetone according to HDL-C levels also correlate well indicating HDL-C may also have indirect effect on endogenous acetone.

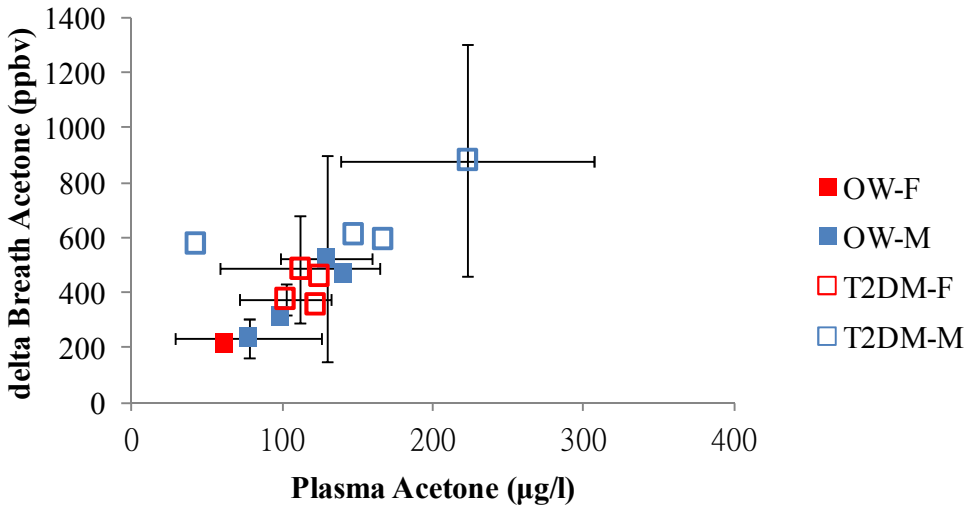

Figure 4.12: Averaged delta Breath Acetone According to HDL-C versus Averaged Plasma Acetone According to HDL-C.

4.5. Methanol in the Human Body

In the human body, methanol can be generated by bacteria in the colon as metabolic product of pectin (Lindinger, Taucher, Jordan, Hansel, & Vogel, 1997). The metabolic products of aspartame, one of the most prevalent sweeteners worldwide, consists of methanol (10%), phenylolamine (50%), and aspartate acid (40 %) (Fisher, Dorman, Medinsky, Welsch, & Conolly, 2000; Garriga & Metcalfe, 1988; Newsome, 1986). Influence of expired methanol relating to fruit or fiber intake has also been reported (Lee, Pahl, Vaziri, & Blake, 2012; Lindinger et al., 1997; Turner, Španěl, & Smith, 2006). Elevated exhaled methanol can result from methanol existing in the ambient air (Turner et al., 2006). Methanol has also been proposed as one of the indexes to monitor the change of blood glucose levels (Minh et al., 2011).

Median exhaled methanol for the OW-F is 100 ppbv (range 87－100 ppbv), for OW-M is 120 ppbv (range 43－230 ppbv), for T2DM-F is 110 ppbv (range 35－260 ppbv), and for T2DM-M is 130 ppbv (range 61－220 ppbv) (Figure 4.13 and 4.14). Statistically, expired methanol for all four groups are similar.

Plasma methanol for the OW-F is 3.5 μg/l. Median plasma methanol for OW-M is 6.7 μg/l (range 4.1－12 μg/l), for T2DM-F is 4.2 μg/l (range 1.6－8.3 μg/l), and for T2DM-M is 7.6 μg/l (range 4.7－15 μg/l) (Figure 4.15). Generally, median plasma methanol for OW-F is lower than OW-M, T2DM-F is lower than T2DM-M, and OW-M is similar as T2DM-M (Figure 4.15). Though the plasma methanol estimated by our assumption is lower than data previously reported (Sarkola & Eriksson, 2001), the trend still provides insight into OW and T2DM. The difference is likely resulting from the estimation of purge efficiency, and fasting condition.

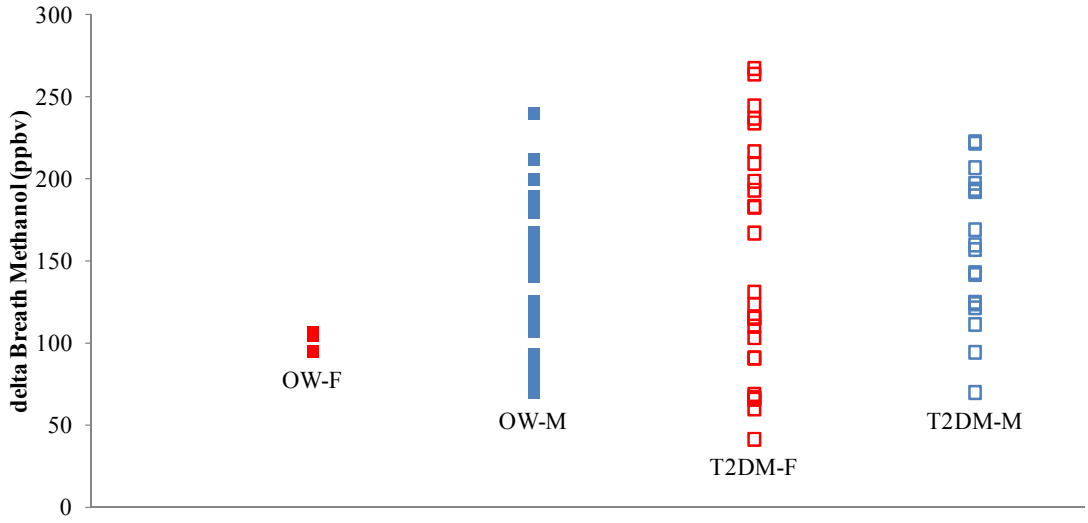

Figure 4.13: delta Breath Methanol Distribution of OW-F, OW-M, T2DM-F, and T2DM-M

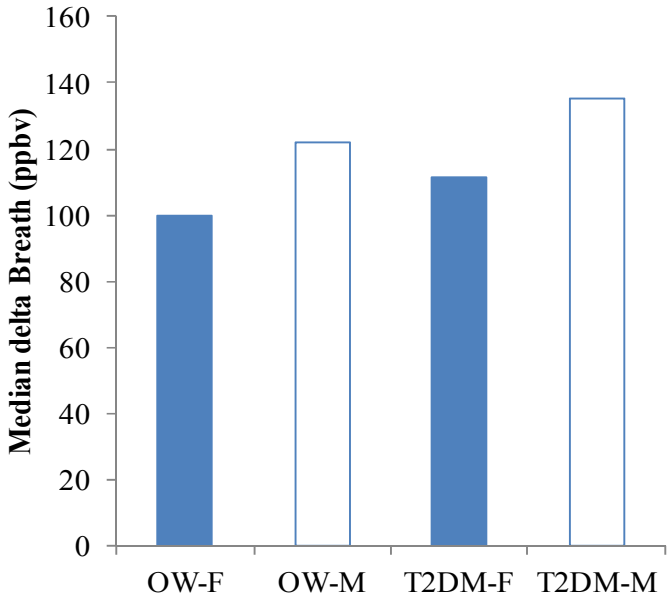

Figure 4.14: Median delta Breath Methanol (ppbv) of OW-F, OW-M, T2DM-F, and T2DM-M

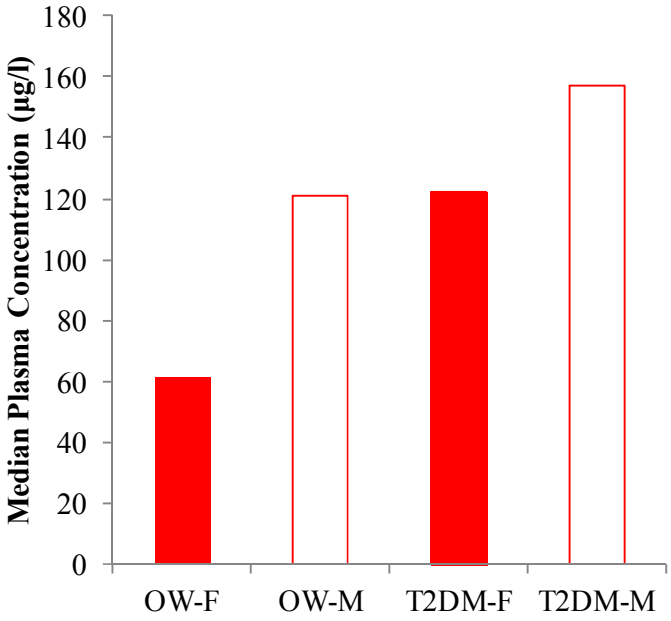

Figure 4.15: Median Plasma Methanol (µg/l) of OW-F, OW-M, T2DM-F, and T2DM-M

4.5.1. Average of delta Breath Methanol versus Plasma Methanol according to Triglycerides

Average delta breath and plasma methanol seem to follow the same correlation for OW-M and T2DM-M (Figure 4.16). Some of the average delta breath and plasma methanol for female groups (both OW and T2DM) fall in the same correlation as OW and T2DM males, but some seem to reflect elevated expired methanol, which are off from the correlation.

Methanol in delta breath is breath methanol minus ambient air (median= 7.7 ppbv, minimum = 3.0 ppbv, maximum = 37 ppbv), which should rule out the contamination from ambient air. Taking methanol's origin in the human body into consideration, the elevated delta breath methanol can be arise from (1) an airway source, (2) altered methanol generation mechanism, (3) altered methanol breath/plasma partition, (4) triglycerides being not the dominant factor of endogenous methanol. Though an airway source is a possible explanation, no evidence of airway methanol generation has been proposed. As forementioned, methanol has been postulated to reflect the change of blood glucose levels (Minh et al., 2011), which implies glucose metabolism involving substance, such as insulin, triglycerides, free fatty acids, etc. can also effect methanol generation. The breath/plasma partition is related to the affinity of substance to plasma constitutes (lipids, proteins). Obesity and T2DM are often characterized with higher lipid contents in the blood stream. Therefore, breath/plasma partition of methanol can be altered. Methanol generated in the human body has been reported to reflect change of glucose levels together with other alcohols (Minh et al., 2011), but not directly involving

triglycerides or other lipids. Maybe this is part of the reason that some data are off from the delta breath and plasma methanol correlation according to triglyceride levels.

However, why only female subjects demonstrate an inconsistency of expired methanol and plasma methanol is not clear. Further investigation of larger subject groups can help elucidate our findings.

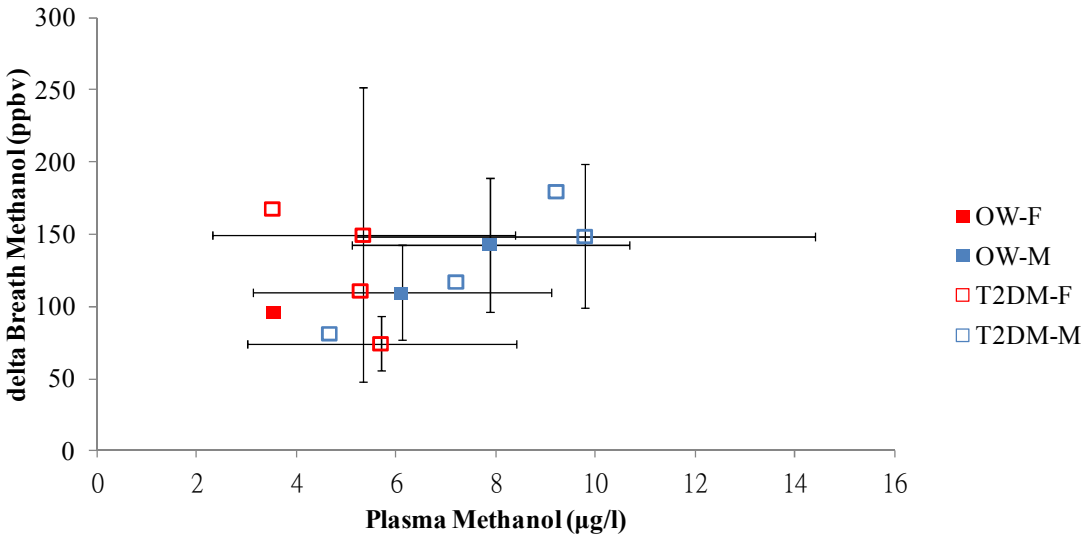

Figure 4.16: Averaged delta Breath Methanol According to Triglycerides versus Averaged Plasma Acetone According to Triglycerides.

4.6. Conclusion

Out of 80 compounds that were monitored, isoprene, acetone, and methanol show significant differences between females and males for both OW and T2DM groups. Elevated triglycerides, free fatty acids are known characteristics of T2DM subjects, but no direct correlation of them between isoprene, acetone, or methanol are observed. Further investigation of a larger group covering different age groups would be helpful to validate current findings.

4.7. References

Claire Turner and Patrik Španěl and David, S. (2006). A longitudinal study of breath isoprene in healthy volunteers using selected ion flow tube mass spectrometry (SIFT-MS). *Physiological Measurement, 27*(1), 13.

Deng, C., Zhang, J., Yu, X., Zhang, W., & Zhang, X. (2004). Determination of acetone in human breath by gas chromatography–mass spectrometry and solid-phase microextraction with on-fiber derivatization. *Journal of Chromatography B, 810*(2), 269-275. doi: http://dx.doi.org/10.1016/j.jchromb.2004.08.013

Eisenreich, W., Bacher, A., Arigoni, D., & Rohdich, F. (2004). Biosynthesis of isoprenoids via the non-mevalonate pathway. *Cellular and Molecular Life Sciences CMLS, 61*(12), 1401-1426. doi: 10.1007/s00018-004-3381-z

Fisher, J. W., Dorman, D. C., Medinsky, M. A., Welsch, F., & Conolly, R. B. (2000). Analysis of Respiratory Exchange of Methanol in the Lung of the Monkey Using a Physiological Model. *Toxicological Sciences, 53*(2), 185-193. doi: 10.1093/toxsci/53.2.185

Galassetti, P. R., Novak, B., Nemet, D., Rose-Gottron, C., Cooper, D. M., Meinardi, S., Blake, D. R. (2005). Breath Ethanol and Acetone as Indicators of Serum Glucose Levels: An Initial Report. *Diabetes Technology & Therapeutics, 7*(1), 9. doi: 10.1089/dia.2005.7.115.

Garriga, M. M., & Metcalfe, D. D. (1988). Aspartame intolerance *Ann. Allergy, 61*, 63-69.

Gelmont, D., Stein, R. A., & Mead, J. F. (1981). Isoprene — The main hydrocarbon in human breath. *Biochemical and Biophysical Research Communications, 99*(4), 1456-1460. doi: http://dx.doi.org/10.1016/0006-291X(81)90782-8

Kalapos, M. P. (2003). On the mammalian acetone metabolism: from chemistry to clinical implications. *Biochimica et Biophysica Acta (BBA) - General Subjects, 1621*(2), 122-139. doi: http://dx.doi.org/10.1016/S0304-4165(03)00051-5

Karl, T., Prazeller, P., Mayr, D., Jordan, A., Rieder, J., Fall, R., & Lindinger, W. (2001). Human breath isoprene and its relation to blood cholesterol levels: new measurements and modeling. *Journal of Applied Physiology, 91*(2), 762-770.

King, J., Koc, H., Unterkofler, K., Mochalski, P., Kupferthaler, A., Teschl, G., . . . Amann, A. (2010). Physiological modeling of isoprene dynamics in exhaled breath. *Journal of Theoretical Biology, 267*(4), 626-637. doi: http://dx.doi.org/10.1016/j.jtbi.2010.09.028

King, J., Kupferthaler, A., Unterkofler, K., Koc, H., Teschl, S., Teschl, G., . . . Amann, A. (2009). Isoprene and acetone concentration profiles during exercise on an ergometer. *Journal of Breath Research, 3*(2), 027006.

King, J., Mochalski, P., Unterkofler, K., Teschl, G., Klieber, M., Stein, M., . . . Baumann, M. (2012). Breath isoprene: Muscle dystrophy patients support the concept of a pool of isoprene in the periphery of the human body. *Biochemical and Biophysical Research Communications, 423*(3), 526-530. doi: http://dx.doi.org/10.1016/j.bbrc.2012.05.159

Kushch, I., Arendacká, B., Štolc, S., Mochalski, P., Filipiak, W., Schwarz, K., . . . Amann, A. (2008). Breath isoprene – aspects of normal physiology related to age, gender and cholesterol profile as determined in a proton transfer reaction mass spectrometry study. *Clinical Chemistry & Laboratory Medicine, 46*(7), 1011-1018. doi: 10.1515/CCLM.2008.181

Kuzma, J., Nemecek-Marshall, M., Pollock, W., & Fall, R. (1995). Bacteria produce the volatile hydrocarbon isoprene. *Current Microbiology, 30*(2), 97-103. doi: 10.1007/BF00294190

Lee, H. J., Pahl, M. V., Vaziri, N. D., & Blake, D. R. (2012). Effect of Hemodialysis and Diet on the Exhaled Breath Methanol Concentration in Patients With ESRD. *Journal of Renal Nutrition, 22*(3), 357-364. doi: http://dx.doi.org/10.1053/j.jrn.2011.07.003

Lindinger, W., Taucher, J., Jordan, A., Hansel, A., & Vogel, W. (1997). Endogenous Production of Methanol after the Consumption of Fruit. *Alcoholism: Clinical and Experimental Research, 21*(5), 939-943. doi: 10.1111/j.1530-0277.1997.tb03862.x

Manolis, A. (1983). The diagnostic potential of breath analysis. *Clinical Chemistry, 29*(1), 5-15.

McGrath, L. T., Patrick, R., & Silke, B. (2001). Breath isoprene in patients with heart failure. *European Journal of Heart Failure, 3*(4), 423-427. doi: 10.1016/S1388-9842(01)00128-3

Mendis, S., Sobotka, P. A., & Euler, D. E. (1994). Pentane and isoprene in expired air from humans: gas-chromatographic analysis of single breath. *Clinical Chemistry, 40*(8), 1485-1488.

Miekisch, W., Schubert, J. K., Vagts, D. A., & Geiger, K. (2001). Analysis of Volatile Disease Markers in Blood. *Clinical Chemistry, 47*(6), 1053-1060.

Minh, T. D. C., Oliver, S. R., Ngo, J., Flores, R., Midyett, J., Meinardi, S., . . . Galassetti, P. R. (2011). Noninvasive measurement of plasma glucose from exhaled breath in healthy and type 1 diabetic subjects. *American Journal of Physiology - Endocrinology and Metabolism, 300*(6), E1166-E1175. doi: 10.1152/ajpendo.00634.2010

Musa-Veloso, K., Likhodii, S. S., & Cunnane, S. C. (2002). Breath acetone is a reliable indicator of ketosis in adults consuming ketogenic meals. *The American Journal of Clinical Nutrition, 76*(1), 65-70.

Musa-Veloso, K., Likhodii, S. S., Rarama, E., Benoit, S., Liu, Y.-m. C., Chartrand, D., . . . Cunnane, S. C. (2006). Breath acetone predicts plasma ketone bodies in children with epilepsy on a ketogenic diet. *Nutrition, 22*(1), 1-8. doi: http://dx.doi.org/10.1016/j.nut.2005.04.008

Newsome, R. (1986). Sweeteners: nutritive and non-nutritive. In: The Scientific Status Summaries of the Institute of Food Technologies Expert Panel on Food Safety and Nutrition. Chicago: Institute of Food Technologies.

Sarkola, T., & Eriksson, C. J. P. (2001). Effect of 4-Methylpyrazole on Endogenous Plasma Ethanol and Methanol Levels in Humans. *Alcoholism: Clinical and Experimental Research, 25*(4), 513-516. doi: 10.1111/j.1530-0277.2001.tb02244.x

Stein, R. A., & Mead, J. F. (1988). Small hydrocarbons formed by the peroxidation of squalene. *Chemistry and Physics of Lipids, 46*(2), 117-120. doi: http://dx.doi.org/10.1016/0009-3084(88)90121-1

Stone, B., Besse, T., Duane, W., Dean Evans, C., & DeMaster, E. (1993). Effect of regulating cholesterol biosynthesis on breath isoprene excretion in men. *Lipids, 28*(8), 705-708. doi: 10.1007/BF02535990

Taucher, J., Hansel, A., Jordan, A., Fall, R., Futrell, J. H., & Lindinger, W. (1997). Detection of isoprene in expired air from human subjects using proton-transfer-reaction mass spectrometry. *Rapid Communications in Mass Spectrometry, 11*(11), 1230-1234. doi: 10.1002/(SICI)1097-0231(199707)11:11<1230::AID-RCM3>3.0.CO;2-Z

Turner, C., Španěl, P., & Smith, D. (2006). A longitudinal study of methanol in the exhaled breath of 30 healthy volunteers using selected ion flow tube mass spectrometry, SIFT-MS. *Physiological Measurement, 27*(7), 637.

Zadak, Z., Hyspler, R., Crhova, S., Gasparic, J., Cizkova, M., & Balasova, V. (1999). Isoprene in expired breath as a marker of cholesterol synthesis for the statin therapy monitoring. *Atherosclerosis, 144*, 206.

Chapter 5: Conclusions

5.1 VOC Profile Study of Water Samples from Different Stages in the OCWD

The first part of this thesis discusses the VOC profiles of water samples including RO feed, RO permeate, UVAOP feed, and UVAOP permeate at the OCWD, a state-of-the-art water reclamation facility. With the ever-increasing demand for water, water reuse can be a reliable and sustainable solution. Reclaimed water need to be carefully processed to thoroughly remove toxics and pathogens before delivery to the public. Some of the commonly used water treatment processes including chlorine disinfection, ozone disinfection, RO purification, UV disinfection have promising pathogen removal power. A complete picture of the effects on treated water by these process is still lacking. An important concern is that most of the current detection and monitoring standard are based on known pollutants. However, with the advancement of techniques, the emergence of compounds that have never been discussed as water treatment byproducts is most likely to increase. Monitoring how impurities evolve during water treatment processes is necessary to ensure the safety of reclaimed water. In our study, five halocarbons: CH_3Cl, $CHCl_3$, $CHBr_3$, $CHBrCl_2$, $CHBr_2Cl$ were observed but were well below the maximum concentration limits. Comparisons to the global budget suggest that the estimated annual production of the five compounds in UVAOP permeate from the OCWD is negligible. The increase of CH_3Cl in

un-quenched RO permeate, and methyl- and *i*-propyl nitrate in UV permeate imply that further investigation of current water treatment processes to elucidate the reaction mechanism is needed. A comprehensive and continuous monitoring of the evolution chemicals and pathogens in ongoing water disinfection and purification processes is very important for safe water reuse.

5.2 VOC Profile Study of OW and T2DM Expired Breath and Plasma

The second part of this thesis examined the VOC profiles of plasma and exhaled breath among four overweight and T2DM groups. Out of all VOCs measured, isoprene, acetone, and methanol show a significant amount in delta breath and plasma. Either plasma and/or delta breath isoprene, acetone, and methanol males are higher in males.

To prevent the damage of diabetic related complications, diabetic patients have to maintain blood sugar levels in a normal range. Monitoring blood sugar three times or more per day with extremely unpleasant pricking fingers blood analysis device has been one of the major hurdles for patients to follow the blood monitoring routine. Non-invasive screening technique using tears (Yan et al., 2011), exhaled breath (Galassetti et al., 2005; Lee et al., 2009; Minh et al., 2011; Novak et al., 2007; Turner, 2011), and molecular sound waves (He et al., 2013; Lin, Lin, Li, & He, 2010) to track

blood glucose levels is highly in need. Investigation of VOC profiles in blood and expired breath among healthy, overweight, and diabetic groups can provide insights for possible non-invasive blood glucose levels tracking techniques. Not only diabetic patients can monitor blood glucose in an easier manner, portable non-invasive techniques based devices can facilitate the screening of pre-diabetic subjects as well. An early alarm for pre-diabetic subjects can urge prevention steps such as increasing exercise time, holding a healthier diet, and decreasing BMI. Some risks for diabetes and cancers are in common. By lowering diabetes risks can also lowering the chances for certain cancers. Therefore, further investigation for larger subject groups and more subject types is important to develop non-invasive blood glucose monitoring and diabetes screening techniques.

5.3 Reference

Galassetti, P. R., Novak, B., Nemet, D., Rose-Gottron, C., Cooper, D. M., Meinardi, S., Blake, D. R. (2005). Breath Ethanol and Acetone as Indicators of Serum Glucose Levels: An Initial Report. *Diabetes Technology & Therapeutics, 7*(1), 9. doi: 10.1089/dia.2005.7.115.

He, Y.-S., Chen, K.-F., Lin, C.-H., Lin, M.-T., Chen, C.-C., & Lin, C.-H. (2013). Use of an Accelerometer and a Microphone as Gas Detectors in the Online Quantitative Detection of Hydrogen Released from Ammonia Borane by Gas Chromatography. *Analytical Chemistry, 85*(6), 3303-3308. doi: 10.1021/ac303694j

Lee, J., Ngo, J., Blake, D., Meinardi, S., Pontello, A. M., Newcomb, R., & Galassetti, P. R. (2009). Improved predictive models for plasma glucose estimation from multi-linear regression analysis of exhaled volatile organic compounds. *J Appl Physiol, 107*(1), 155-160. doi: 10.1152/japplphysiol.91657.2008

Lin, C.-H., Lin, C.-H., Li, Y.-S., & He, Y.-S. (2010). Development and Application of a Milli-Whistle for Use in Gas Chromatography Detection. *Analytical Chemistry, 82*(17), 7467-7471. doi: 10.1021/ac101675z

Minh, T. D. C., Oliver, S. R., Ngo, J., Flores, R., Midyett, J., Meinardi, S., . . . Galassetti, P. R. (2011). Noninvasive measurement of plasma glucose from exhaled breath in healthy and type 1 diabetic subjects. *American Journal of Physiology - Endocrinology and Metabolism, 300*(6), E1166-E1175. doi: 10.1152/ajpendo.00634.2010

Novak, B. J., Blake, D. R., Meinardi, S., Rowland, F. S., Pontello, A., Cooper, D. M., & Galassetti, P. R. (2007). Exhaled methyl nitrate as a noninvasive marker of hyperglycemia in type 1 diabetes. *Proceedings of the National Academy of Sciences, 104*(40), 15613-15618. doi: 10.1073/pnas.0706533104

Turner, C. (2011). Potential of breath and skin analysis for monitoring blood glucose concentration in diabetes. *Expert Review of Molecular Diagnostics, 11*(5), 497-503. doi: 10.1586/erm.11.31

Yan, Q., Peng, B., Su, G., Cohan, B. E., Major, T. C., & Meyerhoff, M. E. (2011). Measurement of Tear Glucose Levels with Amperometric Glucose Biosensor/Capillary Tube Configuration. *Analytical Chemistry, 83*(21), 8341-8346. doi: 10.1021/ac201700c

APPENDIX A: Conversion From Degas Sample Mixing Ratio To Concentration In Water Samples

A total of 760 torr of degas sample was collected at STP from a nine ml water sample.

Total moles of alkyl nitrate in degas sample

= [methyl nitrate mixing ratio] x [total pressure] x [canister volume] / ([gas constant] x [temperature]

Concentration in water (ppt)

= (total mole of alkyl nitrate x molecular weight) x 10^9 (g/ng) / 0.009 L